



Lund University

Faculty of Engineering

Department: Division of Fire Safety Engineering

Year 2015-2016

Reliability of fire barriers

Jonathan Vallée

Promoter: Patrick Van Hees

Master thesis submitted in the Erasmus Mundus Study Programme

International Master of Science in Fire Safety Engineering

DISCLAIMER

This thesis is submitted in partial fulfilment of the requirements for the degree of *The International Master of Science in Fire Safety Engineering (IMFSE)*. This thesis has never been submitted for any degree or examination to any other University/programme. The author declares that this thesis is original work except where stated. This declaration constitutes an assertion that full and accurate references and citations have been included for all material, directly included and indirectly contributing to the thesis. The author gives permission to make this master thesis available for consultation and to copy parts of this master thesis for personal use. In the case of any other use, the limitations of the copyright have to be respected, in particular with regard to the obligation to state expressly the source when quoting results from this master thesis. The thesis supervisor must be informed when data or results are used.

30-04-2016

Jonathan Vallée



Read and approved

Summary/Abstract

A fire barriers are widely used in the industry as a passive fire protection system. Fire barriers are built according to specifications from manufacturer after the construction was tested in full scale furnace in accordance to the appropriate codes. Those tests are made private and the test results are not published apart from the failure/success of the tested sample. In order to accurately protect the life of the occupants and the property, the fire barriers need to be built exactly as its counterpart tested in the furnace test or better. However, it is unknown how a barrier will react to having some higher leakage or lesser insulation property. This study looks at the effect of those two parameters on the fire resistance rating of fire barrier. Numerical tools, ABAQUS and FDS, were used to reproduce the furnace test. Results showed that presence of the insulation material in the cavity can improve the reliability of fire-resistant barrier with regards to the insulation criterion, especially when the fire-exposed gypsum board is breached or altered. Also, results demonstrated that for partitions with equal air tightness, leakage through holes causes earlier failures due to integrity criterion, comparing to leakage through joints or cracks.

Les séparations coupe-feu sont largement utilisées dans l'industrie comme système de protection passive en prévention incendie. Ces murs sont construits à partir des spécifications provenant du fabricant, obtenues suite à des essais rigoureux basé sur les normes en vigueur. Les essais sont effectués auprès de laboratoire privé et seulement le résultat final est publié (échec/succès). Afin de performé tel que prévu, le mur coupe-feu doit être construit exactement comme son homologue testé durant les essais. Cependant, il pourrait y avoir des différences entre le mur testé et le mur construit, spécialement en termes d'isolation et d'étanchéité à l'air. Ces pourquoi une étude est requise afin de connaître l'impact de ces deux propriétés sur la performance des murs coupe-feu. Pour y arriver, plusieurs simulations numériques ont été réalisées sur ABAQUS et FDS. Suite à l'analyse des résultats, il a été constaté que l'utilisation d'isolation dans la cavité murale permet d'obtenir une meilleur performance contre le feu, plus spécialement lorsqu'il y'a une brèche dans la couche de gypse situé du côté de l'incendie. De plus, avec une étanchéité à l'air équivalente, les murs dont la fuite d'air se produit par un trou ou une ouverture concentrée en un endroit précis performe moins bien dans un incendie comparé à un mur qui fuit par des joint ou par une fente distribuée le long du mur.

Table of contents

List of abbreviations.....	vi
List of figures and tables	vii
1 Introduction & Objectives.....	1
1.1 Introduction.....	1
1.2 Objectives.....	2
1.3 Methodology.....	3
1.4 Limitations.....	3
2 Heat Transfer	4
2.1 Radiation	4
2.2 Convection.....	6
2.3 Conduction	6
2.4 Heat flux in furnace test.....	8
3 Hot gas movement.....	9
3.1 Smoke infiltration.....	9
3.2 Air Tightness of walls.....	9
3.3 Pressure difference in a furnace	11
4 Fire barrier construction	13
4.1 Partition investigated.....	13
4.1.1 Construction type A	14
4.1.2 Construction type B	14
4.1.3 Light gauge steel frame.....	16
5 Material Properties.....	17
5.1 Thermal properties of Gypsum Board.....	17
5.1.1 Conductivity	18
5.1.2 Thermal capacity.....	18
5.1.3 Density	19
5.2 Thermal properties of insulation	21

5.2.1	Conductivity	21
5.2.2	Thermal capacity.....	22
5.2.3	Density	22
5.3	Thermal properties of steel.....	23
5.3.1	Conductivity	23
5.3.2	Thermal capacity.....	24
5.3.3	Density	24
5.4	Thermal property of air cavities.....	24
6	Methodology.....	26
6.1	ABAQUS Procedure	26
6.1.1	Geometry and Material Properties.....	26
6.1.2	Initial and Boundary Conditions	27
6.1.3	Interactions and assumptions.....	29
6.1.4	Mesh and Element Type	30
6.2	Validation of the FE model.....	32
6.3	FDS Procedure	34
6.3.1	Dimensions and materials.....	34
6.3.2	Temperature	35
6.3.3	Pressure	36
6.3.4	Leakage	36
6.3.5	Grid selection	38
6.4	Validation of the CFD model	39
6.4.1	Furnace Temperature	39
6.4.2	Furnace pressure distribution.....	41
6.4.3	Heat Flux at sample.....	41
7	Results and discussion	43
7.1	Construction Type A.....	44
7.1.1	Impact of the choice of insulation material.....	44
7.1.2	Impact of reduced amount of insulation	47

7.1.3	Impact of increased amount of insulation.....	50
7.1.4	Impact of hole on the exposed surface	52
7.1.5	Impact of the hole through the barrier	54
7.2	Construction Type B.....	55
7.2.1	Impact of the choice of insulation material.....	55
7.2.2	Impact of hole on the exposed surface	57
7.2.3	Impact of reduced amount of insulation	60
7.2.4	Impact of missing part of insulation	61
7.3	Table of results from the heat transfer simulation with ABAQUS.....	63
7.4	Impact of leakage with FDS.....	66
7.4.1	Localized leakage	66
7.4.2	Distributed leakage on one side	67
7.4.3	Distributed leakage.....	69
7.5	Discussion.....	72
7.6	Limitations and Uncertainties	73
8	Conclusions	75
9	Future Work.....	77
10	Acknowledgements.....	78
11	References	79
	Appendix A: FDS script file	I
	Appendix B: ABAQUS script file	XV

List of abbreviations

HRRPUA – Heat Release Rate Per Unit Area

FRR – Fire Resistance Rating

NRCC – National Research Council Canada

LSF - Light gauge Steel Frame

FE – Finite Element

CFD – Computational Fluid Dynamics

ASTM – American Society for Testing and Materials

ISO – International Organization for Standardization

EN – European Standards

AAMA - American Architectural Manufacturers Association

ASHRAE – American Society of Heating, Refrigerating and Air Conditioning Engineers

NMBCC - National Model Building Code of Canada

DBI – Danish Institute of fire and security technology

List of figures and tables

Figure 1: Heat transfer by radiation on a surface	5
Figure 2: Separation of surfaces into finite element	7
Figure 3: Heat flux measured during a furnace test (reproduced with the permission of the National Research Council of Canada).....	8
Figure 4: Typical light-weight construction assembly	13
Figure 5: Construction Type A.....	14
Figure 6: Construction Type B.....	14
Figure 7: Metal frame	15
Figure 8: joint from gypsum board	15
Figure 9: Conductivity of gypsum type X	17
Figure 10: Specific heat of gypsum board type X	18
Figure 11: Mass loss of gypsum board type X and Contraction of gypsum X.....	19
Figure 12: Change of density of gypsum type X	19
Figure 13: Conductivity of stone wool	20
Figure 14: Conductivity of glass fiber wool.....	21
Figure 15: Conductivity of steel	22
Figure 16: Specific heat of steel	23
Figure 17: Air density change with temperature.....	24
Figure 18: Fire barrier metal frame	25
Figure 19: Unexposed surface temperature.....	28
Figure 20: Exposed surface temperature	28
Figure 21: Temperature at the unexposed surface case a)	30
Figure 22: Temperature at the unexposed surface case b).....	30
Figure 23: Temperature at the unexposed surface case c)	31
Figure 24: Furnace modeled with FDS.....	34
Figure 25: Leakage distributed at every joints.....	36
Figure 26: Leakage distributed on one side.....	36
Figure 27: Leakage localized at the top	37
Figure 28: Acceptable temperature in the furnace according to EN 1363-1	39
Figure 29: Average temperature versus time measured on the surface of the wall sample in FDS	39

Figure 30: Pressure profile in the FDS simulation.....	40
Figure 31: Distribution of the heat flux gauge (reproduced with the permission of the National Research Council of Canada)	41
Figure 32: Heat flux at the surface of the sample in the furnace.....	41
Figure 33: Temperature at the unexposed layer of the Wall with different types of insulation or without insulation.....	43
Figure 34: Temperature inside cross section of walls	44
Figure 35: FRR of each walls insulated or uninsulated	45
Figure 36: Temperature of the exposed side gypsum layer	45
Figure 37: Cross section a partition filled with fiber glass wool, after 60min	46
Figure 38: Wall with reduced insulation.....	47
Figure 39: Temperature in the cross section of wall with reduced insulation	47
Figure 40: Unexposed surface temperature of stone wool partition after 60min.....	48
Figure 41: Ratio of FRR over the expected 60min rating for partition with reduced insulation..	48
Figure 42: Temperature on unexposed surface of the wall with different position of insulation	49
Figure 43: Temperature on the unexposed side of a partition type A with 100mm stone wool insulation.....	50
Figure 44: Temperature in the cross section of a partition type A with 100mm stone wool insulation.....	50
Figure 45: Temperature on the unexposed side for insulated partition with hole on the exposed surface.....	51
Figure 46: Temperature of the partition with hole on exposed surface insulated with stone wool	51
Figure 47: Temperature on the unexposed side of the partition with hole on the exposed surface	52
Figure 48: Temperature of partition without insulation breached on exposed side	52
Figure 49: Temperature on the unexposed surface of a partition type A with a hole of 10mm, first and second scenario	53
Figure 50: Temperature on the unexposed surface of a partition type A with a hole of 50mm radius, first and second scenario	53
Figure 51: Temperature on the unexposed surface of wall type B with different types of insulation and without insulation.....	54
Figure 52: Temperature in the cross section of wall type B for different insulation	55
Figure 53: FRR for different insulation or uninsulated	55
Figure 54: Temperature on the unexposed side for insulated partition with hole on the exposed surface.....	56
Figure 55: Temperature of the partition with hole insulated with stone wool	57

Figure 56: Temperature of the partition for all types of insulation and breach of 10mm and 50mm radius.....	58
Figure 57: Temperature on the unexposed surface of wall type B with reduced insulation	59
Figure 58: FRR for partition with reduce insulation for type B construction	60
Figure 59: Temperature on the unexposed surface of wall type B with missing insulation part	60
Figure 60: The temperature of the two walls with missing portion of insulation, left 50mm radius and right 100mm radius.....	61
Figure 61: The temperature of the two walls with missing portion of insulation, left 50mm radius and right 100mm radius.....	61
Figure 62: Temperature of cotton pad scenario 1 with different level of air tightness.....	66
Figure 63: Temperature of cotton pad with time measured at the top of the sample height	68
Figure 64: Temperature of cotton pad with time measured at the bottom of the sample height	69
Figure 65: Temperature of cotton pad with time measured at the middle of the sample height	69
Figure 66: Temperature on the cotton pad after around 3600 seconds.....	72
Figure 67: Temperature on the unexposed side of the tested sample after 3600 seconds	73
Table 1: Leakage area for different tightness	11
Table 2: Thermal capacity of insulation	21
Table 3: Density of insulation	22
Table 4: Emissivity of material	24
Table 5: Experimental and simulation results	32
Table 6: Thermal properties of ceramic blanket	33
Table 7: Properties of propane	35
Table 8: Comparison of the results obtained with ABAQUS	65
Table 9: FRR of partition with different tightness leaking from a hole on top.....	67
Table 10: FRR of partition with different air tightness leaking from one side	70
Table 11: Percentage change in FRR between localized and distributed leakage	70
Table 12: FRR of partition with different air tightness leaking from every joints	71
Table 13: Percentage change in FRR between leakage in all joints and the other scenarios for the cotton pad at mid height of the furnace	72

1 Introduction & Objectives

1.1 Introduction

In order to restrain fire spread and to contain the fire in one area, a building can be subdivided into compartments separated from one another by fire-resisting constructions. This passive fire protection method helps to reduce the fire size which gives more time for the occupants to evacuate, eases the fire service work and decreases property damage and business interruption time. The fire resistance rating of light weight construction, especially Cold-formed light gauge steel frame (LSF) stud wall systems, has become critical to the building safety design as their use has become increasingly popular in all areas of building construction [1].

The fire resistance rating (FRR), given in unit of time, is the period of time during which a building element can withstand the exposure to defined heating and pressure conditions, until failure. Usually this time period ranges between 60min and 120 min [1]. Traditional fire resistance testing is done in furnace test and based upon the international standard ISO 834. According to the British code BS EN 1363-1, the failure criteria are based on three parameters: integrity, stability and insulation [2]. The insulation criterion relates to the ability of a building component to restrict the heat transfer through its boundaries to a certain level. According to the EN 1363-1 code, failure of the insulation criterion is observed in two ways [2]. The code states that the specimen must maintain its function for the duration of the test without developing temperatures on its unexposed surface such as:

- An increase the average temperature above the initial average temperature by more than 140 °C, called T_{140} ;
- An increase at any location (including the roving thermocouple) above the initial average temperature by more than 180 °C, called T_{180} .

The integrity criterion represents the ability of a building component to prevent the passage, through its boundaries, of flames and hot gases and to prevent the occurrence of flames on the unexposed side. The requirements from the relevant code [2] are the following:

- Prevent the penetration of a 6 mm diameter gap gauge that can be passed through the test specimen, such that the gauge projects into the furnace, and can be moved a distance of 150 mm along the gap
- Prevent the penetration of a 25 mm diameter gap gauge that can be passed through the test specimen such that the gauge projects into the furnace.

- Prevent the ignition of a cotton pad applied for a maximum of 30 s or until ignition positioned at least 30 mm from the unexposed surface and 10 mm from the boundaries of the wall. Charring of the cotton pad without flaming or glowing shall be ignored.

In the industry the fire rated partition are built according to specifications coming from manufacturers, providing fire resistance ratings. Those rating are based on full-scale furnace tests using the required standard [3]. Often, the fire barriers tested in the furnace are highly optimized in order to reach the required fire resistance. The test results remain confidential and the number of samples, which fail is not documented. In practice, the construction of the fire rated barrier can slightly differ from the optimized one tested in the furnace test. Furthermore, with time, the quality of the barrier can be altered, thus, reducing its ability to contain the fire. This raises concerns about the reliability of fire resisting partition as an effective mean of passive fire protection. Little research has been done with respect to the impact of reduced insulation and leakage on the reliability of fire resisting partition. It is not known what kind of safety factor can be expected of fire barrier and often, the designer relies simply on the obtained ratings. For this reason, research is necessary in order to determine the reliability of fire barriers.

In this report the effect of reduced integrity and insulation parameters will be investigated. In order to do so, two fire-rated barriers will be modeled with numerical tools and will be exposed to the standard fire. Then, the same barriers will be modified to exploit different features or defects, affecting the insulation or integrity criterion, and it will be exposed to the same conditions. Finally, the results will be compared to understand how those features affect the FRR. The different defects or features which will be investigated are the following: different type of insulation, different thickness of insulation, missing part of insulation, the absence of insulation, penetration through the drywall on one side or through the entire construction, infiltration of gases through cracks of different size at different location. Additionally, the report will look at the impact of the modeling techniques used such as the difference of grid size, the impact of different heat transfer modes and the assumptions taken.

1.2 Objectives

The first objective of this study is to show how the FRR of partitions is affected by leakage. To do this, the FRR obtained from simulations of partitions with localized leakage, distributed leakage, different leakage size and location will be compared to an airtight partition.

The second objective of this study, is to investigate the effect of a reduced thermal insulation on the FRR of partitions. Insulation can be reduced in multiple ways, the scenarios which will be investigated are: localized missing piece of different size of insulation, reduced thickness of insulation, different type of insulation, partition without insulation, hole of different size on the exposed boundary of the partition and hole through the partition. Those assumed

parameters and features are meant to represent ways in which a fire rated wall could be altered before being exposed to a fire.

1.3 Method

The methods that will be used are hand calculations for basic heat transfer through the wall, hand calculations of infiltration and pressure inside the furnace, CFD modelling using the CFD tool - FDS and Finite element modelling using ABAQUS to replicate the standard fire furnace tests. Case study method will be used in this work. More precisely, the effect on the FRR according to the insulation criterion will be examined for the following parameters: The type of insulation or absence of insulation, the reduction of the insulation thickness inside the cavity, breach in the gypsum board exposed in the furnace, breach through the fire barrier and missing piece of insulation inside the cavity. Also, the effect of leakage on the FRR based on the integrity criterion will be investigated assuming that the barrier leaks before it is submitted to the standard fire. Different level of airtightness will be assumed and different leakage scenario. The first scenario will aim at simulating the effect of hole through the barrier. The second and third scenario will be looking at the effect of leaking joint improperly sealed. In order to validate the models, comparison of model's results to experimental data of wall tested in actual furnace will be made. Thus, the report also holds a study of model validity, to see whether simple calculations and modelling are able to replicate heat transfer in a furnace test.

1.4 Limitations

This study will be limited to walls and will not include doors, windows, ventilation ducts. Studies will be mainly done with respect to smoke leakages and reduced thermal insulation. The stability criterion relates to the structural capacity of the structure at elevated temperature. In this study the stability criterion will not be investigated, thus, it is assumed that the walls do not collapse, do not show excessive deformation or deflection. Also, it is assumed that the defects and features investigated are already part of the wall before the fire, this study will not be looking at the deficiencies due to the fire effects.

2 Heat Transfer

In order to properly model the heat transfer from the furnace to the sample, it is necessary to understand the different modes of heat transfer. There are three basic mechanisms of heat transfer, namely conduction, convection and radiation[4]. Inside the furnace the exposed surface of the partition will be affected by convection and radiation[5]. The contributions of these two modes of heat transfer are independent and must be treated separately. The total heat flux to the exposed surface in the furnace is [6]:

$$q''_{exposed\ surface} = q''_{radiation\ furnace} + q''_{convection\ furnace} \quad (1)$$

The unexposed surface of the fire barrier will be also subjected to heat transfer, but only with the ambient air outside of the furnace. The heat transfer will be done through convection with air at 20°C [7]. Radiation is not considered due to the low temperature expected on the unexposed layer and the unknown distance between the unexposed surface and other objects.

$$q''_{unexposed\ surface} = q''_{convection\ ambient} \quad (2)$$

Heat can propagate inside the barrier by different means depending on its construction. If insulation is used then heat will be transferred to the unexposed side by conduction only, but if there is an empty cavity inside the barrier then radiation is expected due to the high temperature occurring in a furnace test [8].

2.1 Radiation

The net radiative heat flux on a targeted surface is the difference between the absorbed incident radiation and the emitted radiation. Those two parameters depends on the emissivity/absorptivity and absolute temperature, of the surfaces involved. Indeed, as depicted in the Figure 1 (reproduced from a study of SP [5]), part of the incident radiation, coming from the surrounding, is absorbed while the rest is reflected and the surface emit radiation as well. The net radiative heat flux on a surface can be written as [5]:

$$q''_{rad} = \alpha_s q''_{inc} - q''_{emi} \quad (3)$$

The emitted radiative heat flux can be expressed according to the Stefan–Boltzmann equation[4].

$$q''_{rad} = \sigma \varepsilon T^4 \quad (4)$$

Thus the equation (3) can be written as:

$$q''_{rad} = \alpha_s q''_{inc} - \sigma \varepsilon_s T_s^4 \quad (5)$$

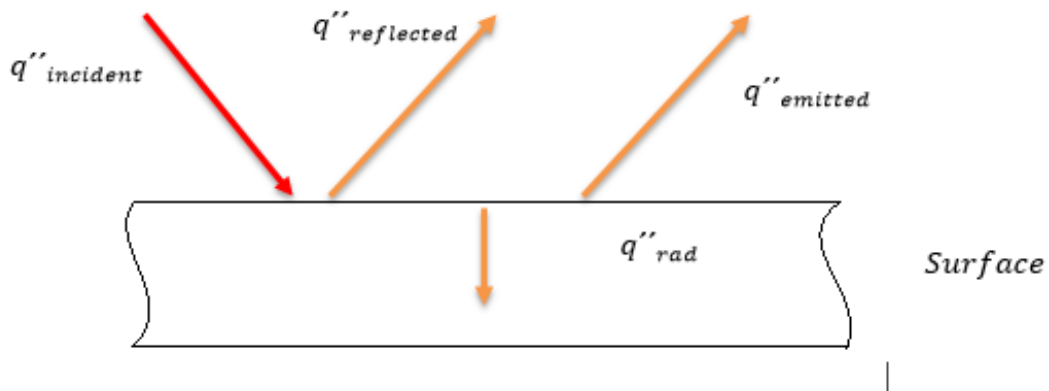


Figure 1: Heat transfer by radiation on a surface

Where

α_s – is the surface target absorptivity

ε_s – is the emitting surface emissivity

σ – is the Stefan–Boltzmann constant, $5.67 \times 10^{-8} \text{ W/m}^2 \text{ K}^4$

T_s – is the target surface temperature, K

However, the surface emissivity and absorptivity are considered equal according to the Kirchhoff's identity[4]. Thus the equation (5) can be rewritten as:

$$q''_{rad} = \varepsilon_s(q''_{inc} - \sigma T_s^4) \quad (6)$$

In the furnace test the incident radiation to the tested surface is emitted by the surrounding gases, by flames and by other surfaces. The heat fluxes are generally very complicated to model. Usually, a summation of the main contributions can give a good estimate of the incoming radiation [6]:

$$q''_{inc} = \sum F_i \varepsilon_i \sigma T_i^4 \quad (7)$$

Where

ε_i – is the surrounding surface emissivity

F_i – is the view factor involving distance and location

T_i – is the surrounding surfaces, flame and gases temperature, K

The view factor for total radiation exchange between two identical, parallel, directly opposed flat plates can be assumed to be 1, when the ratio of the emitting surface dimension over the distance between surfaces is low [4]. Therefore, the heat transfer by radiation from the furnace to the exposed partition surface can be expressed as:

$$q''_{furnace} = \varepsilon_s \sigma (T_{ISO834}^4 - T_s^4) \quad (8)$$

2.2 Convection

Heat transfer by convection occurs between a fluid and a solid. It depends on the target geometry, adjacent fluid velocities and fluid/object temperature. Convection occurs inside the furnace between the furnace gases and the exposed surface of the sample and between the unexposed surface of the sample and the surrounding ambient temperature air, outside of the furnace. The heat transfer equation are expressed as follow [4]:

$$q''_{Exposed\ surface} = h_{exp}(T_{gases} - T_{s_exp}) \quad (9)$$

$$q''_{Unexposed\ surface} = h_{unexp}(T_{s_unexp} - T_{ambient}) \quad (10)$$

Where

h_{exp} – is the convective heat transfer coefficient from the exposed surface, W/m²K

h_{unexp} – is the convective heat transfer coefficient from the unexposed surface, W/m²K

T_{s_exp} – is the exposed surface temperature of the sample (exposed or unexposed), K

T_{s_unexp} – is the exposed surface temperature of the sample (exposed or unexposed), K

$T_{ambient}$ – is the temperature outside the furnace, K

T_{gases} – is the gases temperature inside the furnace, K

The convective heat transfer coefficient, h , inside and outside the furnace will be different due to the flow conditions.

2.3 Conduction

Conduction only occurs inside a medium which can be a gas, liquid, or solid. The distinction between conduction and convection heat transfer is associated with whether the medium has some ordered flow or motion [9]. For very thin solids, or for conduction through solid that goes on for a long time, the process of conduction becomes stationary, and the rate of heat conducted through the solid becomes [4]:

$$q''_{cond} = \frac{k}{\delta}(T_{exp} - T_{unexp}) \quad (11)$$

Where

δ – is the thickness of the sample, m

T_{exp} – is the temperature on the hot side of a sample, K

T_{unexp} – is the temperature on the cold side of a sample, K

k – is the conductive heat transfer coefficient, W/mK

Also a numerical solution can be used to solve heat transfer equations. For one-dimensional heat transfer, the wall needs to be represented by a series of thin, parallel elements of equal thickness, as shown in Figure 2 (reproduced from An Introduction to Fire Dynamics, Third Edition[4]). Transient heat transfer through the barrier is then calculated iteratively, by considering adjacent elements and applying the logic of Equations (12) and (13). Those equations depict the unsteady heating stage where the element numbered 3 receives heat from element 2, but loses heat to element 4. Also, at the two boundaries of the fire barrier, the conditions should be applied to reproduce the convection and the radiation heat transfer from the furnace and the room at ambient conditions. This is shown in the equations (14) and (15) [4], [10].

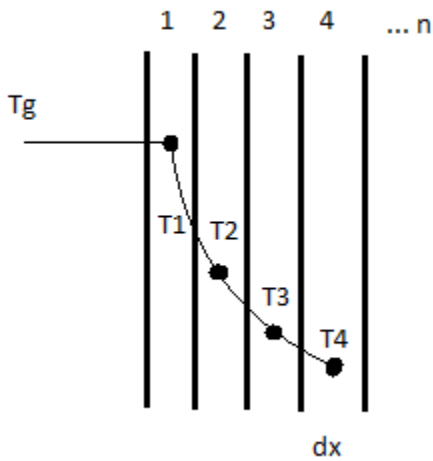


Figure 2: Separation of surfaces into finite element

$$\frac{k}{\Delta x}(T_2 - T_3) - \frac{k}{\Delta x}(T_3 - T_4) = \rho c_p \Delta x (T_3(t + \Delta t) - T_3(t)) \quad (12)$$

$$T_3(t + \Delta t) = T_3(t) + \frac{k}{\rho c_p (\Delta x)^2} (T_2 - 2T_3 + T_4) \quad (13)$$

$$T_1(t + \Delta t) = T_1(t) + \left((h(T_{hot} - T_1) + \varepsilon_i \sigma (T_{hot}^4 - T_1^4) - \frac{k}{\Delta x} (T_1 - T_2)) \frac{2\Delta t}{\rho c_p \Delta x} \right) \quad (14)$$

$$T_m(t + \Delta t) = T_m(t) + \left(\frac{k}{\Delta x} (T_{m-1} - T_m) - (h(T_m - T_{cold})) \frac{2\Delta t}{\rho c_p \Delta x} \right) \quad (15)$$

2.4 Heat flux in furnace test

The total heat flux measured in an ASTM E 119 furnace test, at the National Research Council of Canada, is provided in Figure 3, for a wall furnace. The total heat fluxes were measured using a water-cooled Gardon gauge and the wall furnace was lined with ceramic fiber. The temperature was controlled with ASTM E 119 shielded thermocouples [11]. Though, the time-temperature curves are similar for ISO 834 and ASTM E119, the actual heat flux exposure early in the ASTM E 119 is more severe due to the type of thermocouples used to control the furnace. The same furnace controlled with a plate thermometer provided similar heat flux levels at times after 10 minutes [12]. This heat flux will be used later as means of validation.

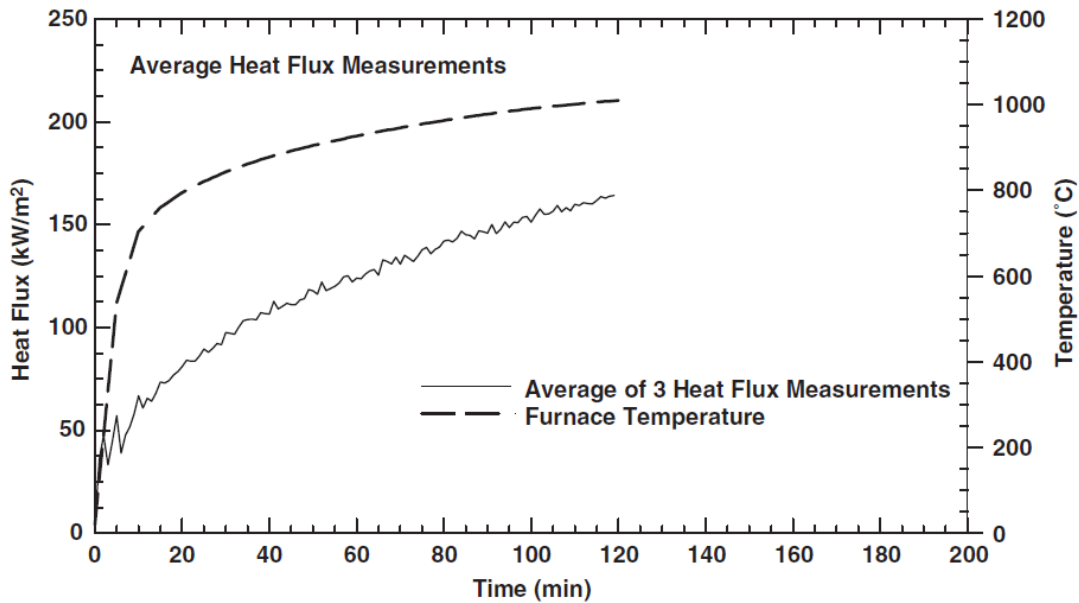


Figure 3: Heat flux measured during a furnace test (reproduced with the permission of the National Research Council of Canada)

3 Hot gas movement

3.1 Smoke infiltration

The driving force for air movement is pressure, air moves from a location of higher pressure to a location of lower pressure. However, for air to move through a surface it needs an open area or leakage area. The total air leakage in a fire rated wall is equal to the sum of all the leakages occurring through holes and cracks in the boundaries. However, the quantity and appearance of the leakage areas is often impossible to predict since when building a fire-rated barrier the aim is not to have any leakages. Still, based on experience, a total opening area can be assumed and it is possible to estimate the total leakage through barriers. By measuring the difference in pressure across the wall from the unexposed side against the exposed side, the flow rate can be obtained from Bernoulli's equation. The orifice equation used to estimate the flow through building is presented below [13]:

$$Q = CA \sqrt{\frac{2\Delta p}{\rho}} \quad (16)$$

where

Q = volumetric airflow rate, m³/s

C = flow coefficient

A = flow area (leakage area), m²

Δ p = pressure difference across flow path, Pa

ρ = density of air entering flow path, kg/m

The flow coefficient depends on the geometry of the flow path, as well as on turbulence and friction. The number of opening also has an impact on the flow coefficient. Literature suggest a flow coefficient in the range of 0.6 to 0.7 [13].

3.2 Air Tightness of walls

Fire-rated barriers should be designed and constructed to be as airtight as possible. This help to prevent any combustible gas to reach the unexposed side of the wall, thus preventing fire spread as much as possible. Nonetheless, it is not possible to build wall that's is perfectly air tight due to the presence of screws, anchors, electrical outlets, etc. Those elements create area or paths for air infiltration, even though effort is made to seal all penetration. Also, materials by themselves are never 100 % impermeable to movement of air and as such they allow for leakage, although, very low leakage.

In North America the Normalized Air Leakage Rate of Building Enclosure is used to define leakage. The average volume of air in L/s that passes through a unit area of the building enclosure in m^2 , is measured and expressed in $L/s \cdot m^2$ when the building enclosure is subjected at 75 Pa of pressure differential, in accordance with ASTM E779 [14].

The American Architectural Manufacturers Association (AAMA) suggests a maximum of $0.3 L/s \cdot m^2$ at 75 Pa [14], while the appendix of the National Model Building Code of Canada (NMBCC) recommends a value of $0.1 L/s \cdot m^2$ at 75 Pa [14] as a maximum allowable leakage rate. Tamura and Shaw, from the NRCC, in the 1980s measured and studied the air leakage of seven high-rise office buildings. Their conclusion was that buildings are tight if they achieve a normalized air leakage rate of $0.5 L/s \cdot m^2$ at 75 Pa [14]. ASHRAE considered that a building is very loose when there is opening in walls equivalent to $0.13 \times 10^{-2} m^2$, average for values of $0.35 \times 10^{-3} m^2$ and tight for values of $0.17 \times 10^{-3} m^2$ per total area of wall (m^2) [13].

With the equation (16), and the density of air at ambient temperature ($20^\circ C$), the previous leakage gives the following opening area/surface ratio:

$$0.5 \frac{L}{s * m^2} = 0.0005 \frac{m^3}{s * m^2} = 0.65A \sqrt{\frac{2 * 75Pa}{1.225 \frac{kg}{m^3}}}$$

$$A = 70 \frac{mm^2}{m^2}$$

$$0.3 \frac{L}{s * m^2} = 0.0003 \frac{m^3}{s * m^2} = 0.65A \sqrt{\frac{2 * 75Pa}{1.225 \frac{kg}{m^3}}}$$

$$A = 42 \frac{mm^2}{m^2}$$

$$0.1 \frac{L}{s * m^2} = 0.0001 \frac{m^3}{s * m^2} = 0.65A \sqrt{\frac{2 * 75Pa}{1.225 \frac{kg}{m^3}}}$$

$$A = 14 \frac{mm^2}{m^2}$$

The wall area investigated will be of dimension equal to 3.6m x 3.1m. The dimensions of cracks which will be considered are presented in the following table.

Airtightness level	Leakage area (mm ²)
Very loose construction	14508
Loose construction	4536
Average construction	1897
Tight construction (NRCC)	780
Tight construction (AAMA)	468
Tight construction (NMBCC)	156

Table 1: Leakage area for different tightness

3.3 Pressure difference in a furnace

Fully-developed fires produce a positive pressure gradient across the boundaries height, relative to ambient conditions. The pressure differential between compartment containing a fire and one containing ambient air will vary due to buoyancy of hot gases, the pressure difference can be found with the equation 17 [12],

$$\Delta p = g(\rho_a - \rho_f)h \quad (17)$$

Where

g - is the gravitational constant, 9.81 m/s²

ρ_f - is the gases density inside the fire compartment, kg/m³

ρ_a - is the ambient air density at the same elevation, kg/m³

h - is the elevation above a reference where the pressure between ambient and the compartment is equal (this reference is called the neutral plane), m

By applying the ideal gas law to equation 17, the differential pressure equation can be transformed into a temperature difference equation [12],

$$\Delta p = 352.8g \left(\frac{1}{T_a} - \frac{1}{T_f} \right) h \quad (18)$$

Where

T_f - is the gas temperature inside the fire compartment, (K)

T_a – is the ambient gas temperature, 293 K

The pressure found in the modeled furnace can be estimate with the equation (18), at height of 3.1m. After 2 hour of the ISO-834 standard fire the temperature inside the furnace reaches 1342 K [2] and the pressure differential is then:

$$\Delta p = 28 \text{ Pa}$$

4 Fire barrier construction

Fire-rated barriers may be constructed in a variety of ways. The required resistance rating will depend on the intended usage and the requirement of building codes. One of the most popular construction type of fire barrier is light weight stud wall system [1]. Lightweight partitions are usually built from various types of sheet materials, supported by timber or metal stud, with sealed joints. The cavity between the boards are filled with insulation layers or left empty. The insulation materials commonly used in the cavity are glass fibre, stone wool insulation [1]. This work will focus on LSF wall system as they are a popular types of installation [1]. Figure 4 shows a typical assembly of a light-weight partition with the insulation. The literature review of fire barrier specifications from Plasterboard manufacturer allowed to define the general component and construction specification required in order to obtain suitable fire rating.

4.1 Partition investigated

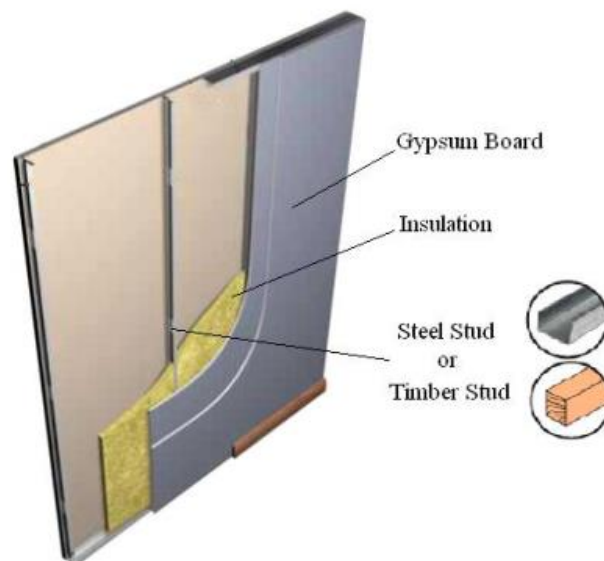


Figure 4: Typical light-weight construction assembly

Two different types of construction will be investigated in this project. The first one, called type A, correspond to a one hour fire resistance wall and the second construction, called type B, correspond to a two hours fire resisting wall. Construction specification of both type come from the literature review of different manufacturer.

4.1.1 Construction type A

The fire barrier of type A, is built of a single layer of fire type gypsum board located on each side of the partition, 12.5mm thick. The gypsum board is supported by 50mm width, 0.5mm gauge, 'C' studs at every 600mm centres, see Figure 5. This type of construction was tested in a furnace test, without the use of any insulation, and was rated 60 minutes of fire resistance [3], [15]. This construction will be investigated with and without the use of thermal insulation. Usually, in order to achieve this resistance, the wall's joints and cracks must be sealed to prevent air infiltration. The impact of the thightness of the wall will be investigated to look at the impact on the barrier's integrity. An example of a section of the wall with and without insulation is given below.

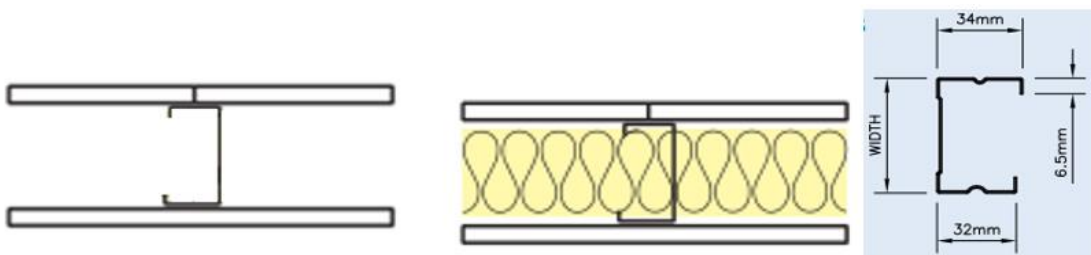


Figure 5: Construction Type A

4.1.2 Construction type B

The fire barrier is built of two layers of fire type gypsum board, located on both side of the partition, 12.5mm thick. The gypsum board is supported by 50mm width, 0.5mm gauge, 'C' studs at every 600mm centres, see Figure 6. This type of construction was tested in a fire resistance test, without the use of any insulation, and was rated 120 minutes fire resistance [3], [15]. This construction was investigated with and without the use of thermal insulation. In order to achieved this resistance, the wall joints and cracks must be sealed to prevent air infiltration. The impact of the thightness of the wall will be investigated to look at the impact on the barrier's integrity. An example of a section of the wall with and without insulation is given below.

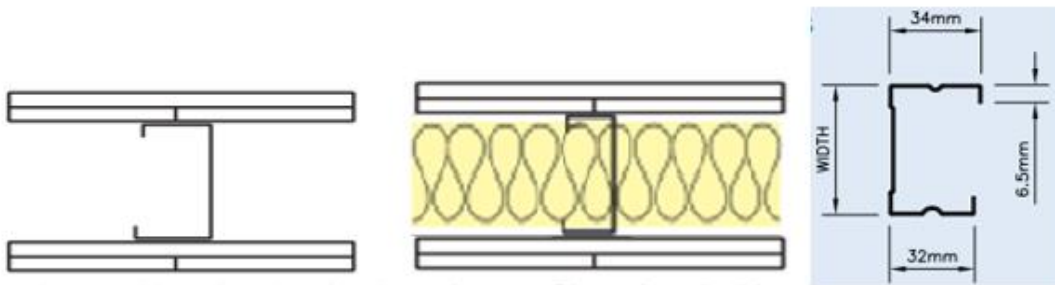


Figure 6: Construction Type B

4.1.3 Light gauge steel frame

The frame used to hold the insulation and on which the gypsum board is fixed to, is presented in the following picture with all related dimensions.

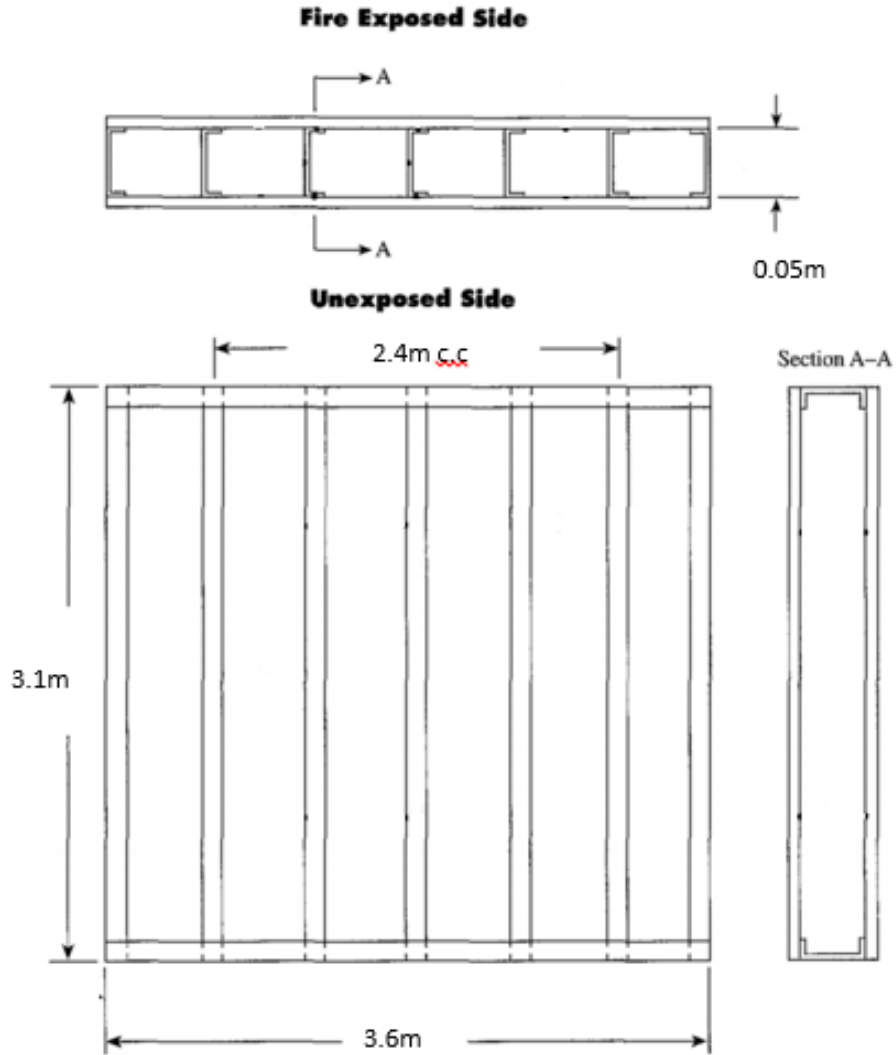


Figure 7: Metal frame

The gypsum boards are usually 1220mm wide by 3660mm long [16], this means that this wall would require 3 gypsum sheets to cover the whole surface. When using multiple sheets of gypsum, joints are formed between each sheet and the surrounding construction as well as between every two sheets. Those joints can be a source of leakage if they are not sealed properly.

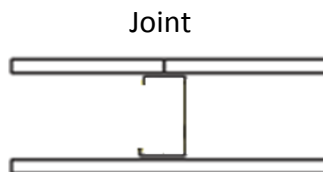


Figure 8: joint from gypsum board

5 Material Properties

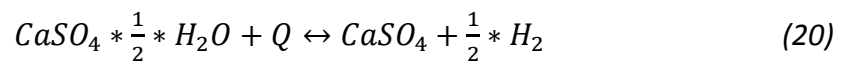
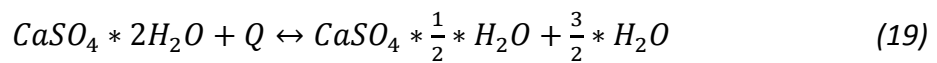
To be able to withstand the furnace increasing temperature, the partition wall must have adequate thermal properties. The properties of each layer constituting the wall are important as they help to slow down heat transfer through partitions. The material properties which should be assessed, in order to investigate the partition reliability with regards to the insulation criterion, are the density, the specific heat and the conductivity. These properties differ from one manufacturer to another, for instance gypsum board type X or Glasroc F FIRECASE. In this study the focus is not on the variation in thermal properties, but on the effects of defects affecting fire-rated barrier. Consequently, material properties will be defined in this section and will not be change in the simulation.

The specific heat or thermal capacity is a measurable physical quantity equal to the ratio of the heat added to or removed from an object to the resulting temperature change. The specific heat is measure in J/kg*K. The thermal conductivity is a material property describing the ability to conduct heat. The thermal conductivity is measure in the units W/m*K. The density is a material attribute defining the weight per volume of a material in kg/m³.

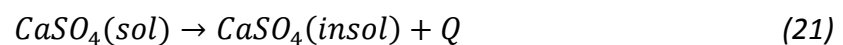
5.1 Thermal properties of Gypsum Board

Gypsum board is constructed of non-combustible products in which gypsum is the primary component with paper-laminated surfaces. In North America the gypsum board called Type X is used for fire barrier. This gypsum board has additives that give better fire-resistive performance compare to the regular gypsum board of the same thickness.

Gypsum is called calcium sulfate dihydrate (CaSO₄ 2H₂O), which is a naturally occurring mineral. The water proportion is a key feature that makes gypsum a fire resistant material. When gypsum is heated, the crystalline gypsum dehydrates and water is released. This process is called Calcination and typically occur in two separate, reversible chemical reactions:



Both of these dehydration reactions are endothermic and generally occur at temperatures between 125 and 225°C. In addition to two dehydration reactions, a third exothermic reaction occurs at a temperature of around 400°C in which the molecular structure of the soluble crystal reorganizes itself into a lower insoluble energy state (hexagonal to orthorhombic) [17]:



The data used in this project is based on a paper from NIST [17], which tested the properties of different type of gypsum board under heat. The results for gypsum board type X from this paper will be used.

5.1.1 Conductivity

The thermal conductivity of gypsum board is a function of the temperature and heating cycle. During the first heating cycle (first time the gypsum board is being heated), the gypsum dehydrates, absorbs some of the energy, and delays the temperature rise. Results from experiment clearly show a huge differences in the thermal conductivity between first heating and second heating cycle [17]. Since it is unlikely that the gypsum board will be reused after a fire, it is reasonable to assume that the gypsum board will be at his first heating cycle. Therefore the conductivity of type x gypsum board will be taken as presented in the Figure 9 [17].

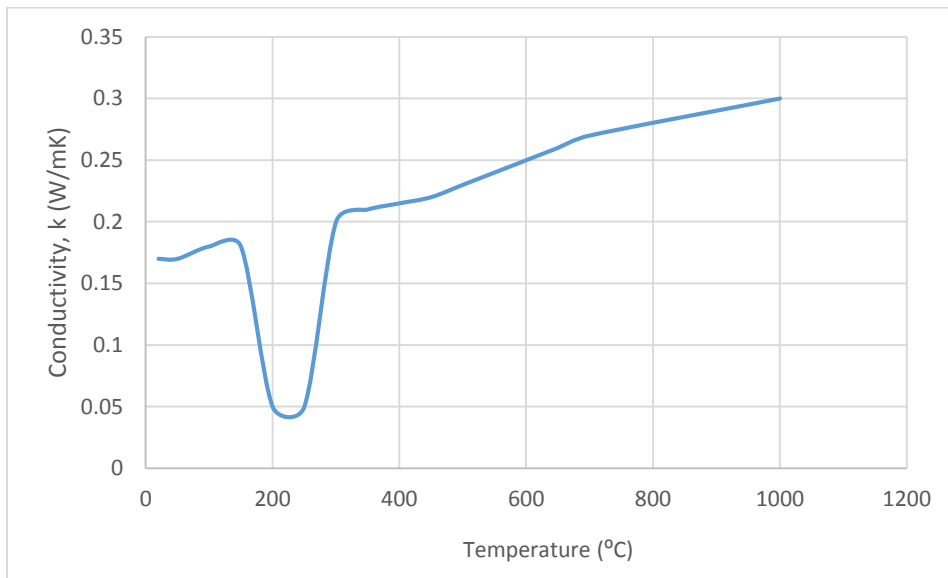


Figure 9: Conductivity of gypsum type X

5.1.2 Thermal capacity

The energy needed to dehydrate the gypsum has a direct effect on the gypsum board thermal capacity. This results in peaks at the moment where the dehydration reaction occurs. The tests from NIST shows relatively the same peak magnitude for different types of gypsum board tested [17]. The resulting specific heat which will be used in the models is presented in Figure 10.

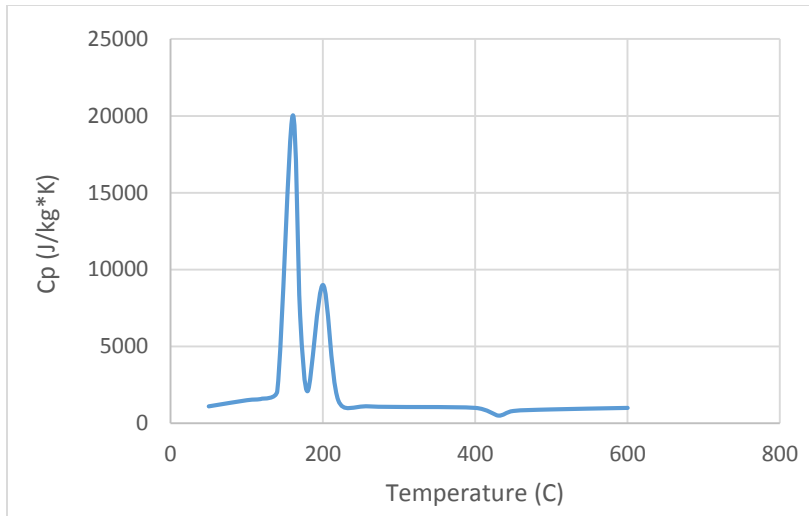


Figure 10: Specific heat of gypsum board type X

5.1.3 Density

At elevated temperatures, gypsum shrinks, test shows that at temperatures above 700°C, shrinkage rapidly increases. Also, experiment indicates that gypsum board loses its mechanical flexibility at about 400°C, and gradually loses its strength starting at about 500°C. Furthermore, when the gypsum board reaches temperature of 700°C, it loses all its strength. Those results suggest that screws should be able to keep gypsum board fixed to the walls for gypsum board's at temperature below 400°C and that it would tend to pull out from the screws at temperatures ranging between 600°C and 700°C [7].

In the series of tests done by NIST [17] the density of gypsum board and its mass loss was investigated. The initial density for gypsum type X is: 711kg/m³. As the temperature of the boards increases the gypsum board loses part of its mass. This occurs due to the crystallised water that evaporates. The results show that the density of gypsum boards changes significantly when the temperature increases. The mass loss was measured and is plotted as a function of temperature and shown in Figure 11. Increase of temperature also affects the size of gypsum board. Indeed, the increase of temperature in gypsum is associated with a contraction of its size, the data found for the gypsum X is presented in Figure 11. This has an effect on the opening of the fire barrier since as the board contracted it let place to gap where combustible gas can infiltrate.

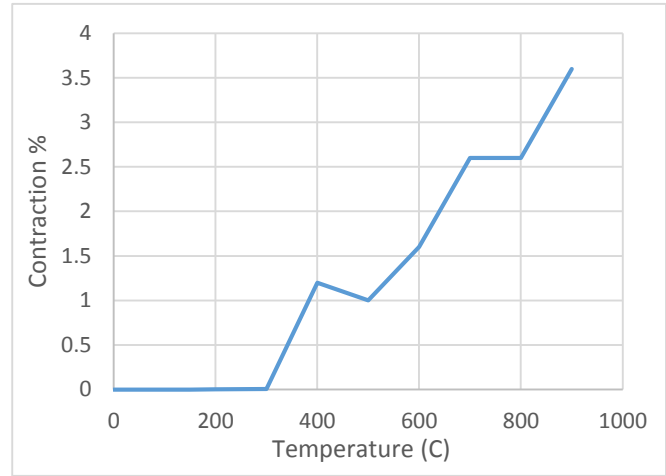
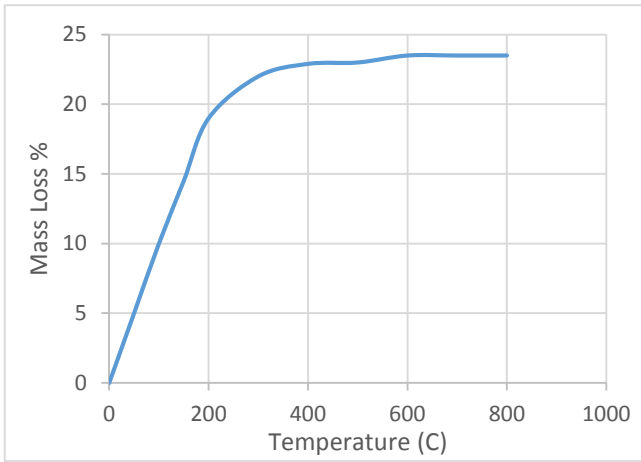


Figure 11: Mass loss of gypsum board type X and Contraction of gypsum X

With the combine effect of mass loss and contraction it is possible to estimate the change of the initial density with the increase in temperature.

$$\rho(T) = \frac{m_i - m_i * \% \text{ mass loss } (T)}{v_i - v_i * \% \text{ contraction } (T)} \quad (22)$$

The density found from the data NIST is presented in Figure 12.

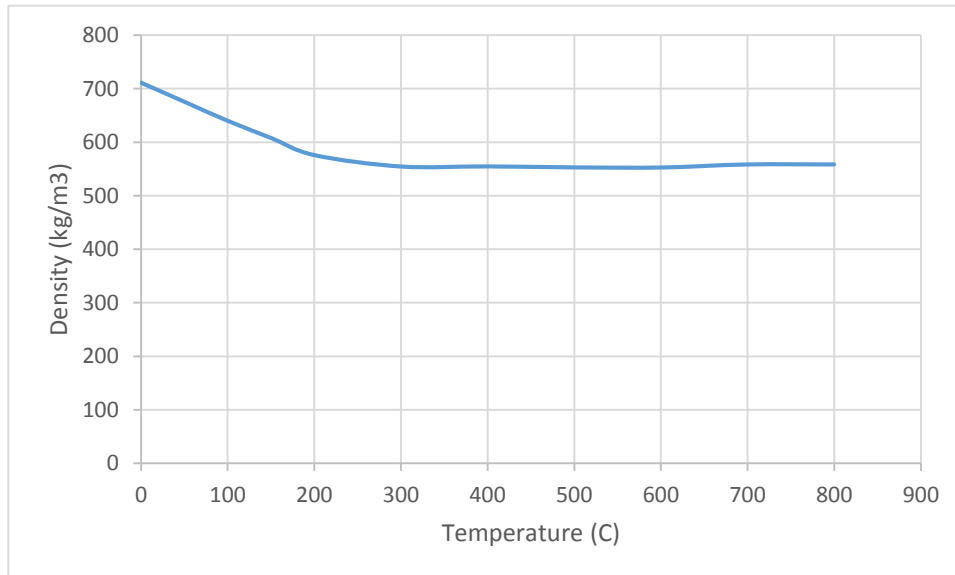


Figure 12: Change of density of gypsum type X

5.2 Thermal properties of insulation

In fire barriers, insulation can be used to delay the temperature rise on the unexposed side of the structure this can increase the FRR of the barrier. This study will focus on the use of stone wool and glass fiber wool, which are two insulation materials widely used in steel-framed walls [1].

5.2.1 Conductivity

Given sufficient time under heat, some materials undergo physical and chemical changes, which results in bonding reduction of the material and removal of successive thin layers from its surface. This process is referred to as ablation [18]. Ablation causes a reduction of the cross-sectional thickness of insulation material and therefore an increase of the heat flux across the insulation. Finite element programs such as ABAQUS, do not allow the user to simulate the change in thickness of the insulation with time. Therefore, ablation can be taken into account inside the thermal properties of materials. Past researches, simulate the effect of ablation by increasing the values of thermal conductivity with the increase of temperature [19]. Thermal conductivities as a function of temperature with consideration of ablation, can be found by the following equations [19].

Stone wool:

$$k = 0.25 + 0.00009T \quad \text{for } 20^{\circ}\text{C} \leq T \leq 550^{\circ}\text{C} \quad (23)$$

$$k = -1.1385 + 0.0026T \quad \text{for } 550^{\circ}\text{C} \leq T \leq 1200^{\circ}\text{C} \quad (24)$$

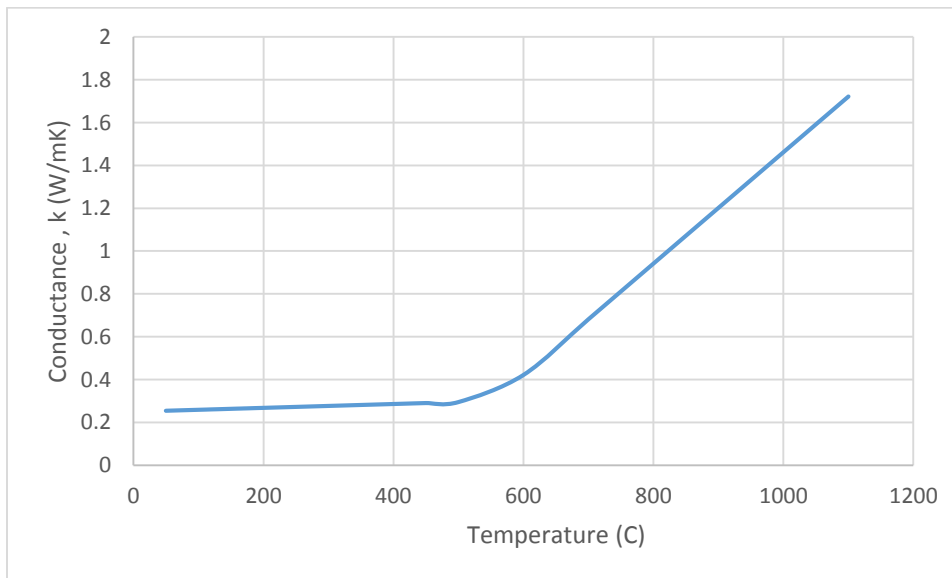


Figure 13: Conductivity of stone wool

Glassfiber:

$$k = 0.5 + 0.0002T \quad \text{for } 20^{\circ}\text{C} \leq T \leq 600^{\circ}\text{C} \quad (25)$$

$$k = -7.8 + 0.014T \quad \text{for } 600^{\circ}\text{C} \leq T \leq 700^{\circ}\text{C} \quad (26)$$

$$k = -0.08T - 54 \quad \text{for } 700^{\circ}\text{C} \leq T \leq 800^{\circ}\text{C} \quad (27)$$

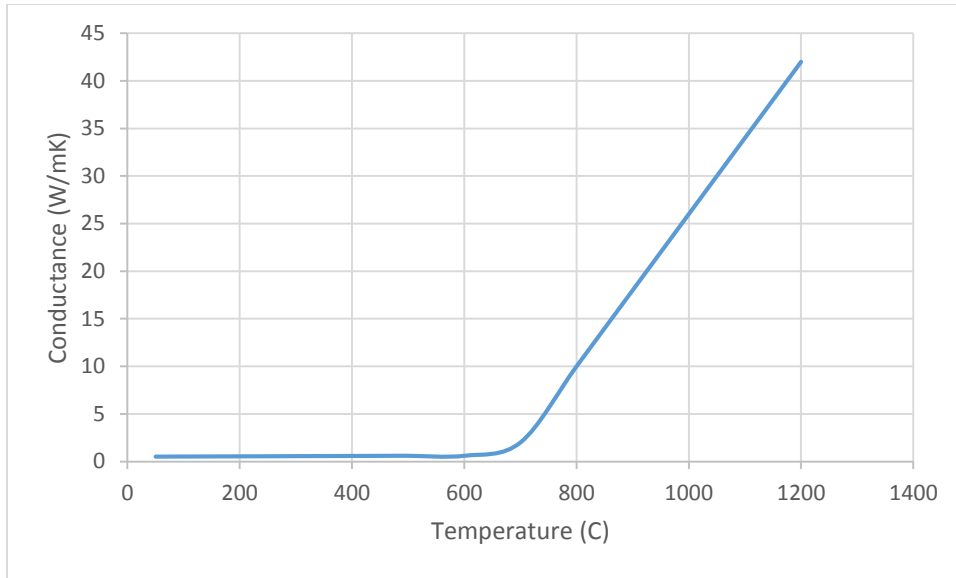


Figure 14: Conductivity of glass fiber wool

5.2.2 Thermal capacity

The specific heat of thermal insulation was found from experimental work [19]. This thermal property was reported to fluctuate very little with the increase of temperature [19]. The value of Stone wool and Fiber glass wool found are presented in Table 2.

	Stone wool	Fibre glass wool
Thermal capacity (J/(kg° C)	850	900

Table 2: Thermal capacity of insulation

5.2.3 Density

The density for insulation material will be assumed constant with increase of temperature because ablation is already considered in the conductivity parameter. The density used for insulation is presented in Table 3 [19].

	Stone wool	Fibre glass wool
Density (kg/m ³)	100	35

Table 3: Density of insulation

5.3 Thermal properties of steel

In light-weight partitions, construction studs are used for structural purpose. The wall needs to maintain its stability, so studs are used throughout the length of the wall to allow the gypsum board to be mounted. Studs are generally made of wood or steel and for this project the use of steel studs will be investigated. Steel is very poor insulator, therefore it is possible that it will create a thermal bridge through the partition wall. Thermal bridges create a highly conductive parallel path through the insulation layer and allow the heat to pass to the unexposed side of the wall. Since thermal resistance of wall is an important criterion in the furnace test, it is essential that the effect of studs is considered in the models.

5.3.1 Conductivity

The conductivity of steel is temperature dependent and can be found by the following equations [20]:

$$k = 54 - 0.0333T \text{ for } 20^{\circ}\text{C} \leq T \leq 800^{\circ}\text{C} \quad (28)$$

$$k = 27.3 \text{ for } 800^{\circ}\text{C} \leq T \leq 1200^{\circ}\text{C} \quad (29)$$

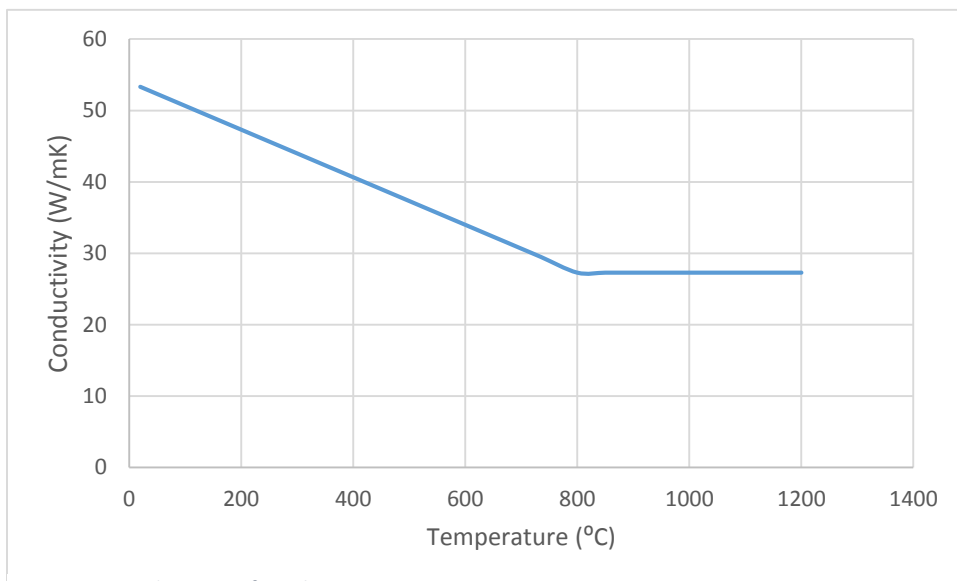


Figure 15: Conductivity of steel

5.3.2 Thermal capacity

The specific heat of steel is also temperature dependent and can be found by the following equations [20]:

$$C_p = 425 + 0.773T - 1.69 \times 10^{-3}T^2 + 2.22 \times 10^{-6}T^3 \quad \text{for } 20^\circ\text{C} \leq T \leq 600^\circ\text{C} \quad (30)$$

$$C_p = 666 + \frac{13002}{738-T} \quad \text{for } 600^\circ\text{C} \leq T \leq 735^\circ\text{C} \quad (31)$$

$$C_p = 545 + \frac{17820}{T-731} \quad \text{for } 735^\circ\text{C} \leq T \leq 900^\circ\text{C} \quad (32)$$

$$C_p = 650 \quad \text{for } 900^\circ\text{C} \leq T \leq 1200^\circ\text{C} \quad (33)$$

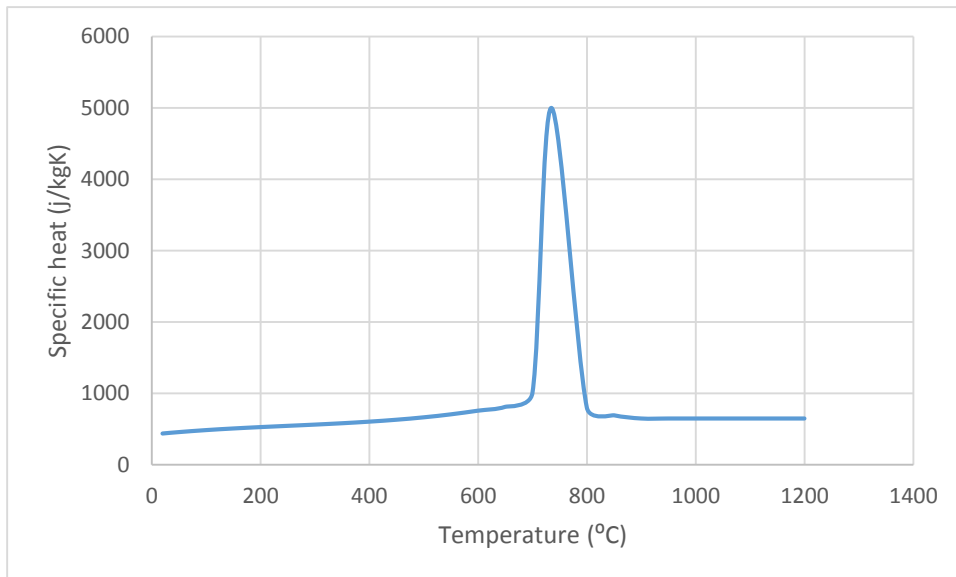


Figure 16: Specific heat of steel

5.3.3 Density

The density of steel can be assumed constant with changes in temperature, at 7850kg/m^3 [20].

5.4 Thermal property of air cavities

When air is enclosed in cavities of limited size, heat transfer through a partition is caused by radiation and conduction. However, due to air high resistance to heat conduction, the main heat transfer parameter to consider, for cavities, is in the form of radiation [8]. The conductivity of air can be found in different tables and depends on the temperature. At ambient temperature

(20°C) conductivity is found at values around 0,026W/m*K and for temperature such as 600 °C at around 0.35W/m*K [21]. The density of air also depends on the temperature and is depicted in Figure 17 [21].The heat transfer by radiation in the cavity is important to consider and it depends on the emissivity of the hot and cold surfaces. The assumed emissivity of the different layer is shown below [22].

Layer	Emissivity
Gypsum	0.8
Insulation	0.8

Table 4: Emissivity of material

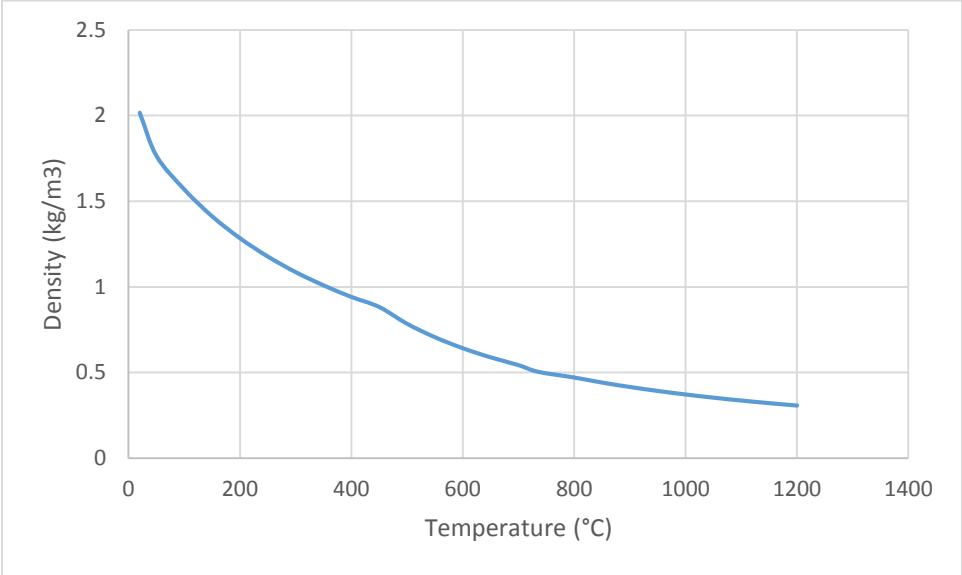


Figure 17: Air density change with temperature

6 Methodology

6.1 ABAQUS Procedure

The heat transfer which occurs in a furnace test is very complex. To investigate the effect of a reduced thermal insulation on the insulation criterion, it is necessary to have recourse to finite element method. ABAQUS allows to solve transient heat transfer on various type of construction. This can be achieved via defining a transient “Heat transfer” step in the model. The objective of this analysis is to obtain the temperatures on the unexposed side of the wall after the sample is subjected to the ISO-834 standard fire.

6.1.1 Geometry and Material Properties

The geometry of the model is based on the types of construction described in section 0. Figure 18 shows the construction of the light gauge steel frame using ABAQUS.

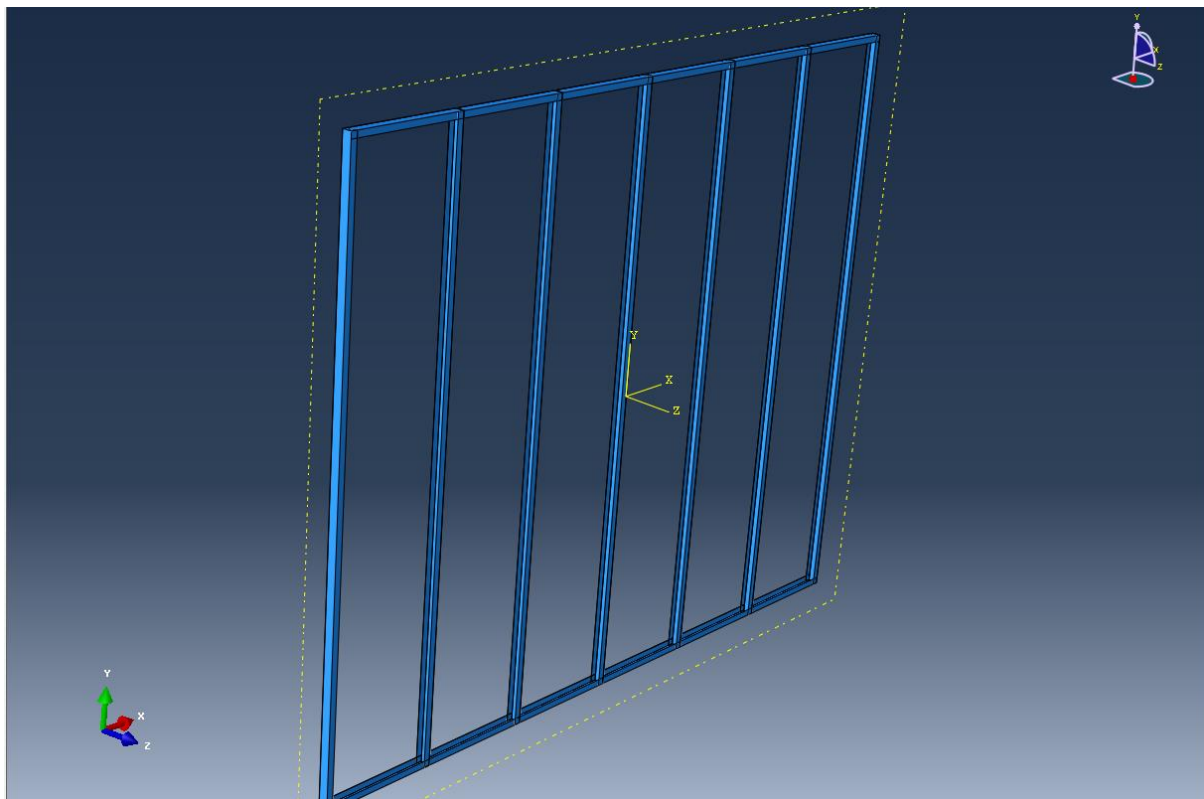


Figure 18: Fire barrier metal frame

The thermal properties of materials used in the model correspond to the one presented in section 5. ABAQUS allows defining thermal properties as function of temperature.

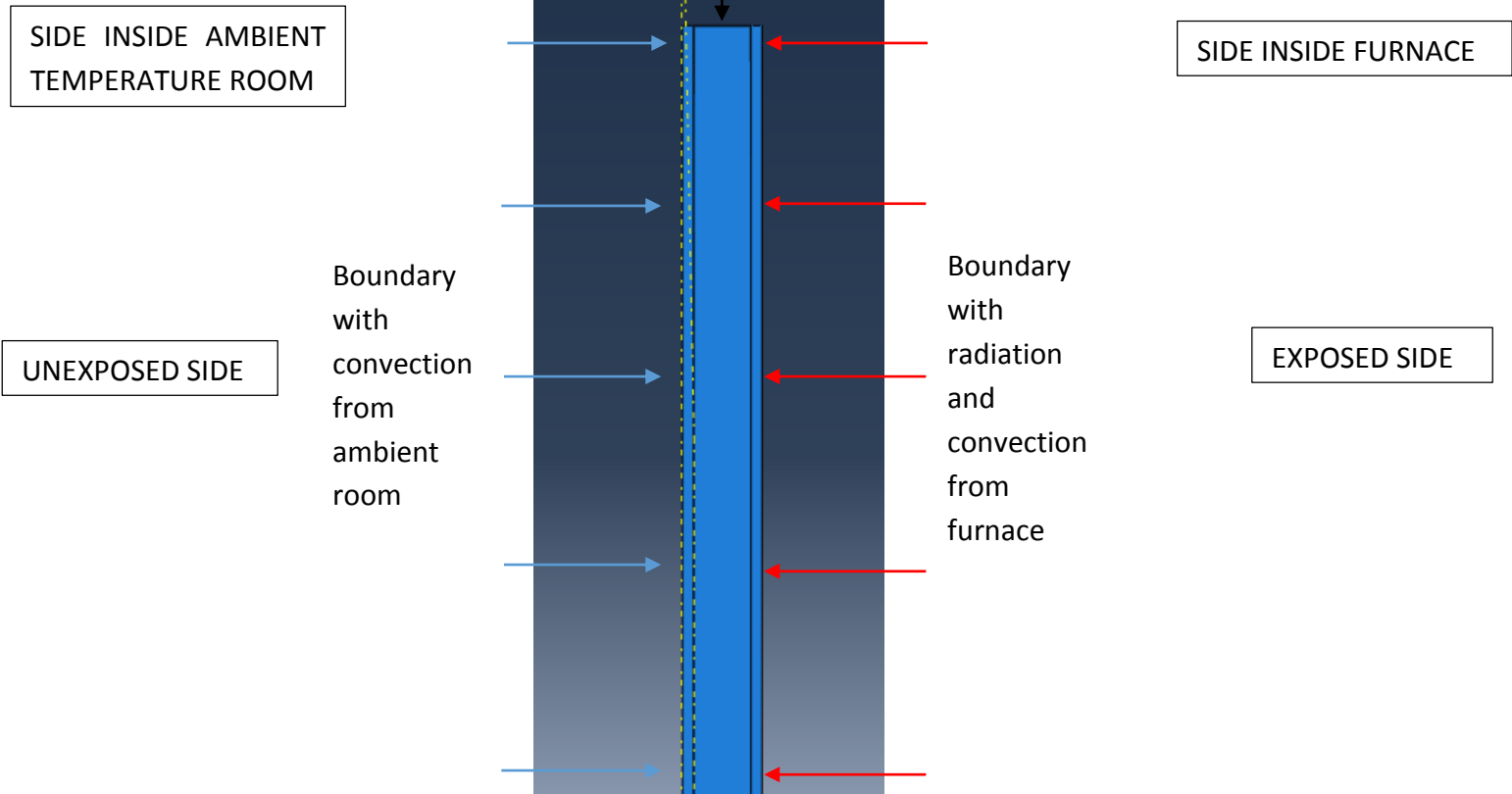
The different scenarios investigated required some changes to the original model. To test the effect of insulation, a layer of insulation filling the whole cavity was created. The insulation was in contact with the two layers of gypsum board. The thermal properties of fiberglass and

stone wool were used. Then, the thickness of the insulation was reduced to 75%, 50% and 25%, while keeping the same cavity depth. This was done to see how the FRR would change if less insulation was used in the construction of the partition, compare to the original tested in the furnace. Also, when the insulation thickness is reduced by half, two models were created. One with the insulation located on the exposed side and one on the unexposed side, this allows seeing the worst case scenario. Then, different sizes of hole in the exposed gypsum board layer were added to the original wall insulated and non-insulated to investigate the effect of breaches in the gypsum layer located in the furnace. The holes dimension used were a large hole of 50mm radius and a small hole of 10mm radius. Also, partitions with hole through were modeled to investigate the effect of penetration in fire-rated partition. Again two holes were used, one large hole of 50mm radius and one small hole 10mm radius. Finally, to investigate what would happen if at one specific location insulation would be missing, two partitions insulated with stone wool were modeled with missing piece of insulation. Round missing pieces were used of 100mm and 50mm radius. The dimension of the different features used is assumed. Indeed, other size could have been used and investigate, however it is more probable that small holes and small missing pieces of insulation will go unnoticed compare to bigger one.

6.1.2 Initial and Boundary Conditions

The initial temperature of the boards was assumed to be uniform and equal to 20°C. Convection and radiation boundary conditions were defined for the surface of the wall located inside the furnace while only convection boundary conditions were defined for the surfaces of the wall outside the furnace. The boundary conditions were set using 'Interactions'. The interaction types, used for convection and radiation boundary conditions, were 'Surface film condition' and 'Surface radiation to ambient', respectively. The gypsum board on the furnace side was exposed to the standard fire temperature, and the gypsum board on the room side was exposed to a constant temperature of 20°C. The effective emissivity from the fire at the exposed surfaces was set to 0.8 [10]. The convection heat transfer coefficients were assigned according to European code on fire interaction with structures [31], i.e. 4 W/m²K for the unexposed surface and 25 W/m²K for the exposed surface. The other surfaces, which were located inside the temporary construction, are considered fully insulated since in actual test a great amount of insulation must be used to prevent the wall from leaking via the supporting construction.

Perfectly insulated boundary



To investigate if the boundary conditions used in ABAQUS are appropriate, another simulation was performed. In this simulation the surface of the wall inside the furnace is exposed to the experimental heat flux given in section 2.4. Temperatures on the unexposed and exposed gypsum surfaces of the wall were measured. The following figures show the difference between the temperatures obtained using the two methods.

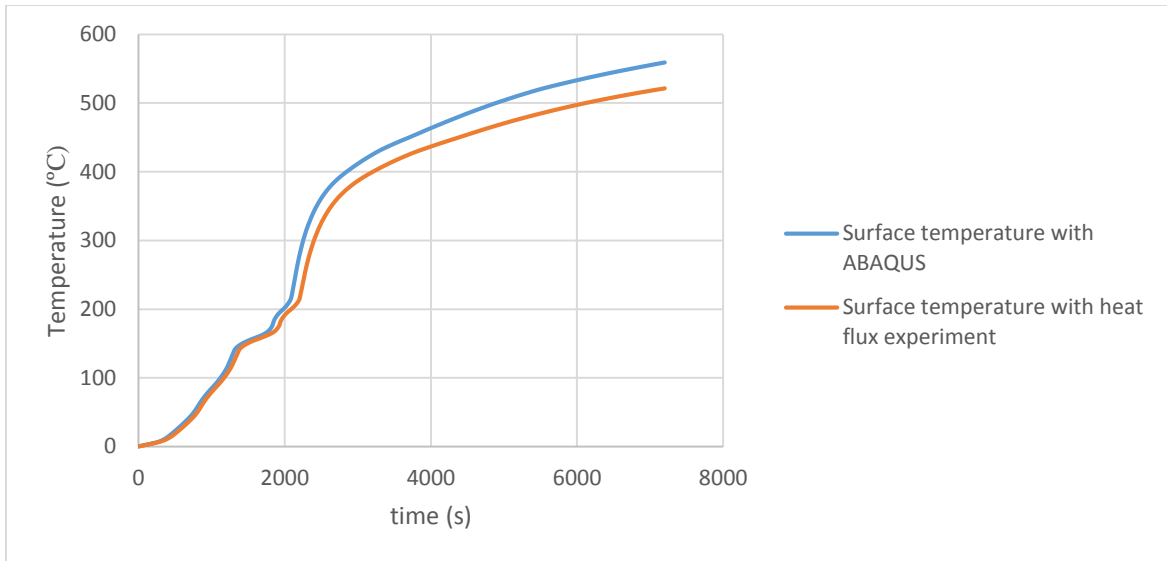


Figure 19: Unexposed surface temperature

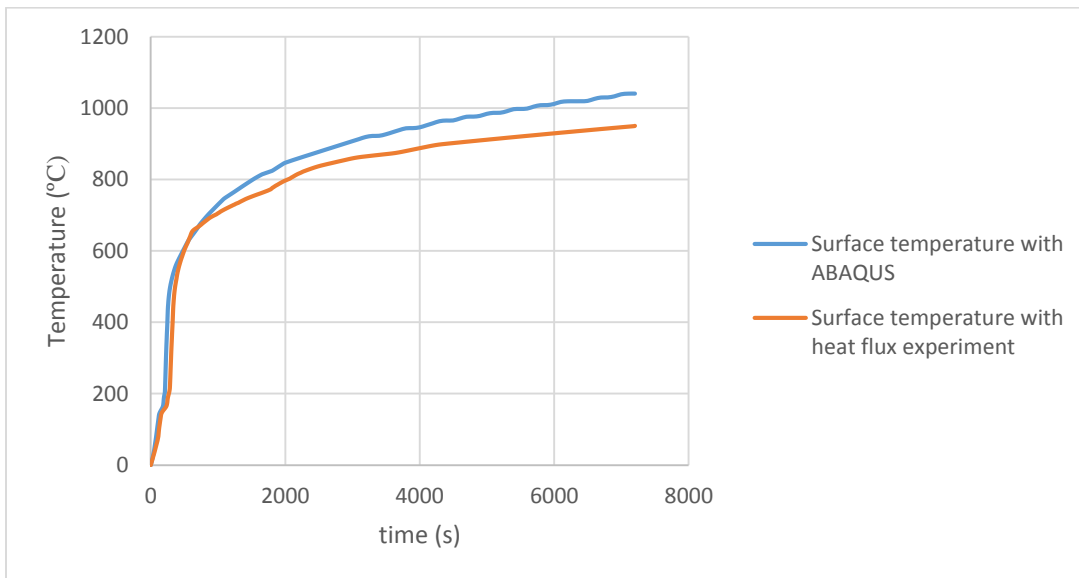


Figure 20: Exposed surface temperature

As we can see from the figures above, the modelling method used in the simulation gives slightly higher exposure temperature, but still quite similar. Therefore, the results should be considered to be conservative, especially since it is known that the ASTM E119 is also slightly more strict than the ISO 834 [12].

6.1.3 Interactions and assumptions

To accurately model the heat transfer inside the wall from the unexposed to the exposed surface different assumption were used. ABAQUS calculates heat transfer inside a building element with its thermal properties and conduction equation. In the model it was assumed that

the surface between different components of the wall in contact were at the same temperature. This was set using TIE interaction.

The cavity radiation was modeled with the interaction, SURFACE CAVITY RADIATION, for every scenario where a space inside the wall was not filled with insulation. ABAQUS estimate the heat transfer by radiation, in cavities, from the equation (37). The temperature and emissivity values come from the surfaces inside the cavity and F is the view factor which depends on the distance between the surfaces.

$$q''_{Cavity\ Radiation} = F\varepsilon\sigma(T_{S1}^4 - T_{S2}^4) \quad (37)$$

The conduction through air was modeled using the SURFACE TO SURFACE conduction interaction. This defines conduction between two surfaces by using the defined thermal conductivity only. This was used for every scenario where air cavity was present. Since the main heat transfer mode at elevated temperature when a cavity is present is radiation, it was assumed that the cavity do not heat up, but conduct heat through radiation and conduction. This allowed for simpler model and was the most conservative scenario. All the thermal properties defined in the section 5 were used.

6.1.4 Mesh and Element Type

For the heat transfer analysis, a standard heat transfer element type is chosen. In the ABAQUS there is no advantage in using higher order of elements than four node linear quadrilateral element, DC3D8 [30]. The number of elements is an important parameter to consider as the precision of the results will be greatly affected by this factor. The grid size across the thickness is not relevant since only the temperature at the surface is analyzed. To choose the optimum element size on the surface, a sensitivity study has been performed. For the analysis, the wall, insulated with stone wool, was selected with the following different mesh sizes:

Case a) mesh size: 0.1 m

Case b) mesh size: 0.05mm

Case c) mesh size: 0.03mm

The following figures show the difference between different grid sizes. It can be observed that the maximum temperature measured on the surface is seen from the case B (Figure 22) and does not change in case C, therefore it is not required to run simulation with a finer grid.

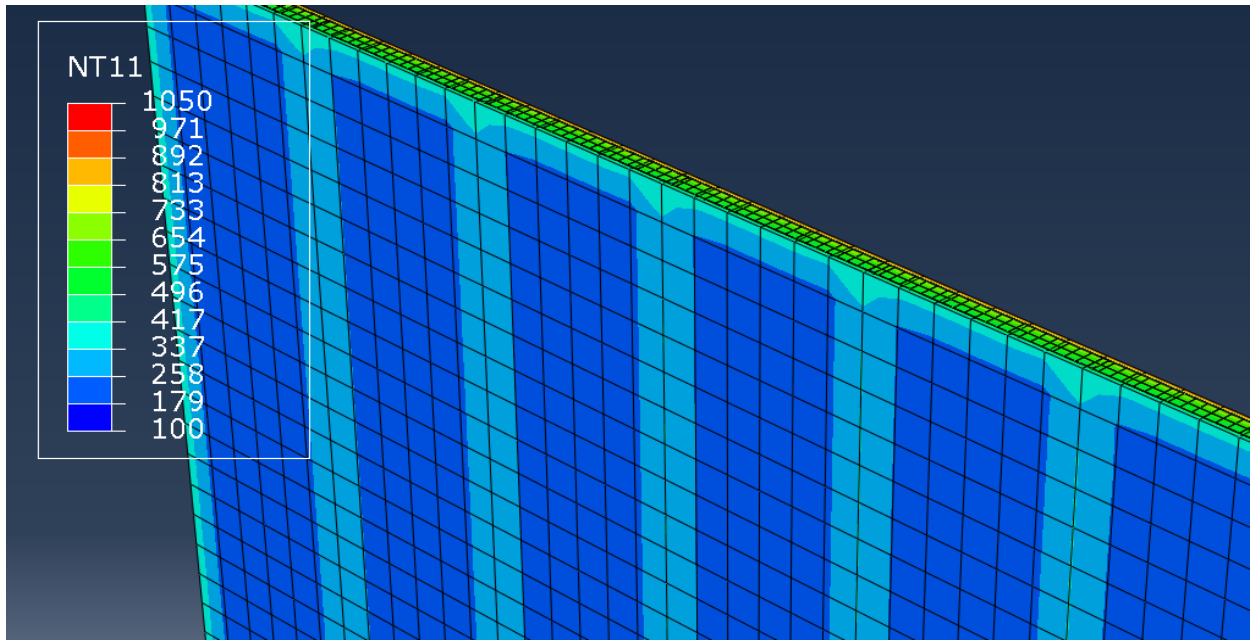


Figure 21: Temperature at the unexposed surface case a)

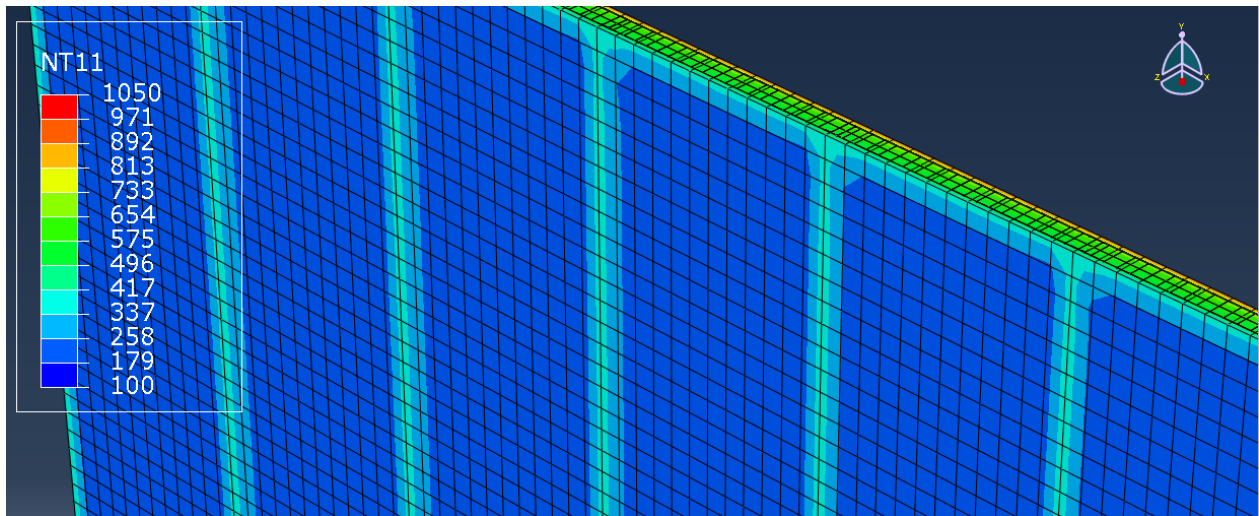


Figure 22: Temperature at the unexposed surface case b)

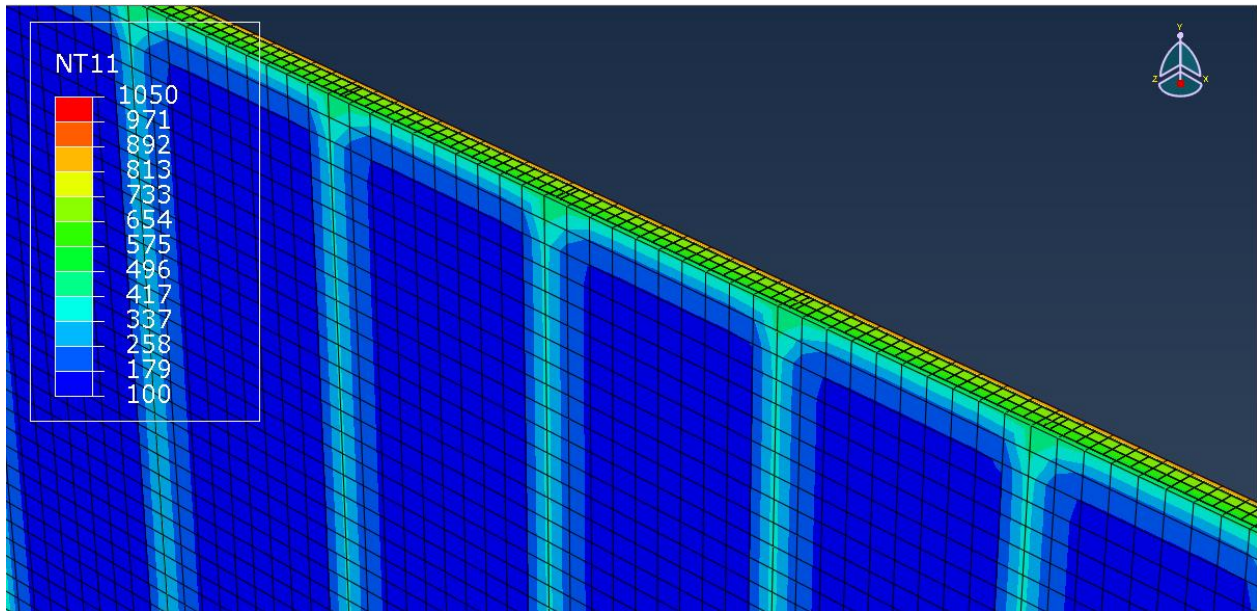


Figure 23: Temperature at the unexposed surface case c)

6.2 Validation of the FE model

The literature review allowed to find different experimental data on the FRR of LSF when tested in a furnace test based on codes. The literature review focused on LSF construction with the use of stone wool, fiber wool insulation and empty cavity. The FRR obtained for different test samples were compared with the results obtained with numerical model built with ABAQUS. A model, corresponding to each experimental sample, was produced in order to validate the modeling technique used in ABAQUS. Table 5 depicts the results obtained for the numerical model and the experimental data as well as the relative error of the numerical model. Some experimental FRR were given with respect to the criterion where the average temperature increased above the initial temperature by more than 140°C (T_{140}). Other used the criterion where an increase at any location (including the roving thermocouple) above the initial average temperature was more than 180°C (T_{180}). The information about the thickness of gypsum and insulation and the type of insulation used is given in Table 5. However, for every simulation the thermal properties used were similar to ones presented in section 5.

For example the assembly: 1 x 2 - 15.9mm gypsum 90mm air cavity, can be interpret as 1 layer of 15.9mm gypsum board exposed in the furnace – 2 layers of 15.9mm gypsum board on the cold side – Steel studs of 90mm width – Wall cavity 90mm width non insulated.

Type of assembly	Experimental test			ABAQUS	
	FRR (min)	Criterion	REF	FRR (min)	Relative error
1 x 1 - 9.5mm gypsum + 50mm Stone wool insulation	42, 41	T ₁₈₀	[32]	45	+8%
1 x 1 - 12.5mm gypsum 50mm air cavity	38, 33, 34, 33, 36, 36	T ₁₈₀	[32]	31	-11%
2 x 2 - 12.5mm gypsum 50mm air cavity	78, 77, 89, 91	T ₁₈₀	[32]	89	+6%
2 x 2 - 15.9mm gypsum 90mm air cavity	52 min	T ₁₄₀	[33]	37	-28%
1 x 2 - 15.9mm gypsum 90mm air cavity	66 min	T ₁₄₀	[33]	78	+20%

Table 5: Experimental and simulation results

The Table 5 shows the results of the validation test with ABAQUS. It is possible to see that the relative error obtained is generally low, ranging from 6 to 28%. The Wall with an empty cavity yields good results if compared to the data taken from the passive fire safety document from Ghent University [32]. When the model is compared with the results of SULTAN [33], the findings seems to be more confusing. The error could come from the different standard used in the experimental test, different material properties or the testing methods. However, results in the range of 6-28% are deemed acceptable considering that experiment results can differ by as much as 15% and maybe more.

6.3 FDS Procedure

To investigate the effect of leakage on the integrity criterion a furnace test is reproduced using the CFD tool FDS. For this purpose, the wall furnaces of the NRCC, was reproduced as precisely as possible with FDS, see Figure 24, from data [23], [11]. However, due to lack of information available, assumptions were needed. Also, the furnace was modeled to cope with the requirement of the European standard EN-1301-6, not the ASTM E119. This means that the ISO-834 temperature-time curve was used in the simulation. All parameters, assumptions and dimensions used to replicate the furnace test with FDS will be presented in this section.

6.3.1 Dimensions and materials

The furnace dimensions are 3600 mm wide by 3100 mm high by 600 mm deep. The furnace walls were lined with 38-mm-thick fibrous ceramic blanket. The overall dimensions of the sample were 3600 mm wide by 3100 mm high. The fire barrier sample used correspond to the type B construction, presented in section 4. To simulate the integrity criterion, a cotton pad was modeled and positioned in front of the leakage area. The thermal properties presented in section 5 were used for all material related to the fire-rated barrier. For the thermal properties of the ceramic blanket, data from the work of Sultan [11] were used. For the cotton pad generic thermal properties were used from engineering toolbox [24], [25], [26]. The properties of the cotton pad and the ceramic blanket are presented in Table 6. The Temperature of ignition of the cotton pad was assumed to be at 400 °C as experimental results shows [12].

	Ceramic fibre blanket	Cotton Pad
Thermal conductivity (W/mK)	0.04	0.23
Specific heat (J/kgK)	1150	1339
Density (kgm³)	160	150

Table 6: Thermal properties of ceramic blanket

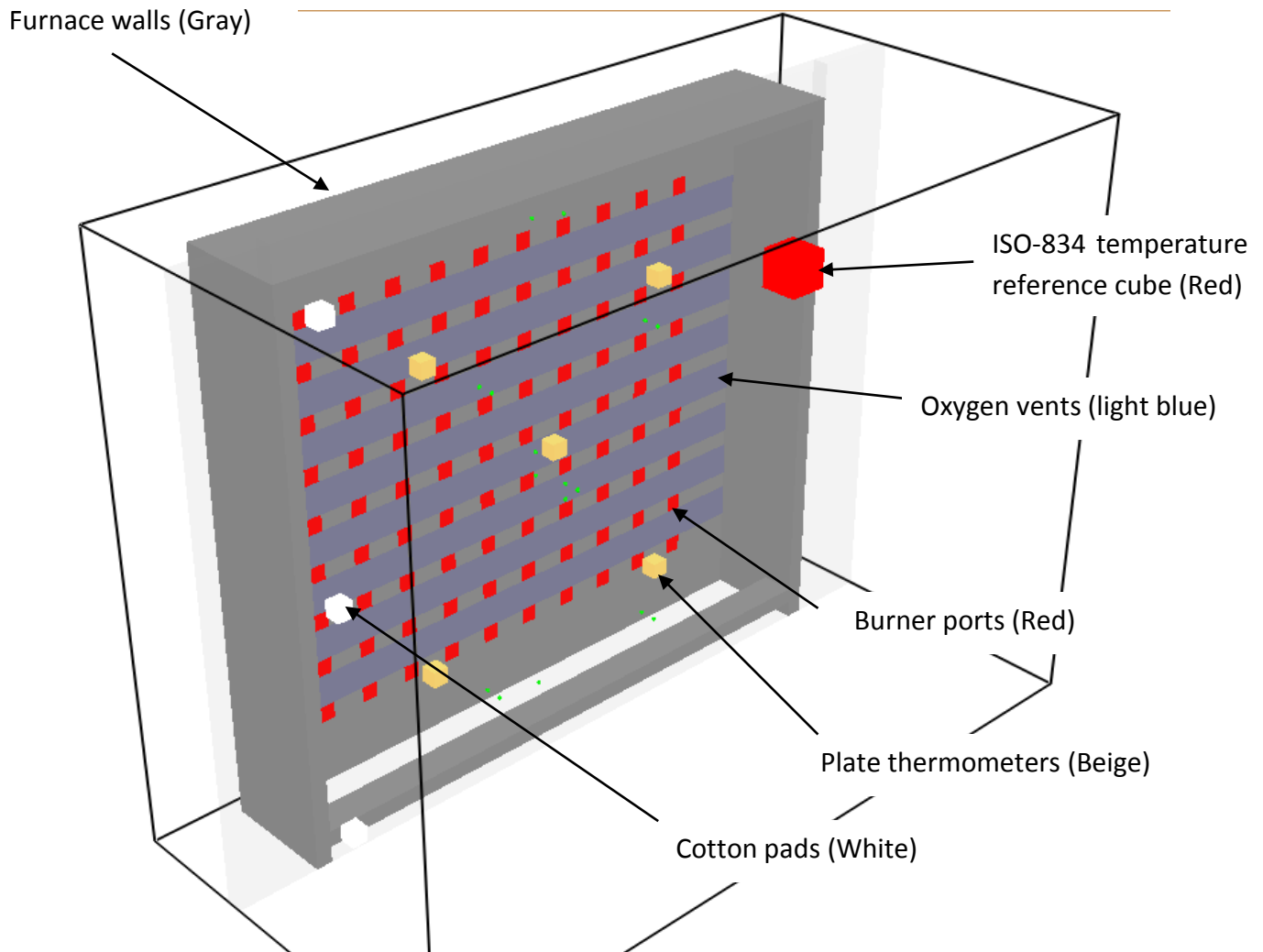


Figure 24: Furnace modeled with FDS

6.3.2 Temperature

Furnaces use premix air and gas burners, using different types of combustible, in order to heat up the space at the required temperature. The NRCC wall furnace, which was used as model and validation (section 2.4), has 90 propane burner ports. Those were implemented in the model as 90 vents of one grid size area with a set HRRPUA. Propane was used as fuel with the properties presented in Table 7 [27], [28]. One issues with FDS is that it is not possible to simulate pre-mixed air-fuel burners. In order to overcome this issue vents were added close to the burner ports from which air is introduced inside the furnace. Those vent are controlled, in FDS, to keep the oxygen level between 15 and 20 %. The air is introduced inside the furnace at the temperature of the ISO-834 temperature time curve, in order to reduce the extra heat necessary to warm the new air. Another major issue when it comes to modelling a fire resistance test with FDS, is to keep temperature in the furnace within the range required by the code. This was done by setting up a control system which open or close burner ports depending on the temperature inside the

furnace. The temperature is measured with plate thermometer modelled as required by the standard [2]. The plate thermometers temperature is compared to a 1 cell thick reference cube at the temperature of the standard fire. The burner ports were associated to the local plate thermometer and the ports closed if the plate thermometer temperature exceeded the reference cube's temperature and opened if the plate thermometer temperature was less than the reference cube's temperature.

Fuel	Radiative fraction (%)	Heat of combustion, ΔH_c (kJ/kg)	Soot Yield (kg/kg)
Propane	0.3	46450	0.01

Table 7: Properties of propane

6.3.3 Pressure

As shown in the literature review, pressure difference is very important when it comes to leakage between two compartments. Therefore, it was necessary to measure and control the pressure inside the furnace in order to keep it inside the required boundaries. The code EN-1301-6 requires that the neutral plane inside the furnace should be located 0.50 m above the bottom of the test sample and that the pressures at the top of the test sample should not exceed 20 Pa. However, other experts suggested that the neutral plane in furnace test should be maintained at the bottom of the test specimen and that the pressure in the furnace is more representative of the pressure exerted by a real fire [12]. This was estimated at 28 Pascal in section 3.3. Because of the complexity required to move the neutral plane and to keep the pressure at 20 Pascal, in FDS, the boundaries selected, for pressure at the top of the furnace, was set between 28 and 30 Pascal. Indeed, the extra air inserted inside the furnace to fix the pre-mixed burner problem, caused an increase of the internal pressure of the furnace. This made it hard to keep the pressure, inside the furnace, at 20 or even 30 Pascal. To minimize the pressure at the top of the furnace, a vent at the bottom of the furnace and a controlled vent at the top of the furnace were created. The controlled vent opened if pressure increased more than 30 Pascal and closes when pressure passed under 28 Pascal.

6.3.4 Leakage

There are different ways to model leakage with FDS, but since the leakage area is usually very small it was not possible to define a leak directly on the numerical mesh. A better way to handle leakage was by exploiting the HVAC model of FDS. With this feature, leakage can be presented as a large HVAC vent that connects via a very small duct linking both sides of the wall. This allows for the leakage area to be distributed over the vent area. Leakage in the simulations was modeled in three ways, with the area of leakage distributed over all the joints of the wall, over only one joint or localized in a small area. To do this, the vent area was distributed as

presented in the Figure 25, Figure 26 and Figure 27. Where blue color represent the location of the leakage through the wall.

Failure of integrity was investigated for different location on the sample: at the top, at the bottom and in the middle of the furnace. The volume flow, through a leak of certain area is given by a form of the equation (16), with the friction flow coefficient assumed to be 1 [27].

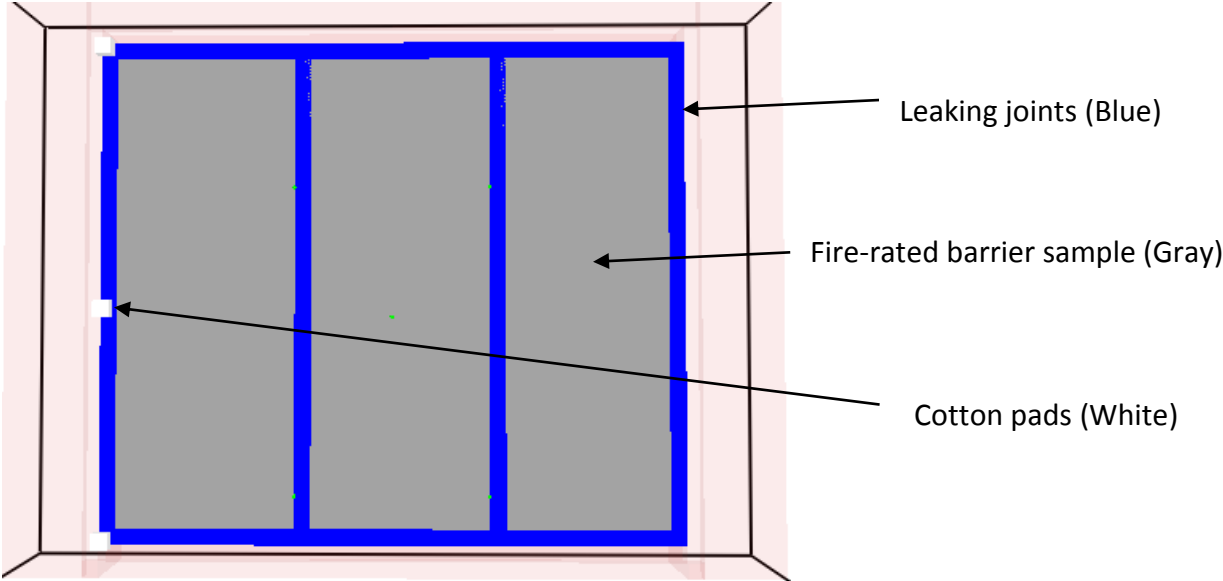


Figure 25: Leakage distributed at every joints

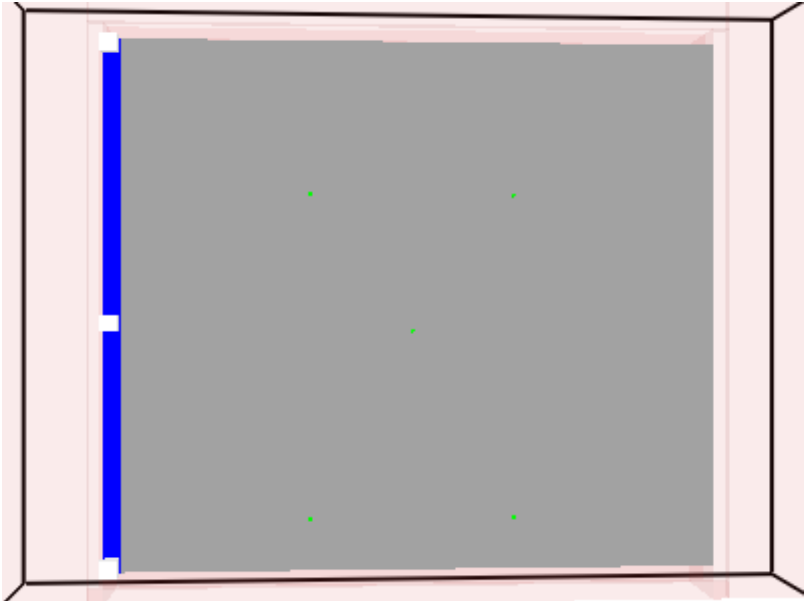


Figure 26: Leakage distributed on one side

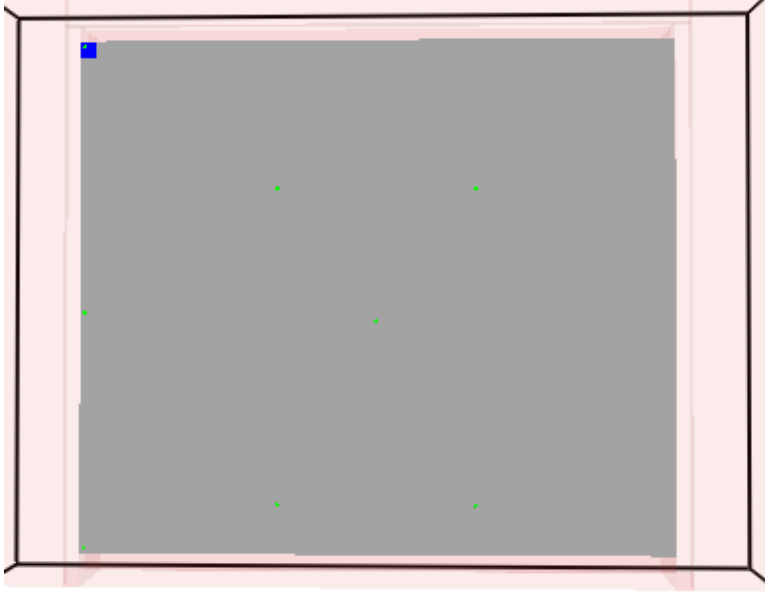


Figure 27: Leakage localized at the top

6.3.5 Grid selection

The duration of the fire resistance test is 7200 seconds, consequently the computational time for every simulation to be high. To decrease this time, a coarse grid was applied. However, this had an impact on the precision of the results due to increased averaging. For simulations involving buoyant plumes, a measure of how well the flow field is resolved can be used [27]. Even though, a perfect buoyant plume is not exactly used this method shall be used as a gauge to verify the grid size. This method use the characteristic fire parameter calculated with the following equation:

$$D^* = \left(\frac{\dot{Q}_{Fire}}{\rho_{\infty} c p_{\infty} T_{\infty} \sqrt{g}} \right)^{\frac{2}{5}} \quad (34)$$

Then the characteristic fire parameter shall be compared with the grid size (dx):

$$\frac{D^*}{dx} \quad (35)$$

The U.S. Nuclear Regulatory Commission used a range of $4 \leq \frac{D^*}{dx} \leq 16$ for their validation studies [29] and Danish best practice use $10 \leq \frac{D^*}{dx}$. In the simulation the HRR increases and reaches a peak located around 5500 kW, for a grid size of 100 cm, this yield $\frac{D^*}{dx} \sim 19$, which is over the range required by the U.S. Nuclear Regulatory Commission and as required by the Danish best practice.

6.4 Validation of the CFD model

In this project the furnace model will be validated against the code EN 1363-1 and experimental data. EN 1363-1 regulates how and what should be done during the furnace test so that the fire resistance test is deemed valid. Also, the heat flux at the boundary of the sample from the furnace will be compared to experimental data corresponding to the similar furnace.

6.4.1 Furnace Temperature

The Heating curve inside the furnace shall be controlled so that the average temperature of the furnace derived from the thermocouples follows the following relationship:

$$T = 345 \log_{10}(8t + 10) + 20 \quad (36)$$

Where

T - is the average furnace temperature, in degree Celsius;

t - is the time, in minutes.

The code stipulates that the percentage deviation in the area of the curve of the average temperature recorded by the specified furnace thermocouples versus time from the area of the standard temperature/time curve shall be [2]:

15%	<i>for</i> $5 < t \leq 10 \text{ min}$
$(15 - 0.5(t - 10))\%$	<i>for</i> $10 < t \leq 30 \text{ min}$
$(5 - 0.083(t - 30))\%$	<i>for</i> $30 < t \leq 60 \text{ min}$
2.5%	<i>for</i> $t > 60 \text{ min}$

The Temperature inside the furnace according to the code EN 1363-1 is presented in Figure 28.

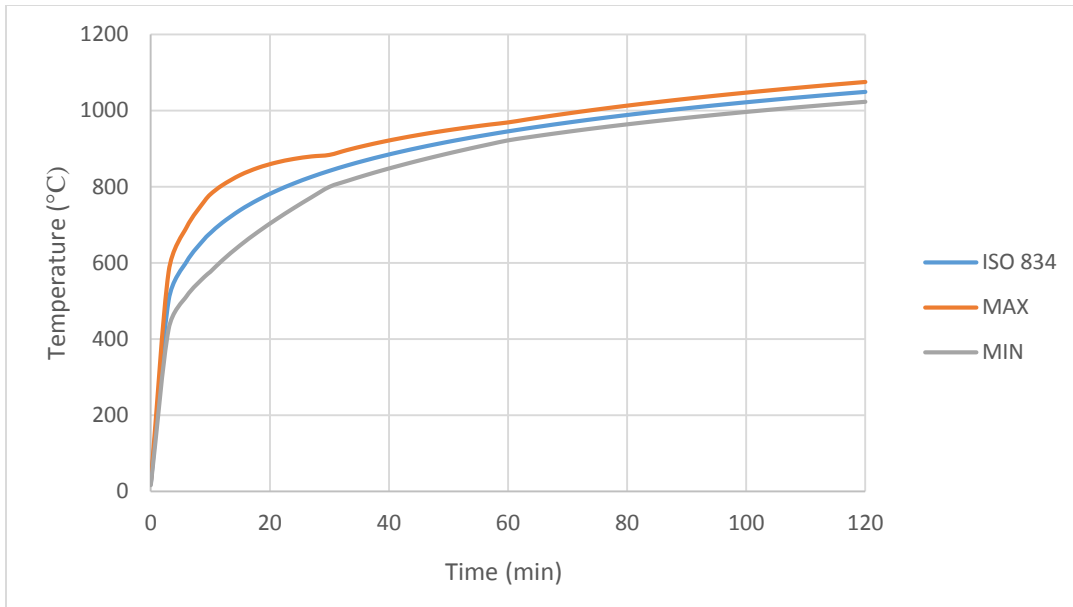


Figure 28: Acceptable temperature in the furnace according to EN 1363-1

The average temperature measured inside the FDS furnace by the plate thermometers is shown in the following graph. It is possible to see that the temperature follows the requirement of the code. The plate thermometers used are located as presented in Figure 31. It is possible to see that the temperature is within the requirement of the code.

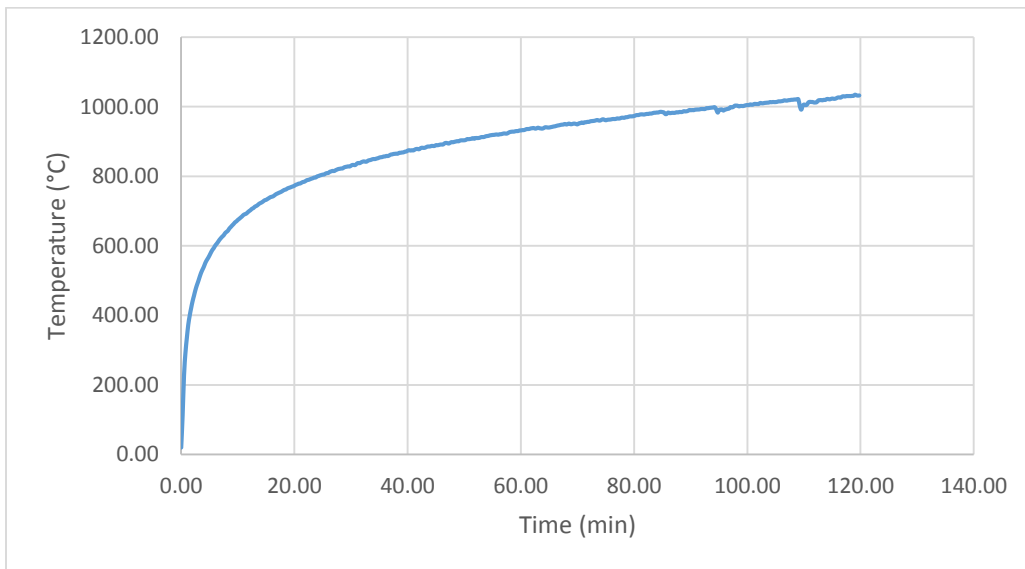


Figure 29: Average temperature versus time measured on the surface of the wall sample in FDS

6.4.2 Furnace pressure distribution

As mentioned in section 6.3.3, the pressure at the top of the furnace needs to stay at approx. 30 Pascal. The figure below shows the average pressure measure at the top and in the middle of the furnace.

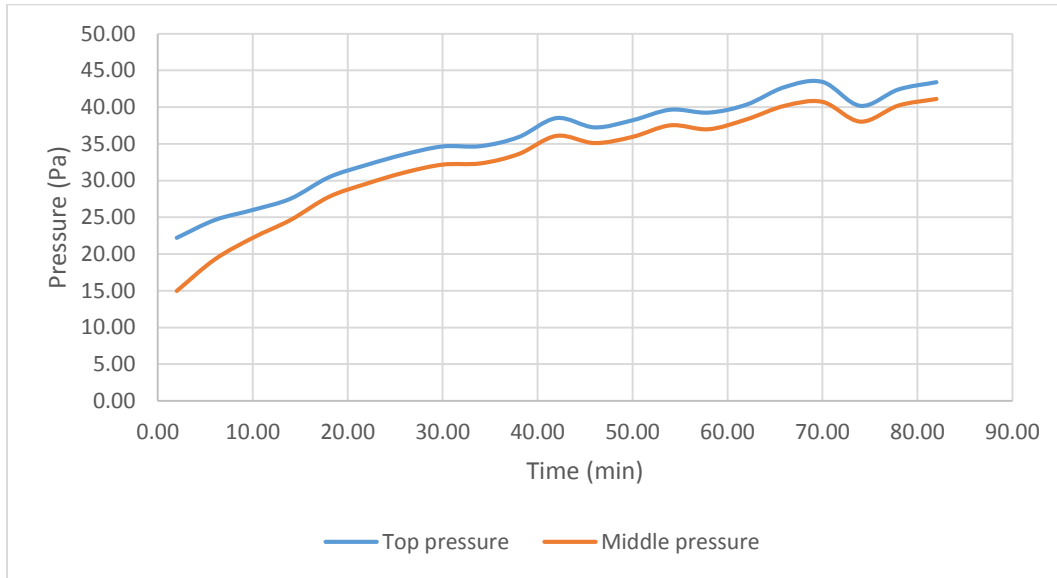


Figure 30: Pressure profile in the FDS simulation

It is possible to see that the pressure is slightly over the expected 30 Pascal so this will causes the volume flow of hot gases through the partition to increase. The impact of this pressure difference will be discussed further in the results section.

6.4.3 Heat Flux at sample

The total heat flux from a furnace to a sample, presented in section 2.4, will be compared to the one obtained during the simulation. The heat flux is measured by 5 gauge heat flux devices, similar to the one used in the experiment. These are located at the surface of the sample in FDS as seen Figure 31 [11]. The heat flux measured is presented in the Figure 32.

It is possible to see in the graphs that the average heat flux measured in FDS is comparable to the one obtained by SULTAN, presented in Figure 3. Although the heat flux measured in FDS is slightly higher, an increase of 10% in the heat flux was noticed.

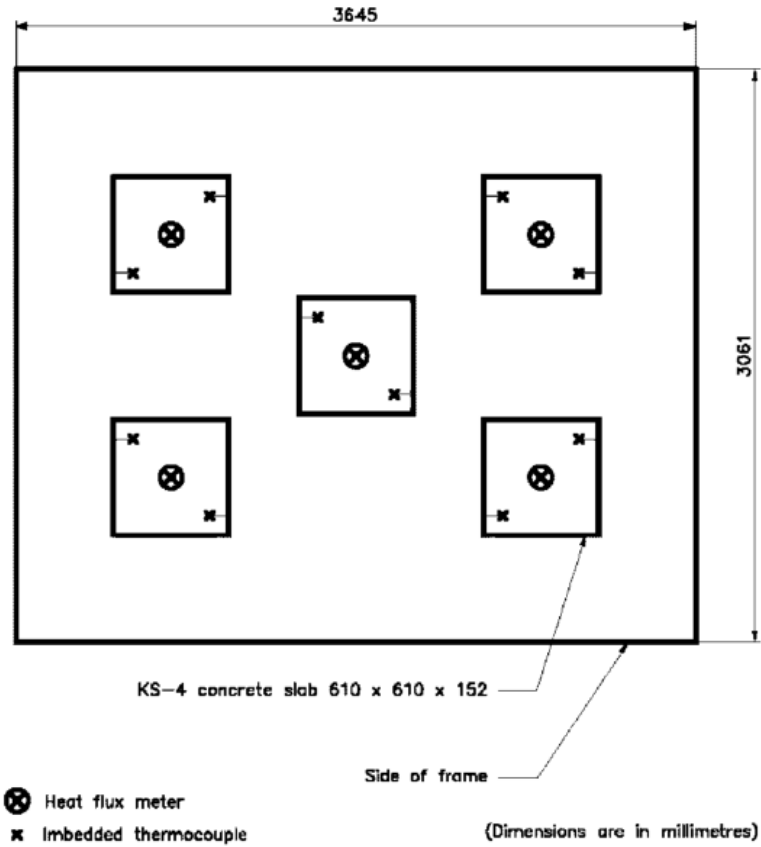


Figure 31: Distribution of the heat flux gauge (reproduced with the permission of the National Research Council of Canada)

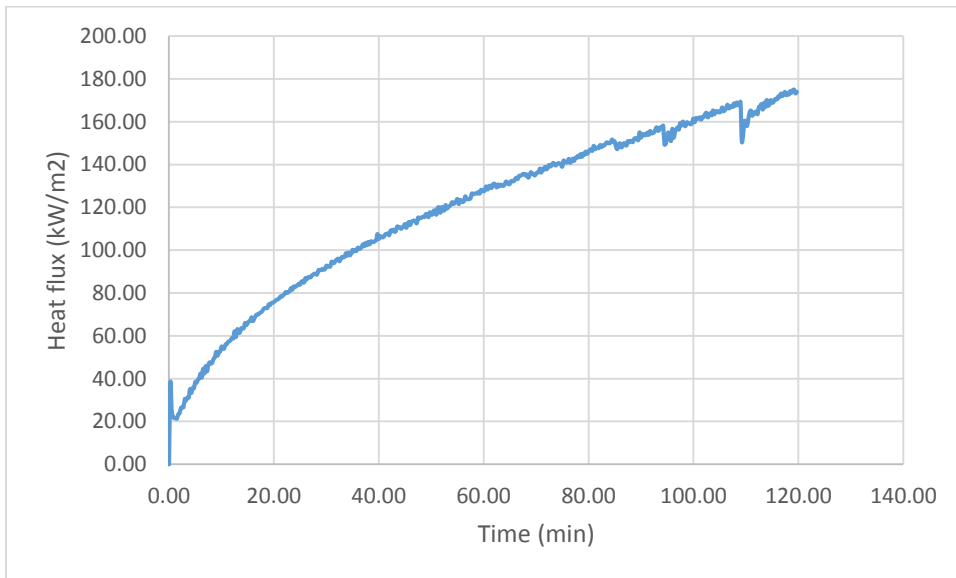


Figure 32: Heat flux at the surface of the sample in the furnace

7 Results and discussion

First, the results obtained from the simulations made with ABAQUS will be presented for the two type of construction and the following scenario:

- The type of insulation (Stone wool, Fiber glass wool) and uninsulated
- Reduced amount of insulation with stone wool insulation (Full depth (50mm), three quarter, half and quarter) using the same cavity depth 50mm
- When the insulation is reduced by half, the impact of the location of the insulation (exposed versus unexposed side) for the partition type A only
- Hole in the gypsum board at the exposed surface of the barrier insulated with stone wool, fiberglass wool and without insulation (Large hole 50mm radius against small hole 10mm radius).
- Hole through the fire barrier, with stone wool insulation, type A only (Large hole 50mm radius against small hole 10mm radius).
- Missing portion of stone wool insulation of different size for the partition of type B only (Large portion 100mm radius against small portion 50mm radius).

The failure criterion considered for the different partition depends on the scenario. The scenario, which leads to higher temperatures at specific locations, is considered to fail based on the criterion T180 (Holes through, holes on one side, missing portion of insulation). Other scenarios with a more uniform unexposed surface, temperature used the failure criterion T140 (reduced insulation, type of insulation).

Secondly, the results obtained from FDS concerning the integrity tests are going to be introduced. Since it is not possible to reproduce the gap gauge test, all the leakage areas were distributed over a surface limiting the width of the crack to 6mm (distributed leakage) or 25mm (localized leakage). Failure was considered once the temperature inside the cotton pad, located in front of the leakage area, reached the ignition temperature of 400 °C as obtained in experiment[12]. The scenarios considered are the following:

- Leakage localized on the surface of one cell, see Figure 27. This represents the effect of small breach or hole through the partition.
- Leakage area distributed on one side of the wall as presented in Figure 26. This represents the scenario where the sealing of the partition was not done properly at one specific location.

- Leakage area distributed over all joints of the construction, see Figure 25. This is to investigate the effect of an improper sealing work of all the joints of the partition.

7.1 Construction Type A

7.1.1 Impact of the choice of insulation material

The maximum temperature found on unexposed side of the fire resisting barrier is shown in the Figure 33 for the partitions filled with different type of insulation or empty.

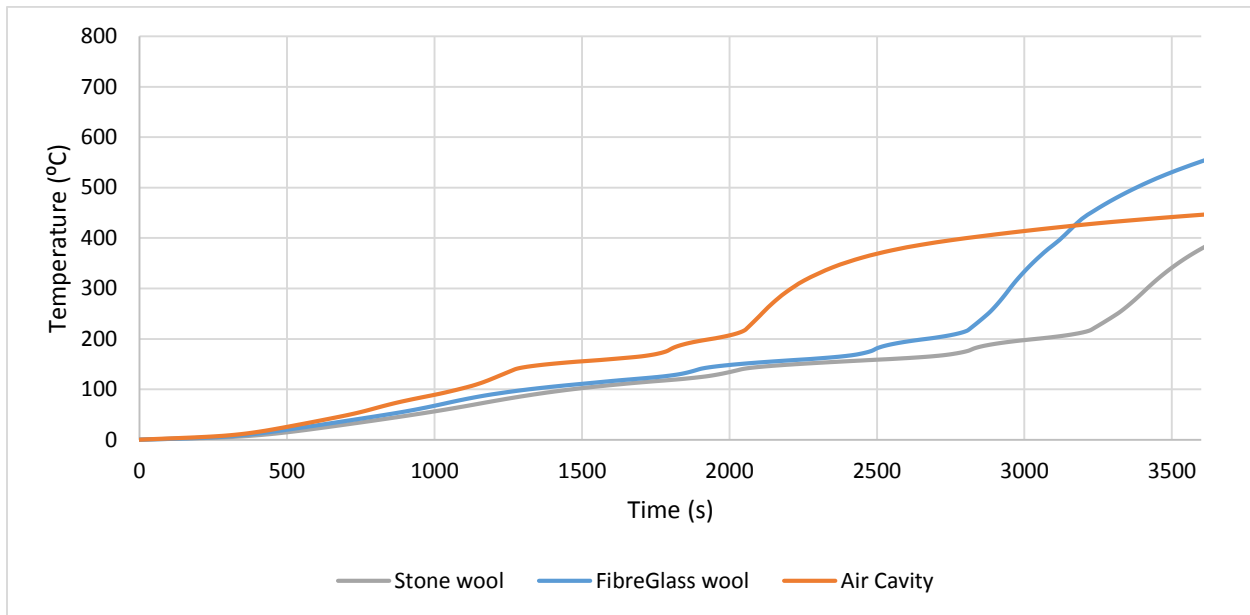


Figure 33: Temperature at the unexposed layer of the Wall with different types of insulation or without insulation

The first thing that should be noticed is that the three walls do not perform as expected. Because the FRR for all three constructions was supposed to be 60 minutes, but the temperature T_{180} was exceeded for all cases before this time, see Figure 35. Of course, the models could have been altered in order to obtain the rating specified by the manufacturer. However, it was decided to keep the method presented in section 6.1 and used in the validation section 6.1.4. The difference in the FRR obtained with ABAQUS could be explained by different properties of material or simply by the modeling method since the validation section showed error in the range of 30%. It does show however that the fire-rated barrier should not perform much more than 60 minutes in reality.

It can be observed that the wall with insulation yields better results compare to the wall without insulation in term of FRR, see also Figure 35. However, after 60min the temperature is higher for fiber glass insulation compare to an empty partition, this is due to two factors. First, as the temperature increases, the properties of fiber glass wool insulation falls, leading to higher

heat transfer by conduction as seen in section 5. Second, the heat transfer by radiation inside the empty cavity decreases, as the temperature of the gypsum layer on the cold side increases.

Also, the previous graph shows that Stone and fiber glass wool give comparable temperature until around 2500 seconds, at this point ablation of fiber glass wool causes the partition temperature to rise. Figure 35 depicts the FRR found for the different cases. The critical temperature was observed at the steel studs location for stone wool insulation (see Figure 40) and at the center point between each studs for fiber glass wool (see Figure 37). This is explained by the difference between the thermal conductivity of insulation material and steel. At high temperature the fiber glass wool conducts more heat than steel, due to ablation.

The Stone wool insulation gives the best result being able to resist 70% of the 60min expected. However, fiber glass wool and the partition without insulation are able to provide fire resistance only 62% and 55% respectively, of the expected 60min rating. Figure 34 shows the propagation of heat inside the different type of insulation after 60 min. In order the cross section are: air cavity, stone wool and fiber glass wool.

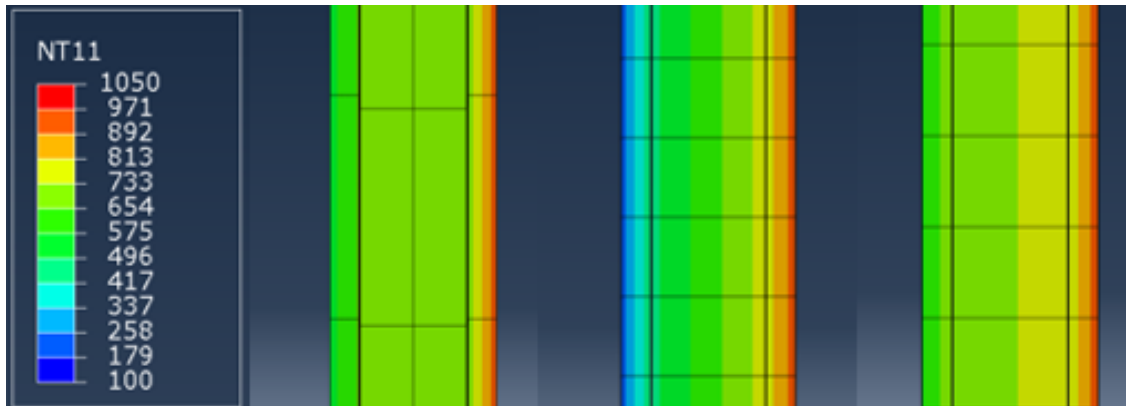


Figure 34: Temperature inside cross section of walls

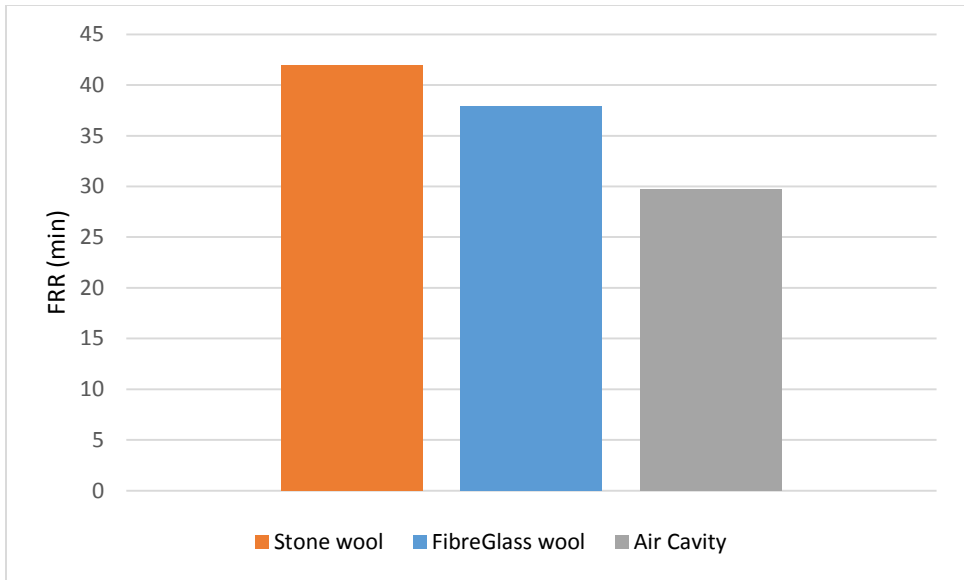


Figure 35: FRR of each walls insulated or uninsulated

One important impact of the insulation material, as it is possible to observe in Figure 34 and Figure 36, is the difference of temperature in the exposed gypsum layers. Due to insulation material, which slows down the heat transfer through the cross section of the wall, the temperature on the inside face of the exposed gypsum layer is increased, as seen below.

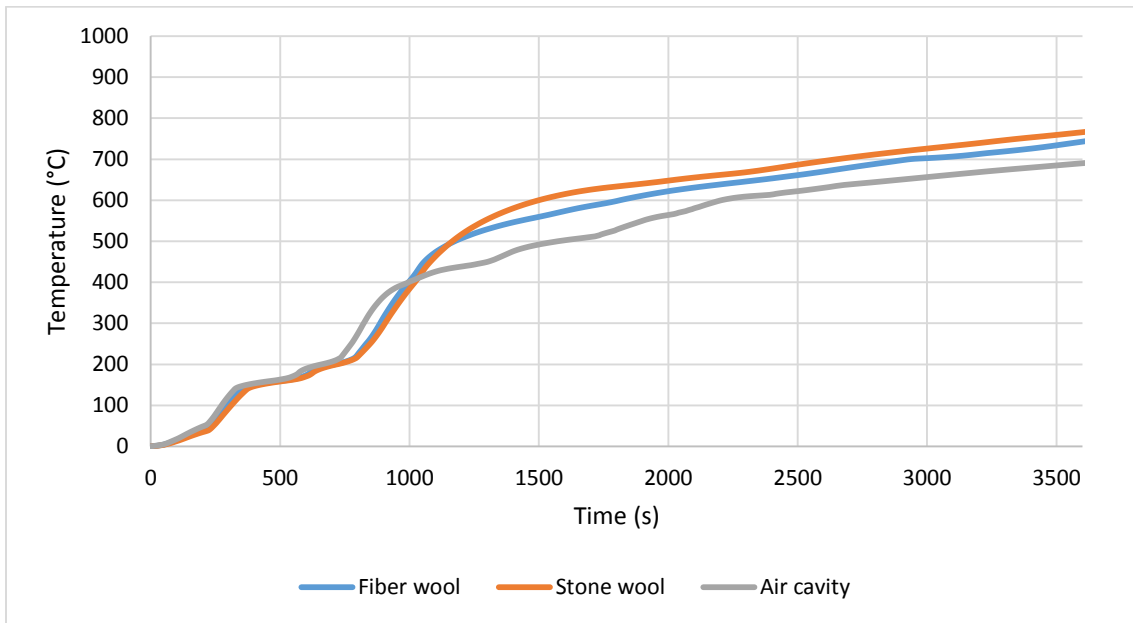


Figure 36: Temperature of the exposed side gypsum layer



Figure 37: Cross section a partition filled with fiber glass wool, after 60min

7.1.2 Impact of reduced amount of insulation

The maximum temperature found on unexposed side of the fire barrier, for barrier with different thickness of insulation, is presented in Figure 38. This graph shows that the temperature on the unexposed side increases with the decrease of insulation, as expected. The increase of temperature seems proportional to the amount of insulation reduced. Figure 41 shows that the FRR is reduce by around 5% for every 25% of reduced insulation. Also, the Figure 39 shows temperature in the cross section of each scenario, after 60 min. The cross sections are introduced in this order: the color-temperature legend; the partition with 25% insulation; the partition with 50% insulation; the partition with 75% insulation; and the partition 100% insulation. We can see from this figure that in general, the cross section is hotter for scenario with reduced insulation.

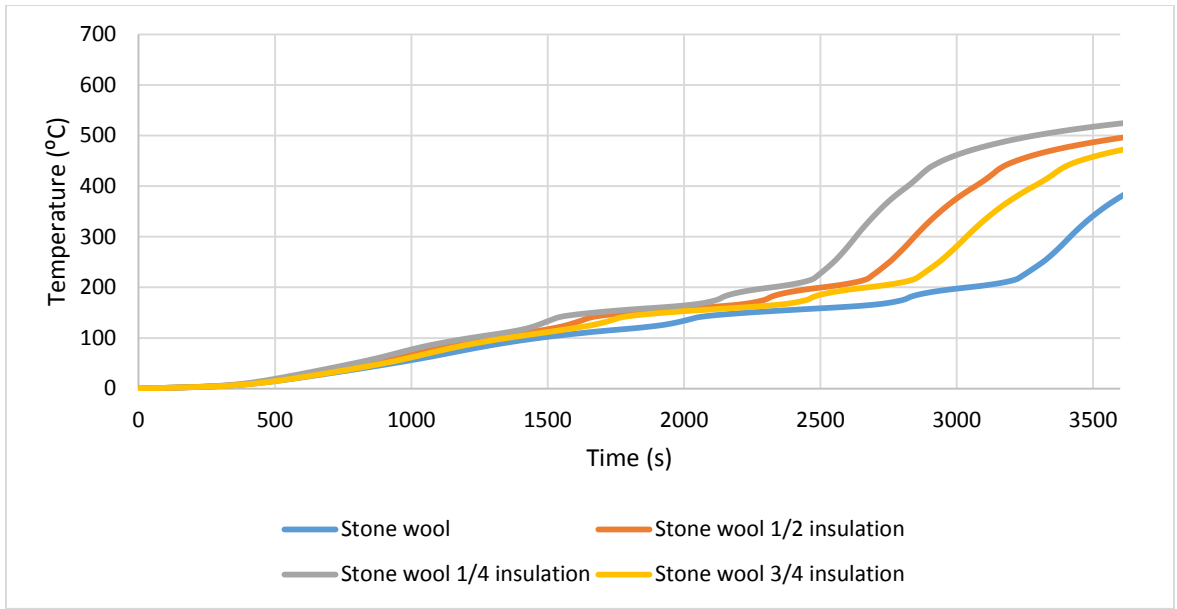


Figure 38: Wall with reduced insulation

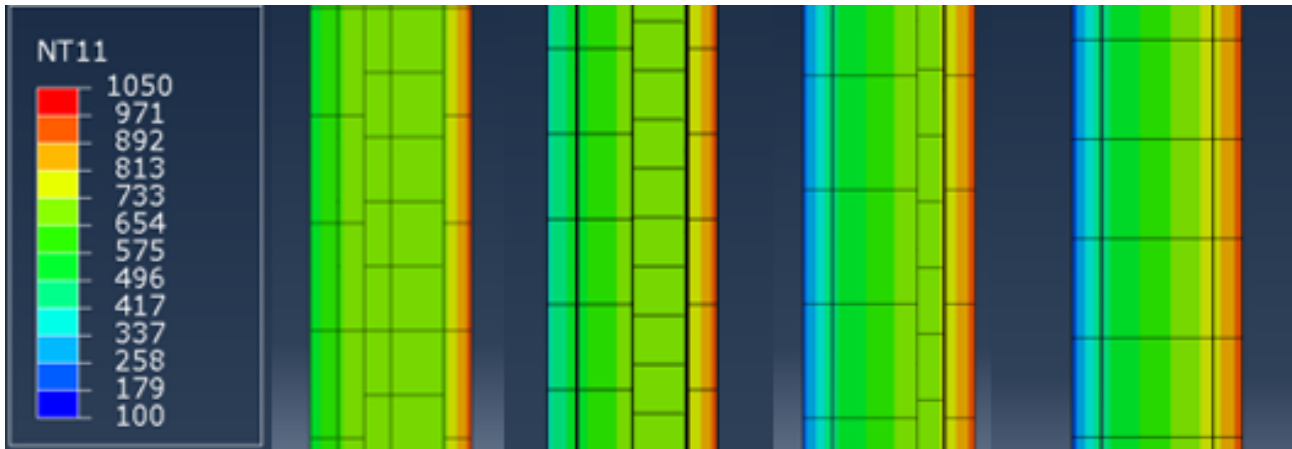


Figure 39: Temperature in the cross section of wall with reduced insulation

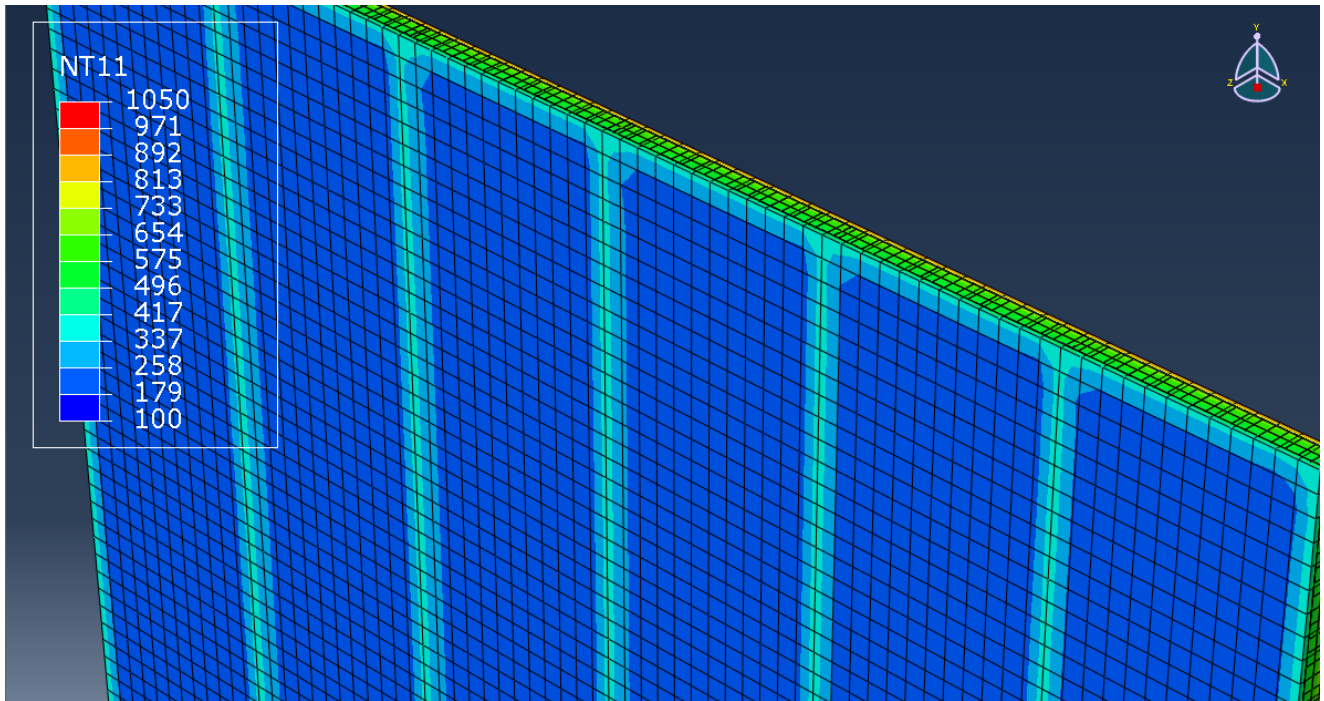


Figure 40: Unexposed surface temperature of stone wool partition after 60min

Figure 40 demonstrates the temperature on the unexposed surface of the partition insulated with 50mm of stone wool insulation, after 60min of exposure to the standard fire. As it is possible to see the maximum temperature is reached at the location of the steel studs. This is due to the high thermal conductivity of steel compare to the stone wool.

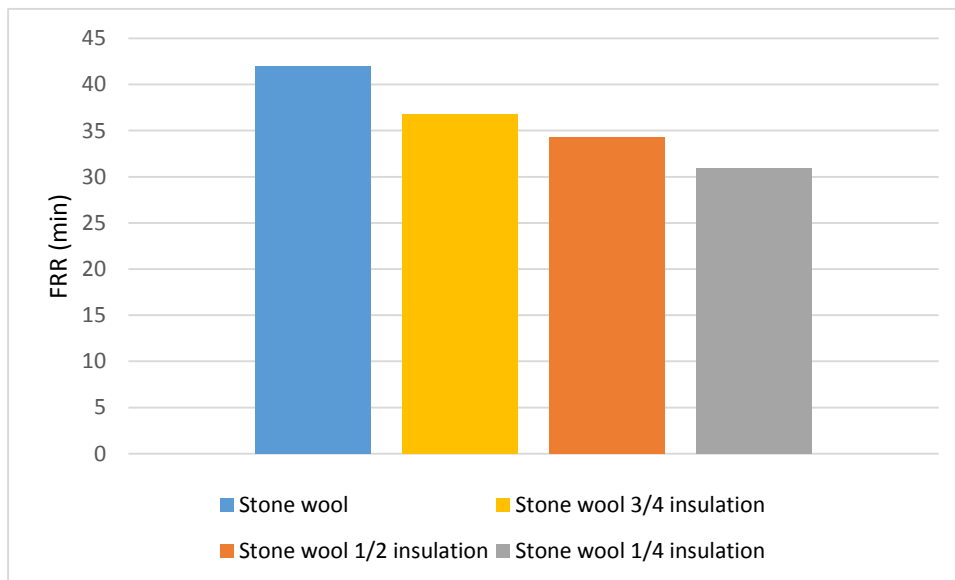


Figure 41: Ratio of FRR over the expected 60min rating for partition with reduced insulation

The following graph displays the temperature measured on the unexposed side depending on the position of insulation. The 25mm thick insulation inside the 50mm cavity was set in contact with the exposed layer of gypsum (fire side) or on the unexposed layer of gypsum (cold side).



Figure 42: Temperature on unexposed surface of the wall with different position of insulation

Figure 42 depicts that for higher temperature it is better to have insulation located on the side of the fire. This reduces the amount of cavity radiation within the construction and lower the temperature on the unexposed surface. It is possible to observe a difference of 20% in temperature on the unexposed surface, between the two cases.

7.1.3 Impact of increased amount of insulation

The following figure shows the temperature on the unexposed side of the partition when the insulation thickness is doubled (100mm). This will be compared later to the effect of doubling the thickness of gypsum board.

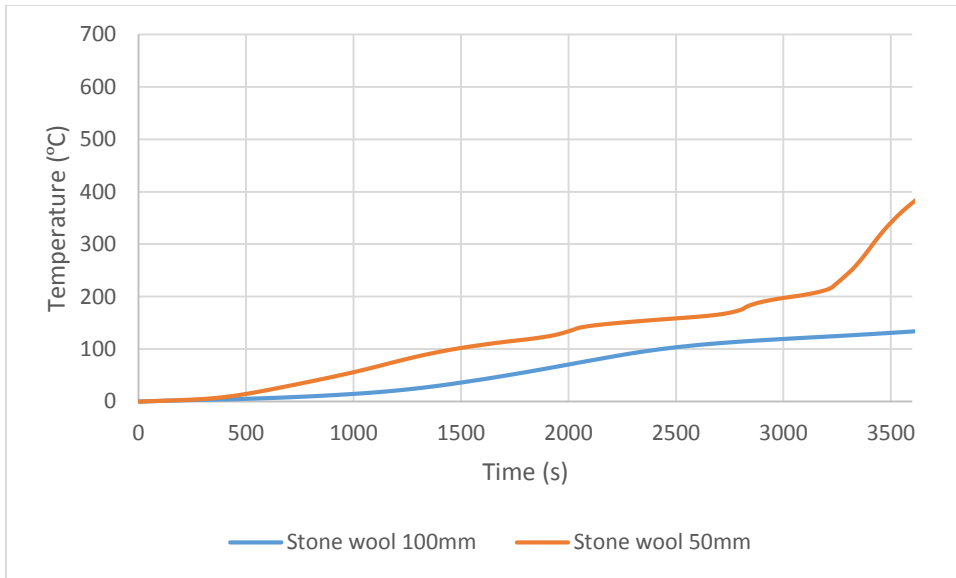


Figure 43: Temperature on the unexposed side of a partition type A with 100mm stone wool insulation

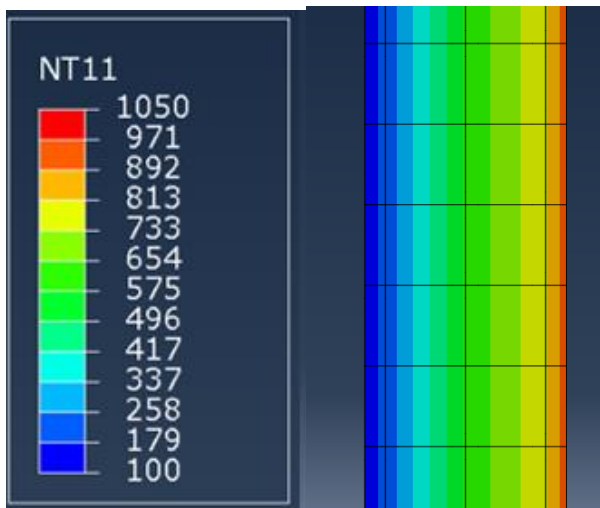


Figure 44: Temperature in the cross section of a partition type A with 100mm stone wool insulation

Figure 43 shows that when the insulation is doubled the FRR of the partition is increased by 175% passing from 43min to 75min.

7.1.4 Impact of hole on the exposed surface

The maximum temperature found on the unexposed side of the partition is shown in the following figures, for partition with hole on the fire-exposed surface with insulation.

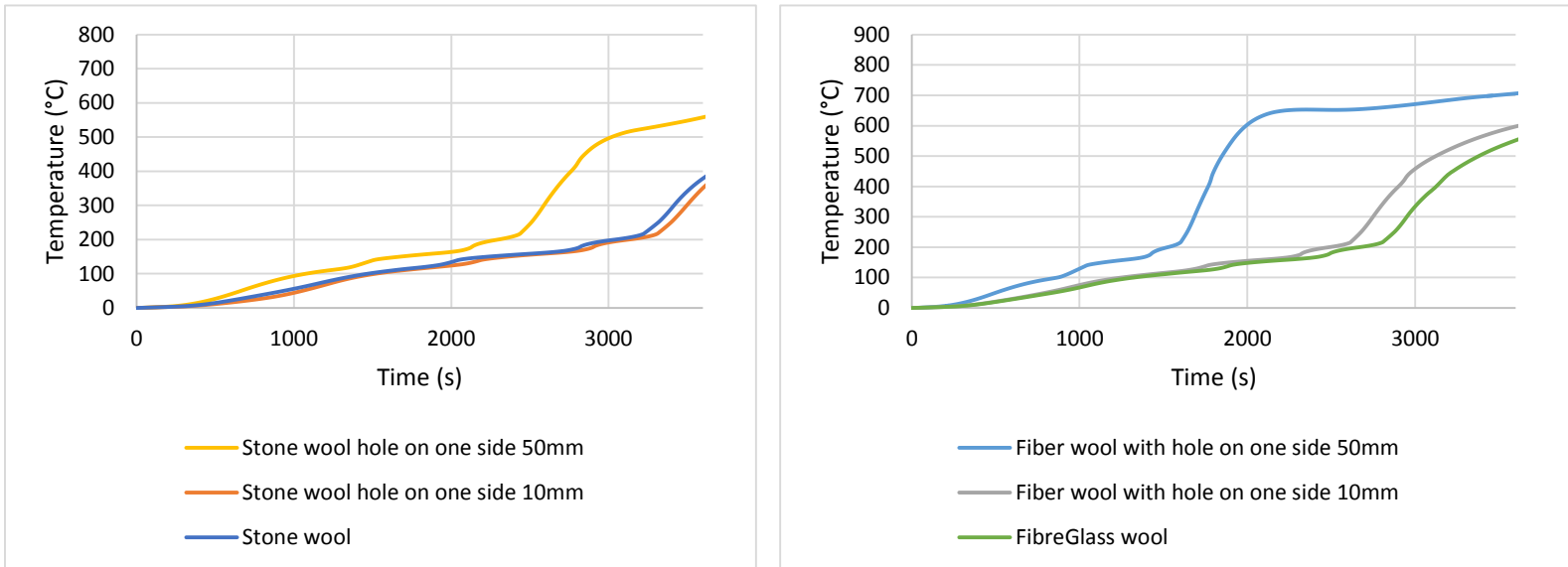


Figure 45: Temperature on the unexposed side for insulated partition with hole on the exposed surface

Figure 45 shows the impact of a hole on the exposed surface on the temperature on the unexposed surface. It can be seen that if the hole is small enough the temperature on the unexposed side will be comparable to the temperature found at the steel studs. However, if the area is increased, the heat transfer is increase and the FRR is reduced. The FRR is reduced by 20% (stone wool) and by 37% (fiber glass wool) when the diameter is increased 5 times. The following picture (Figure 46) shows the temperature through the wall insulated with stone wool, left side is a hole of 50mm radius and right side is a hole of 10mm radius.

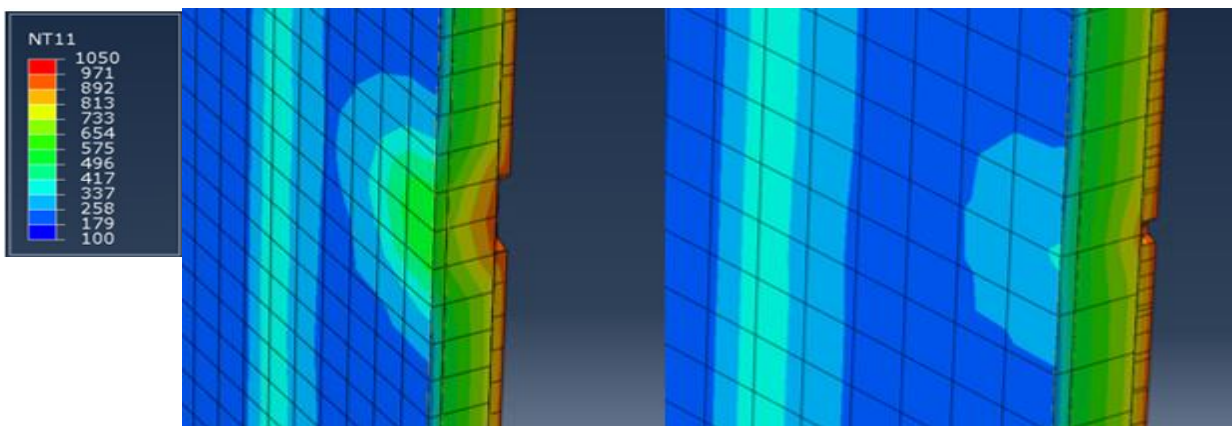


Figure 46: Temperature of the partition with hole on exposed surface insulated with stone wool

The Figure 47 shows the temperature on the unexposed surface for the different scenarios. It shows clearly that for partition without insulation the FRR is drastically reduced. A reduction of the FRR by 67% and 50% is notice for an empty partition with hole of 10mm and 50mm radius, when compare to an empty partition without hole on the exposed surface. This was expected since nothing prevents the radiation from reaching the unexposed gypsum layer, see Figure 48.

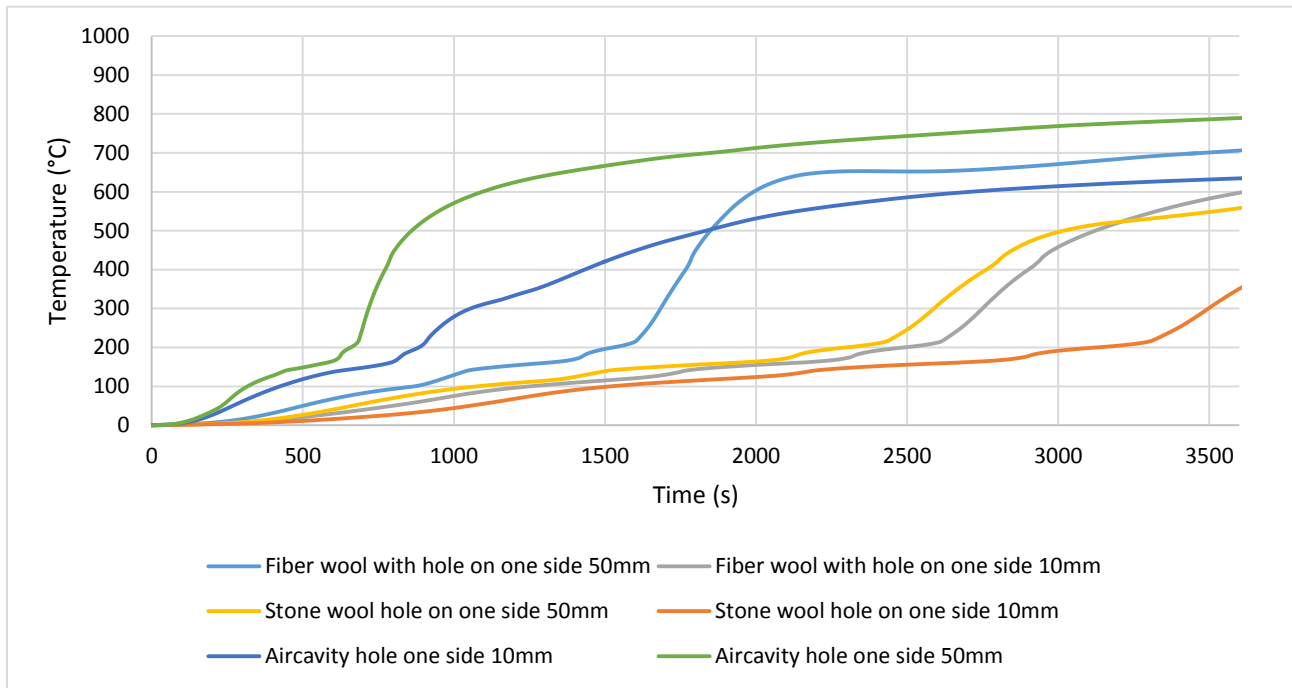


Figure 47: Temperature on the unexposed side of the partition with hole on the exposed surface

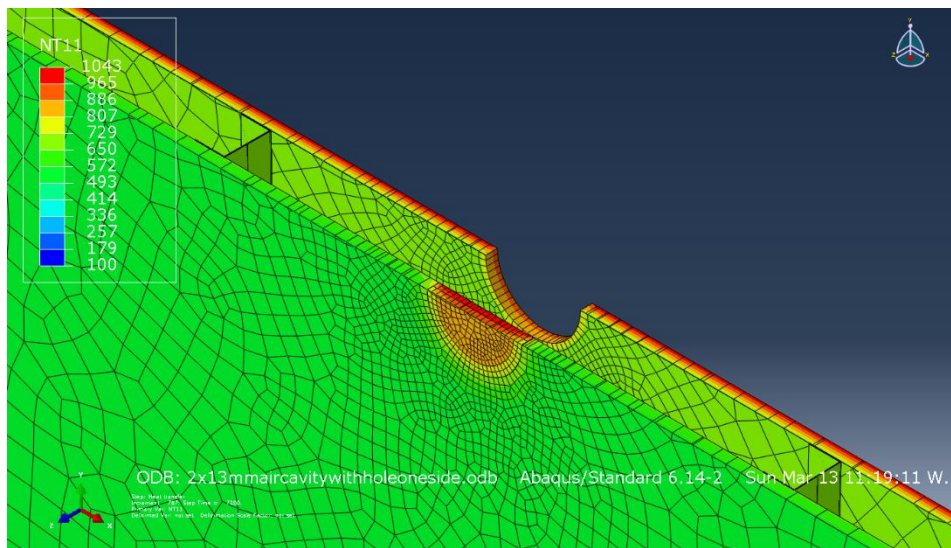


Figure 48: Temperature of partition without insulation breached on exposed side

7.1.5 Impact of the hole through the barrier

In this section the maximum temperature found on unexposed side of a fire rated barriers with a penetration through its boundaries is examined. For this scenario the wall insulated with stone wool was used because it was found to provide the best FRR. When the wall is breached through, it is possible to consider two scenarios. First, where the radiation and convection from hot gases affect all the area inside the hole. Second, where only the convection from the hot gases affect the area of the hole. For the first scenario the temperature at the surface will be almost equivalent to the standard temperature-time curve and therefore the FRR is as low as 5min regardless of the penetration dimension. In the second scenario the FRR is increased to around 12min also regardless of the dimension. The following pictures show the temperature on the unexposed side of the partition for both scenarios and for each penetration size (10mm, 50mm radius). On the left the pictures show the temperature with only radiation and on the right with only convection.

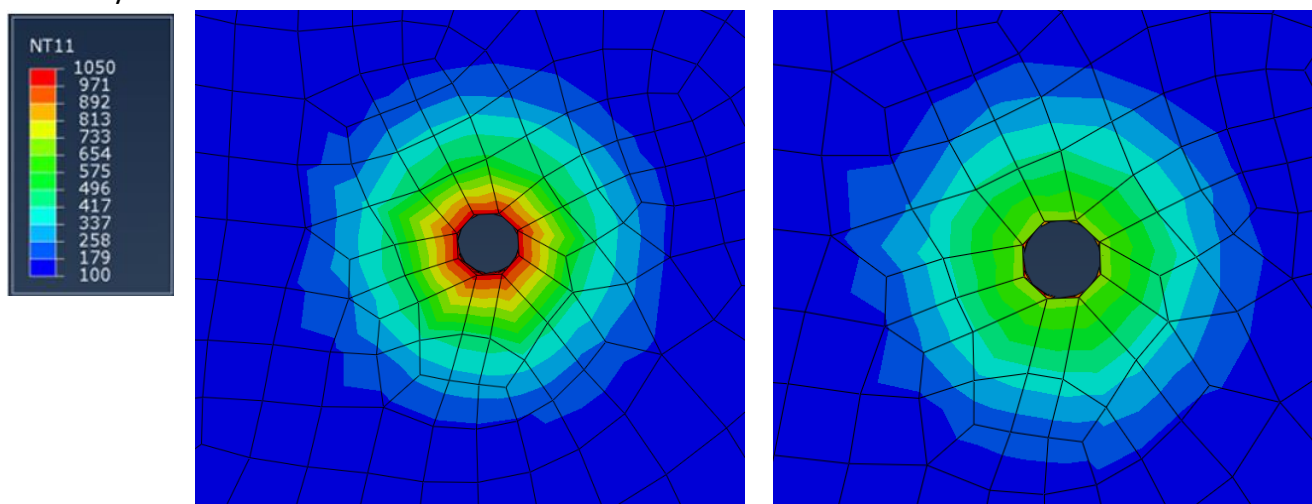


Figure 49: Temperature on the unexposed surface of a partition type A with a hole of 10mm, first and second scenario

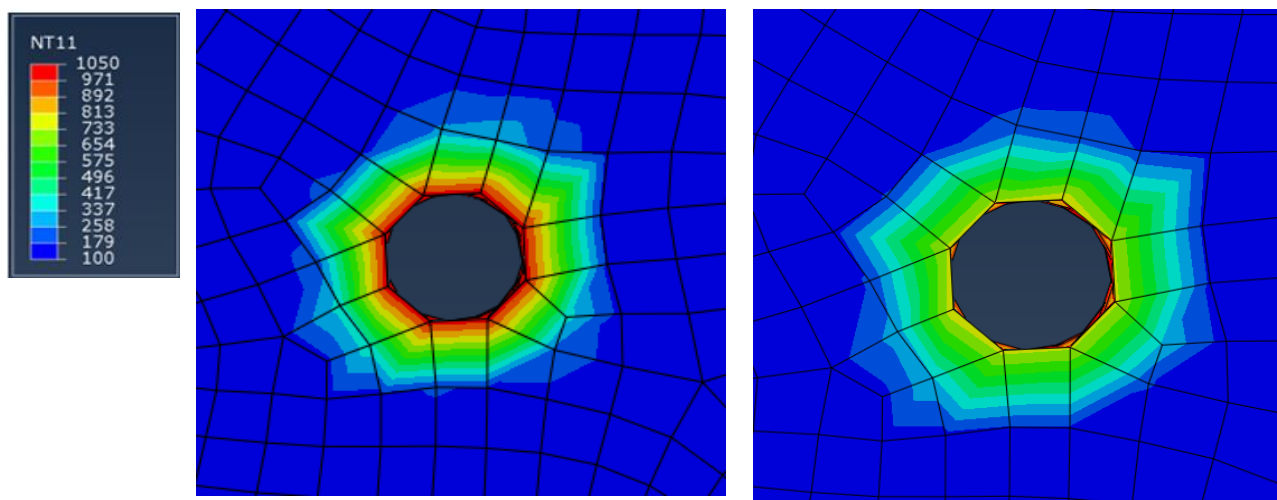


Figure 50: Temperature on the unexposed surface of a partition type A with a hole of 50mm radius, first and second scenario

7.2 Construction Type B

7.2.1 Impact of the choice of insulation material

The maximum temperature found on unexposed side of the fire-resisting barrier is shown in the Figure 51, for partitions with different type of insulation or without insulation.

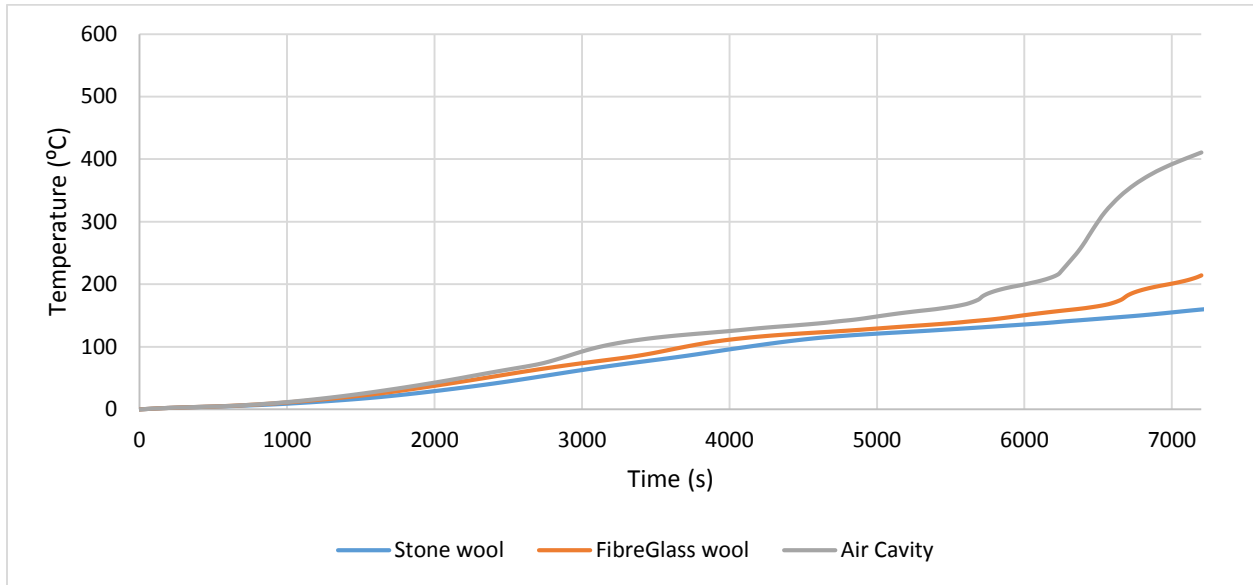


Figure 51: Temperature on the unexposed surface of wall type B with different types of insulation and without insulation

Again the fire-rated walls with different insulation do not perform as expected, still the results are closer to the manufacturer rating than the results obtained in section 7.2.1.

The previous figure shows that the temperature on the unexposed side for all three cases is within 25% difference, until approximately 83min. At this point the temperature of the wall with an empty cavity starts to increase much faster since radiation is affected by temperature at a power of 4. Figure 53 shows that the FRR for the partition insulated with stone wool is 15% higher than the fiber glass wool and 226% higher than the empty cavity. Also, the results here can be compared with the results from section 7.1.1 and it is possible to see that the FRR, with twice the thickness of drywall, increases by 280% for insulated wall and by 180% for the non-insulated wall. The Figure 52 shows the temperature at different thickness of the wall, from left to right the partition are built without insulation, with stone wool insulation and with fiber glass wool insulation.

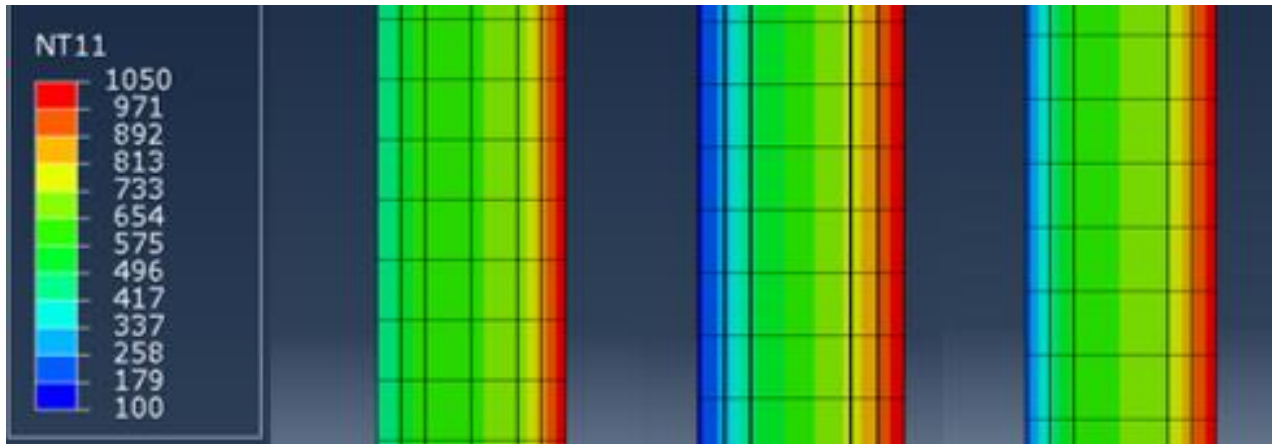


Figure 52: Temperature in the cross section of wall type B for different insulation



Figure 53: FRR for different insulation or uninsulated

7.2.2 Impact of hole on the exposed surface

The maximum temperature found on the unexposed side of the partition with a breach or penetration on the fire-exposed gypsum surface is shown in the following figures, for partition with and without insulation.

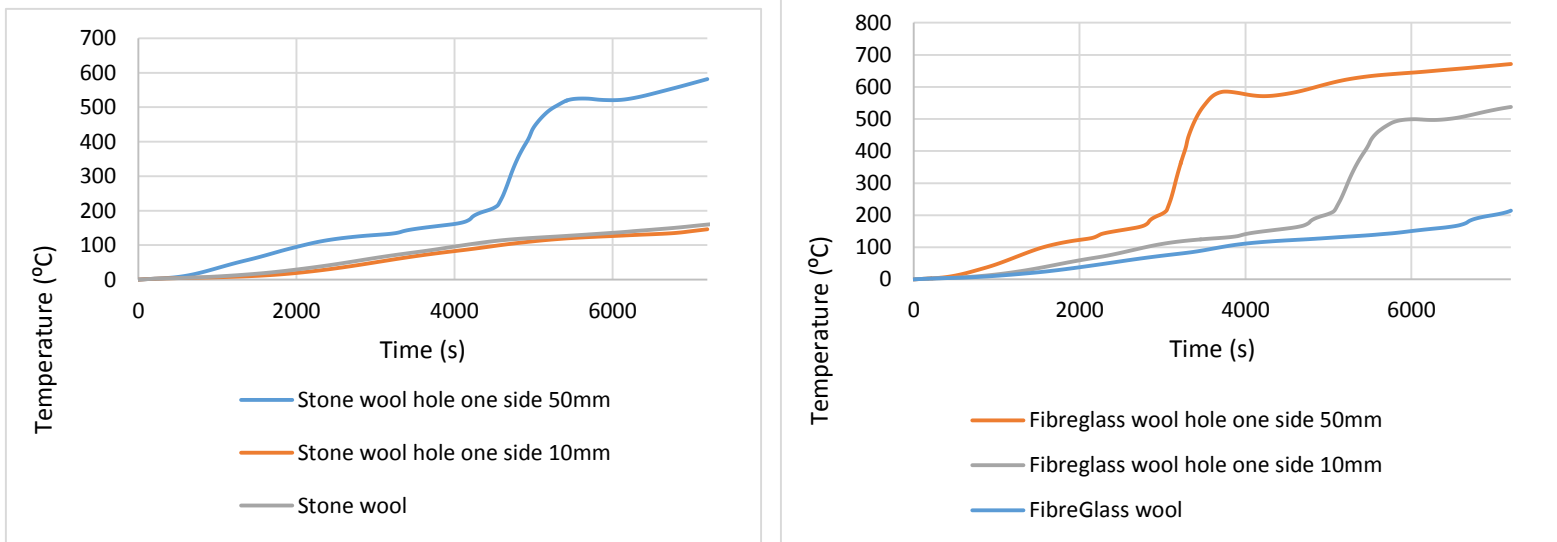


Figure 54: Temperature on the unexposed side for insulated partition with hole on the exposed surface

The two graphs above depict the difference between a wall insulated with stone or fiber glass wool. A major difference can be observed for partition with a 10mm radius penetration. For the wall with stone wool insulation the temperature at the surface remains unaffected as the temperature does not penetrate through the partition. While with fiberglass wool temperature rise very fast resulting in an early failure of the partition, a reduction of 20% of the FRR can be observed. This can also be seen in the Figure 56. For a penetration of larger dimensions, both types of insulation do not restrain the heat transfer, thus the FRR is found reduced. Still, stone wool insulation provides better fire resistance. For the larger hole, 50mm radius, a 40% and 50% reduction of the FRR can be observed for Stone wool and Fiberglass wool respectively.

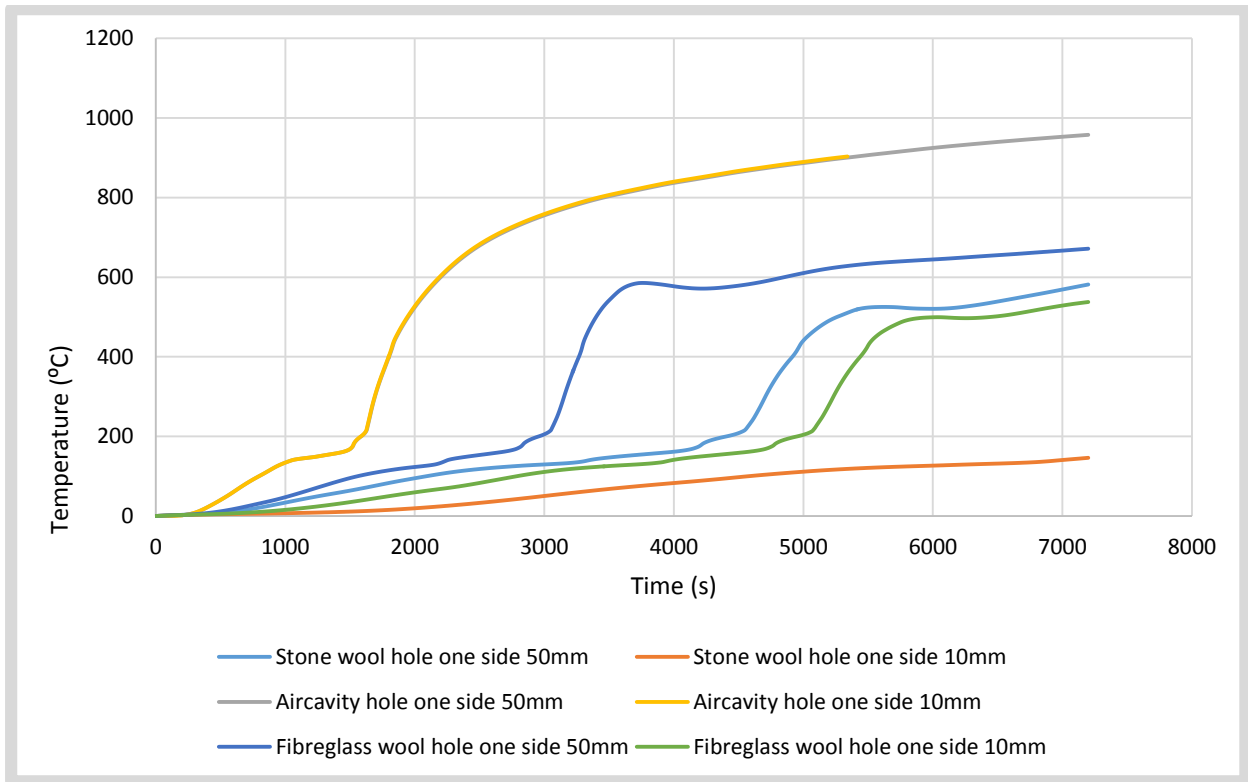


Figure 55: Temperature of the partition with hole insulated with stone wool

The figure above illustrates the temperature on the unexposed surface for the different scenarios. Again, for partition without insulation, the FRR is dramatically reduced. A reduction of the FRR by 50% is noticed for an empty partition with hole of 10mm and 50mm radius, when compare to an empty partition without hole on the exposed surface. As explain before, since nothing prevent the radiation from reaching the unexposed gypsum layer, the temperature rises very fast. This can also be seen in the following pictures.

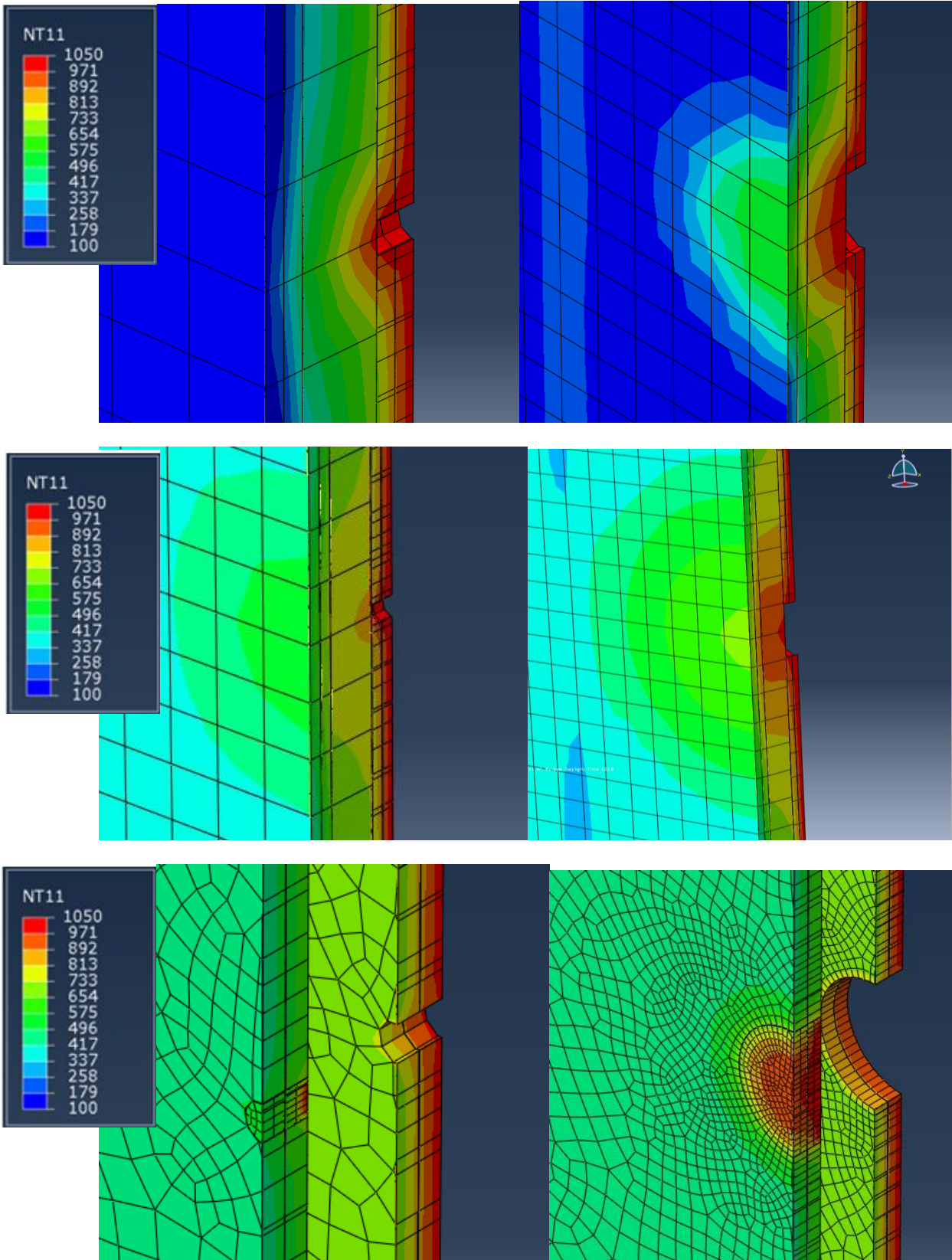


Figure 56: Temperature of the partition for all types of insulation and breach of 10mm and 50mm radius

7.2.3 Impact of reduced amount of insulation

The maximum temperature found on unexposed side of the barrier is shown in the figure below, for the partition with different thickness of insulation.

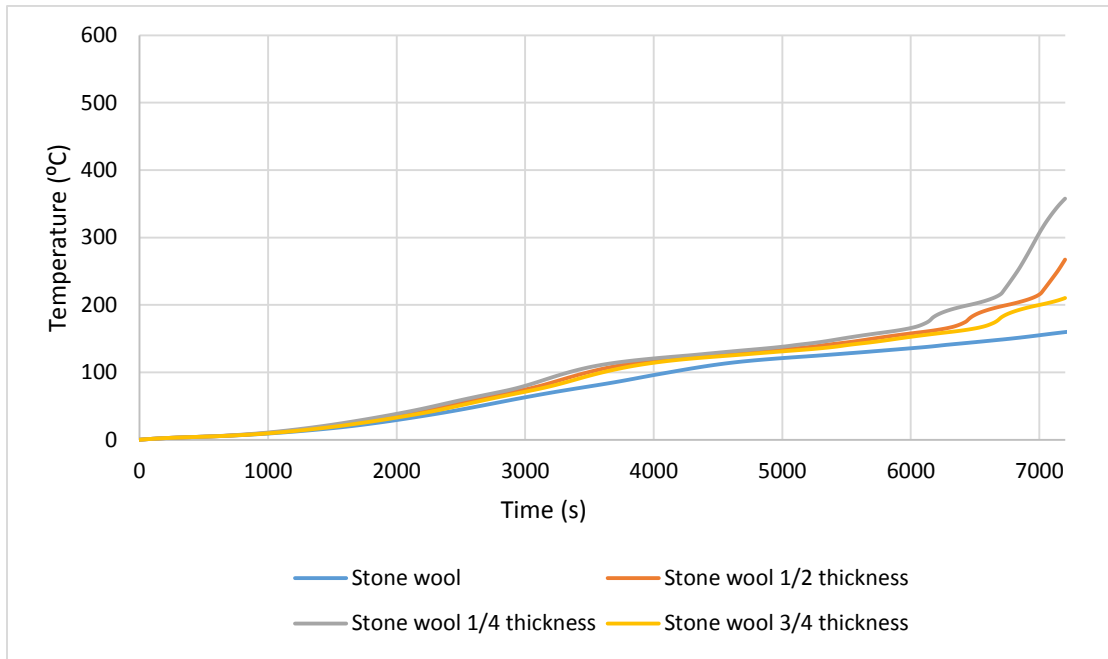


Figure 57: Temperature on the unexposed surface of wall type B with reduced insulation

Again the temperature on the unexposed side of the wall insulated with different thickness of insulation, is not significantly different, up to 80% of the test duration. Still, the FRR is slightly affected, as it can be seen from Figure 58. After 120 min the FRR is reduced by up to 20% for a 75% reduction in insulation, 15% for a 50% reduction in insulation and 12.5% for a 25% reduction in insulation. This is comparable to the data obtained with the type A construction.

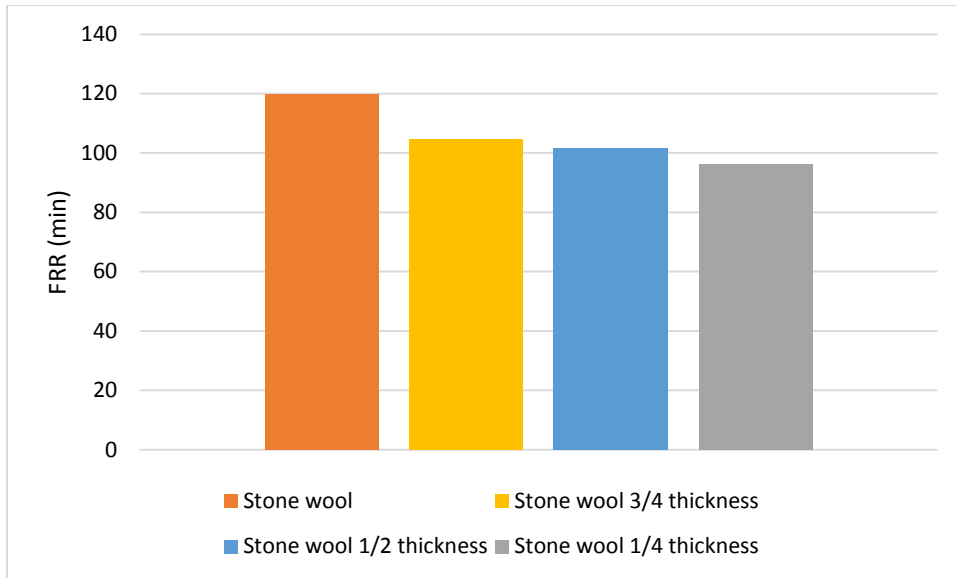


Figure 58: FRR for partition with reduce insulation for type B construction

7.2.4 Impact of missing part of insulation

The maximum temperature found on unexposed side of the fire-resisting barrier is shown in Figure 59, for the barrier fully insulated against two fire barrier with missing portion of insulation.

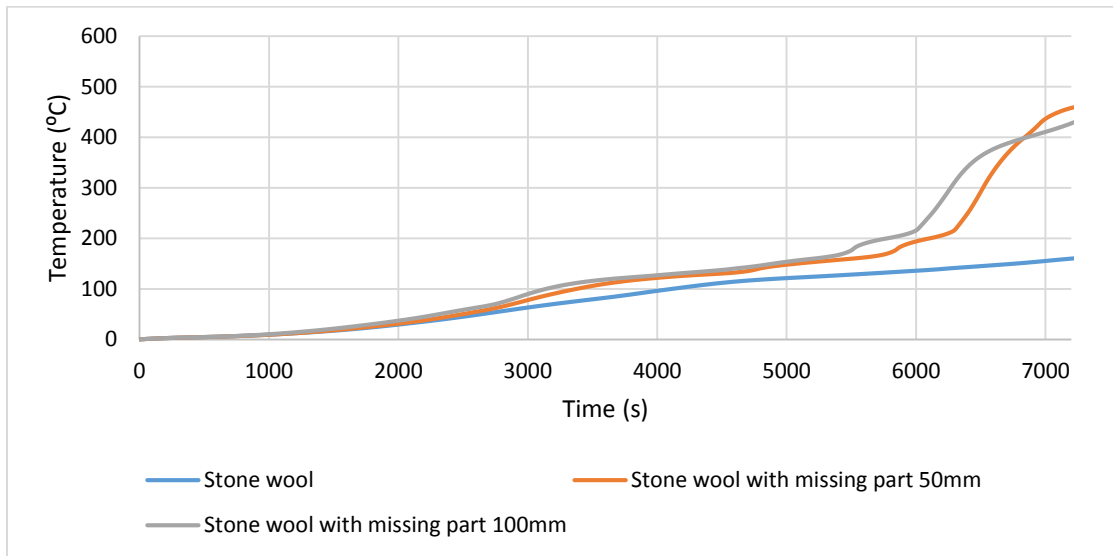


Figure 59: Temperature on the unexposed surface of wall type B with missing insulation part

As it is possible to see in the graph above and following picture, the temperature at the surface increased for the scenario with missing portion of insulation compare to the full insulated partition. Cavity radiation occurs where insulation is missing, and as seen in the previous cases, it results in higher temperature at the surface of the gypsum board. This causes the FRR to be

reduced to 96min for the wall with 100mm radius missing part and 102min for the one with 50mm radius missing part. A reduction equivalent to 20% and 15% respectively. The pictures presented below show the temperature through the partition at the location where the insulation is missing. Heat is transferred only by conduction and radiation.

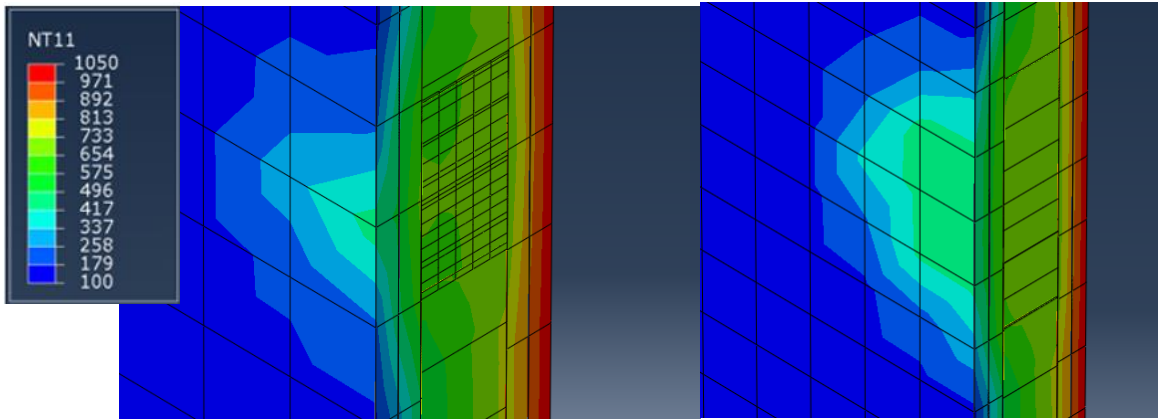


Figure 60: The temperature of the two walls with missing portion of insulation, left 50mm radius and right 100mm radius

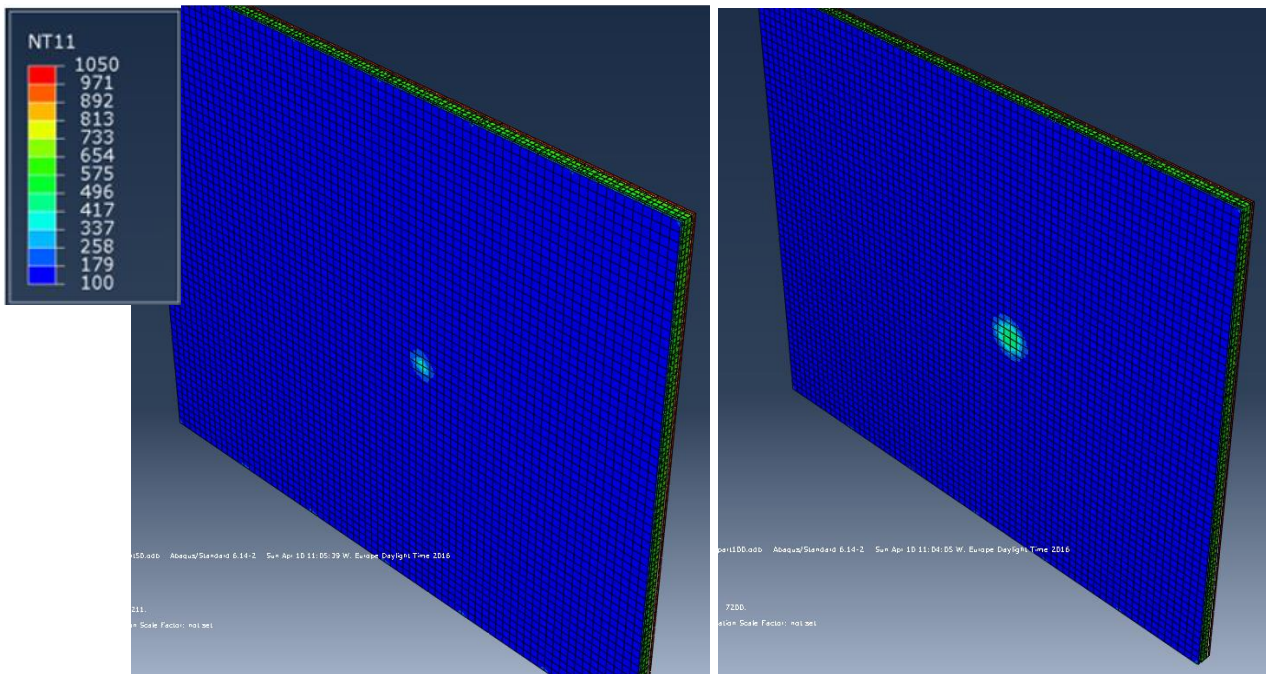


Figure 61: The temperature of the two walls with missing portion of insulation, left 50mm radius and right 100mm radius

7.3 Table of results from the heat transfer simulation with ABAQUS

The following table resumes the findings with ABAQUS. This table shows the reduction of the FRR of different features compare to a specific partition assembly.

Type	Partition features	Reduction of the FRR				
A/B		No reduction	Between 0- 25%	Between 25-50 %	Between 50-75 %	More 75%
Comparison with partition type A insulated with stone wool (no deficiencies)						
Type A	Empty cavity			■		
	Fiberglass wool		■			
	Stone wool insulation reduced by 25%		■			
	Stone wool insulation reduced by 50%		■			
	Stone wool insulation reduced by 75%			■		
	Stone wool partition exposed gypsum breach 10mm radius	■				
	Stone wool partition exposed gypsum breach 50mm radius		■			
	Hole through partition 10mm radius					■
	Hole through partition 10mm radius					■
Comparison with partition type A insulated with Fiberglass wool (no deficiencies)						
Type A	Empty cavity		■			
	Fiberglass wool partition exposed gypsum breach 10mm radius	■				

	Fiberglass wool partition exposed gypsum breach 50mm radius					
Comparison with partition type A uninsulated (no deficiencies)						
Type A	Empty partition exposed gypsum breach 10mm radius					
	Empty partition exposed gypsum breach 50mm radius					
Comparison with partition type A insulated with Stone wool with fire-exposed gypsum breach 10mm radius						
Type A	Fiber glass wool partition exposed gypsum breach 10mm radius					
	Empty partition exposed gypsum breach 10mm radius					
	Empty partition exposed gypsum breach 10mm radius					
Comparison with partition type A insulated with Stone wool with fire-exposed gypsum breach 50mm radius						
Type A	Fiber glass wool partition exposed gypsum breach 50mm radius					
	Empty partition exposed gypsum breach 50mm radius					
Comparison with partition type B insulated with Stone wool (no deficiencies)						
Type B	Empty cavity					
	Fiberglass wool					

	Stone wool insulation reduced by 25%		■			
	Stone wool insulation reduced by 50%		■			
	Stone wool insulation reduced by 75%		■			
	Stone wool partition exposed gypsum breach 10mm radius	■				
	Stone wool partition exposed gypsum breach 50mm radius			■		
	Hole through partition 10mm radius					■
	Hole through partition 10mm radius					■
Type A	Stone wool insulation				■	
Comparison with partition type B insulated with Fiberglass wool (no deficiencies)						
Type B	Empty cavity			■		
	Breach on exposed gypsum 10mm radius		■			
	Breach on exposed gypsum 50mm radius			■		
Type A	Fiberglass wool insulation				■	
Comparison with partition type B non-insulated (no deficiencies)						
Type B	Breach on exposed gypsum 10mm radius			■		

	Breach on exposed gypsum 50mm radius					
Type A	Empty Cavity					
Comparison with partition type B insulated with Stone wool with fire-exposed gypsum breach 10mm radius						
Type B	Fiberglass wool partition exposed gypsum breach 10mm radius					
	Empty partition exposed gypsum breach 10mm radius					
Comparison with partition type B insulated with Stone wool with fire-exposed gypsum breach 50mm radius						
Type B	Fiberglass wool partition exposed gypsum breach 50mm radius					
	Empty partition exposed gypsum breach 50mm radius					

Table 8: Comparison of the results obtained with ABAQUS

7.4 Impact of leakage with FDS

7.4.1 Localized leakage

Figure 62 shows the temperature at different time inside the cotton pads. The leakage was considered localized in one area, at the top of the furnace (one cell thick 100mm). The cotton pad is located in front of the leakage area, as required by the code [2]. Since the thickness of the opening should not exceed 25mm (gap gauge criteria) only the construction with an opening smaller than 2500mm² (25mm x 100mm) can be considered. This means that the very loose and loose construction are not investigated, see Table 1. The temperature of the cotton pad with time, found with the FDS models, is presented below for the fire-rated wall with different air tightness construction: Average ASHRAE, tight NRCC, tight AAMA and tight NMBCC. As mentioned in section 6.3.1 the ignition temperature assumed is 400°C.

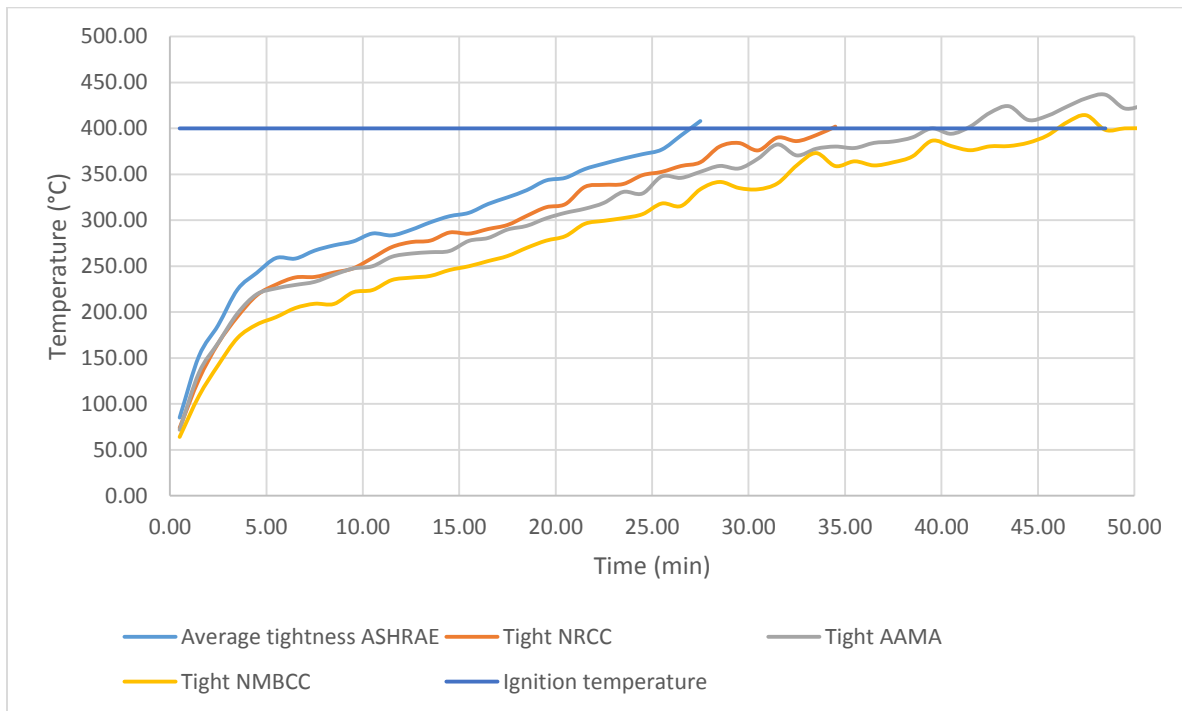


Figure 62: Temperature of cotton pad scenario 1 with different level of air tightness

Table 9 shows the FRR according to the integrity criteria of partition with localized leakage.

Scenario	Time until ignition of cotton pads (min)
Average construction	27
Tight construction (NRCC)	34
Tight construction (AAMA)	41
Tight construction (NMBCC)	46

Table 9: FRR of partition with different tightness leaking from a hole on top

As it is possible to see in the table above the FRR is reduced with an increase of the leakage volume rate. The FRR is reduced to 27min for an average construction this represents a reduction of 55% for a 60min fire-rated wall and 77% reduction for a 120min fire-rated wall. For a tight (NRCC) construction the FRR represents a reduction of 43% for a 60min fire-rated wall and 72% reduction for a 120min fire-rated wall. For a tight (AAMA) construction the FRR represents a reduction of 32% for a 60min fire-rated wall and 66% reduction for a 120min fire-rated wall. Finally, for a tight construction, according to the NMBCC, the FRR represents a reduction of 23% for a 60min fire-rated wall and 62% reduction for a 120min fire-rated wall.

7.4.2 Distributed leakage on one side

The following figures show the temperature at different times inside the cotton pads, for the fire-rated partition with air tightness according to the Table 1. The leakage area, in those models, was distributed over one joint of the wall only, as seen in Figure 26. The temperature for the cotton pads was measured at different heights. One located at the floor level, the second one at mid-level and the last one at the top level of the furnace.

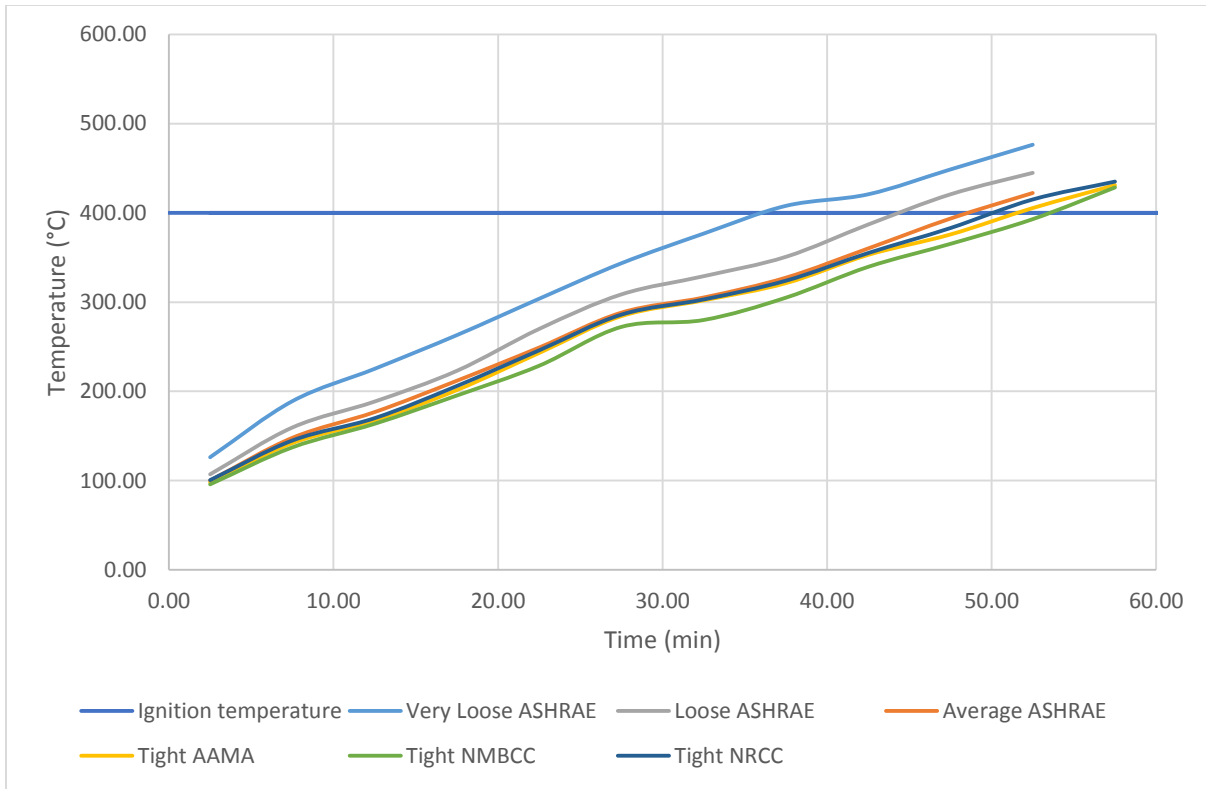


Figure 63: Temperature of cotton pad with time measured at the top of the sample height

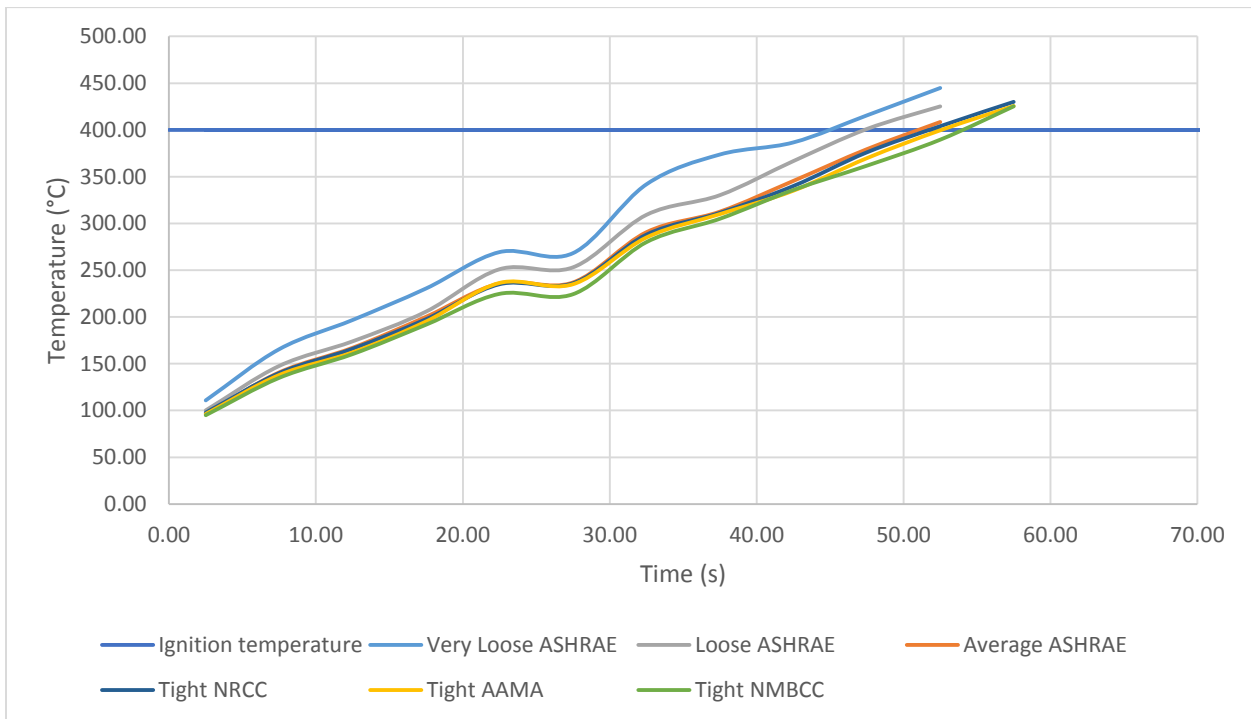


Figure 64: Temperature of cotton pad with time measured at the bottom of the sample height

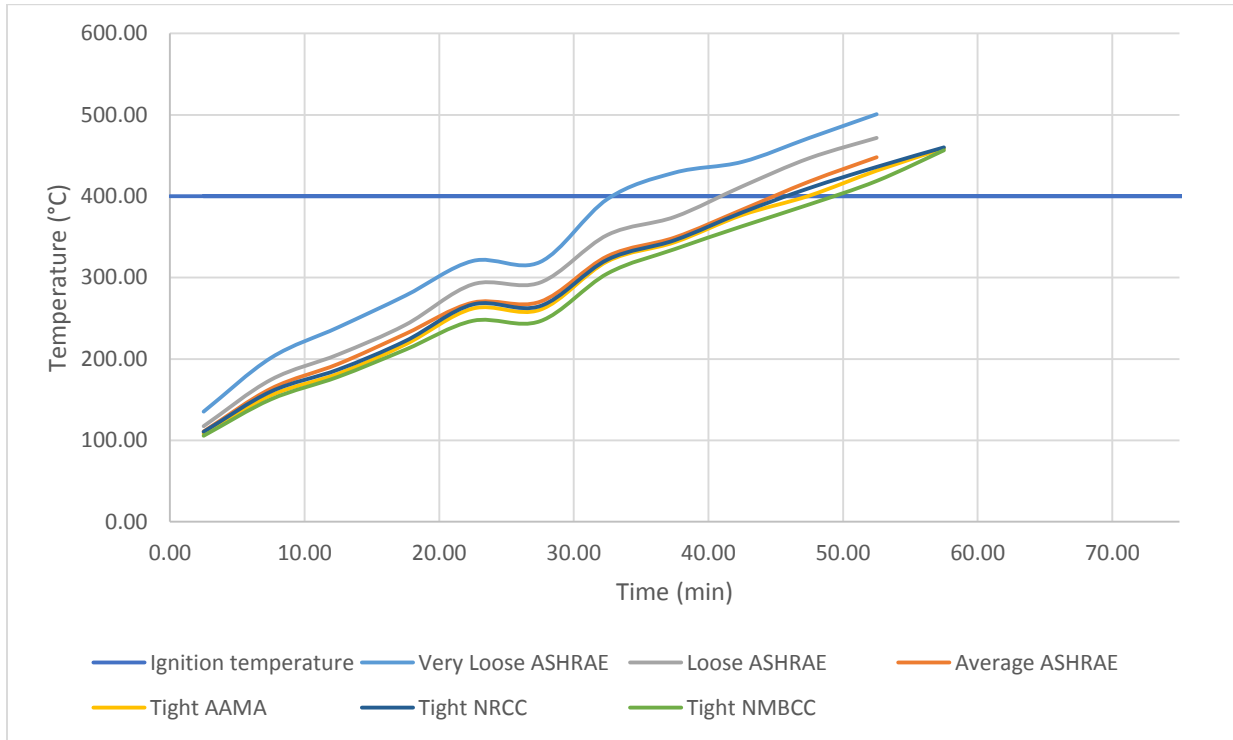


Figure 65: Temperature of cotton pad with time measured at the middle of the sample height

The Table 10 shows the time until ignition of cotton pad, for each position, taken from the graphs shown above. This time represent the time until failure according to the integrity criterion.

Scenario	Time until ignition of cotton pads (min)		
	Bottom of furnace	Middle of furnace	Top of furnace
Very loose construction	45	32	37
Loose construction	47	40	44
Average construction	51	44	47
Tight construction (NRCC)	52	46	50
Tight construction (AAMA)	53	48	53
Tight construction (NMBCC)	55	50	54

Table 10: FRR of partition with different air tightness leaking from one side

Results show, as expected, that when the leakage area increases the cotton pad reaches ignition temperature earlier, thus the FRR is reduced. This is caused by the increased quantities of hot gases allowed through the partition. Also, ignition is noticed earlier for the cotton pad located at the middle of the sample height. We can see from the Table 10 a difference of about 32% between a very loose constructions and a tight construction according to NMBCC. Moreover, if the results are compared to the one obtained with a localized leakage, section 7.4.1, we can see an increase of the FRR as presented in the Table 11, comparing to the values from Table 10 corresponding to the cotton pad in the middle of the furnace. However, the gain percentage of FRR decreases with the increase of air tightness. This implies that the leakage in a very tight construction is a less significant issue than a leakage in a loose construction.

Scenario	Increase of the FRR (%)
Average construction	62
Tight construction (NRCC)	35
Tight construction (AAMA)	17
Tight construction (NMBCC)	8

Table 11: Percentage change in FRR between localized and distributed leakage

7.4.3 Distributed leakage

Table 12 shows FRR for the sample with leakage area distributed over all the joints of the wall, as seen in Figure 25. The leakage area considered is presented in the Table 1.

Since, the leakage is distributed over all the joints of the wall, the volume of smoke going through the partition decreases. This causes the FRR to increase a little. The Table 12 shows a difference of 11% in the FRR between a very loose constructions and a tight construction according to NMBCC, which is less than in the previous section. Table 13 shows the increase of the FRR compare to the localized leakage, section 7.4.1, and to the distributed leakage on the right side, section 7.4.2. Leakage from every joints gives much better FRR compare to penetration, but the results do not increase much when compare to the results from section 7.4.2.

Scenario	Time until ignition of cotton pads (min)		
	Bottom of furnace	Middle of furnace	Top of furnace
Very loose construction	52	46	48
Loose construction	51	50	52
Average construction	54	52	54
Tight construction (NRCC)	54	50	54
Tight construction (AAMA)	54	53	54
Tight construction (NMBCC)	54	52	54

Table 12: FRR of partition with different air tightness leaking from every joints

Scenario	Increase of the FRR compared to section 9.3.1 (%)	Increase of the FRR compared to section 9.3.2 (%)
Average construction	92	18
Tight construction (NRCC)	47	8
Tight construction (AAMA)	29	10
Tight construction (NMBCC)	13	4

Table 13: Percentage change in FRR between leakage in all joints and the other scenarios for the cotton pad at mid height of the furnace

Figure 66 and Figure 67 show the temperature of the unexposed surface of the partition and of the surface of the cotton pad, for the scenario with leakage according to AAMA. By looking at the unexposed surface of the partition it is possible to see that the temperature on the unexposed surface is very high in the surrounding of the leakage area, compare to the rest of the sample. This causes the heat transfer by radiation to increase greatly, between the tested sample and the cotton pad. This could explain why the FRR does not change much, for very little values of leakage. Most of the heat transferred to the cotton pad seemed to be done by radiation and not by convection from hot gases. Also, this explains why the cotton pad located at the middle of the sample height gives the lower FRR. The cotton pad at this location is subjected to a higher heat flux by radiation, compare to the other two location measured.

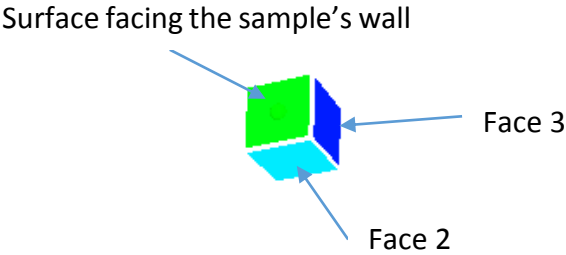


Figure 66: Temperature on the cotton pad after around 3600 seconds

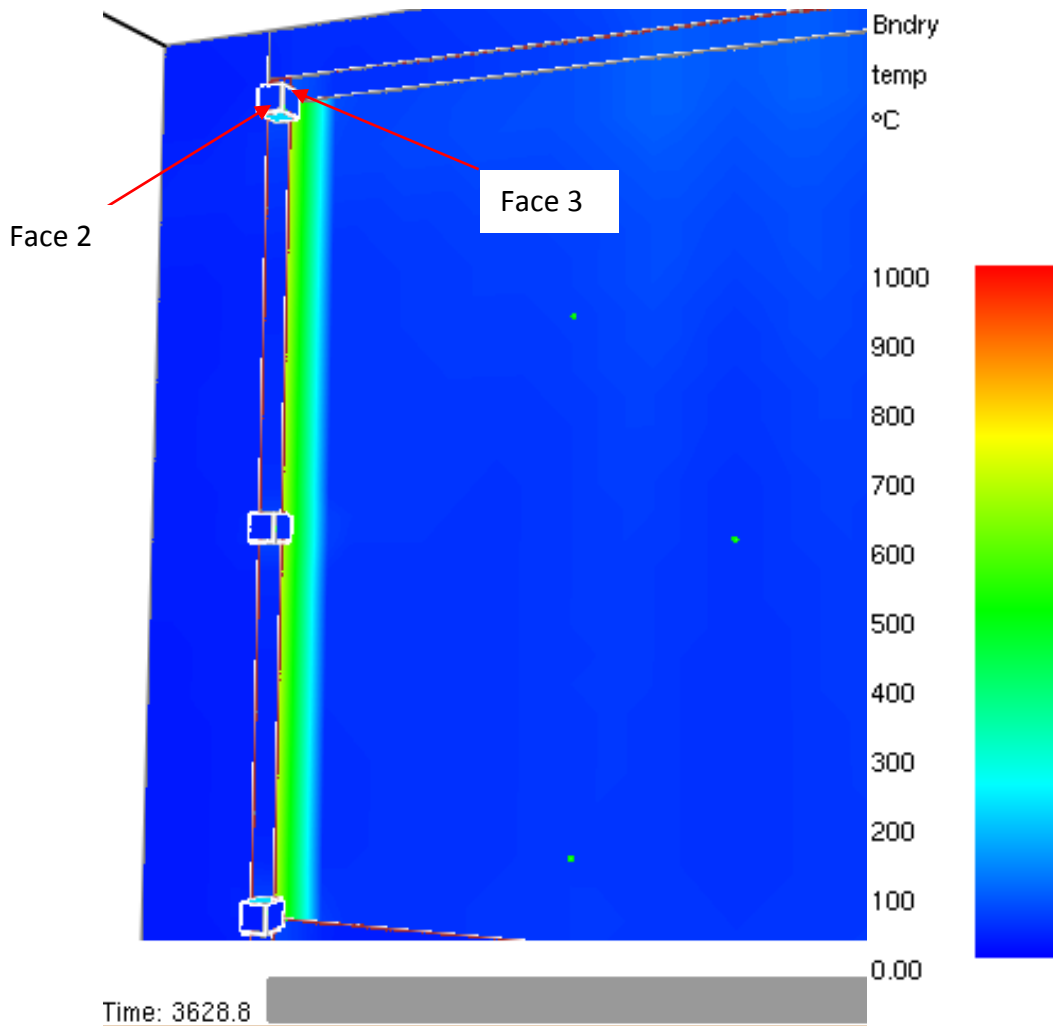


Figure 67: Temperature on the unexposed side of the tested sample after 3600 seconds

7.5 Discussion

The previous sections have presented simulation results in the form of time–temperature graphs, FRR-cases figures and temperature of cross section figures. Results help to understand how fire barriers are affected by different parameters. These graphs were used to describe the performance of each panel in term of insulation and integrity.

First, the impact of the thickness of plasterboard will be discussed. As seen from the data, plasterboard has a very huge impact on the FRR. By doubling the thickness of plasterboard the FRR is increase by 280%. This can be compared to insulation, which shows an increase of 175% of the FRR when the insulation is twice as thick, see section 7.1.3. Therefore, it seems more efficient for size limitation to increase the quantity of gypsum board. Still, it should be kept in mind that gypsum fails after prolonged time subjected to high temperature.

It was also found that if portion of insulation is missing from the cavity, higher temperatures are expected at the unexposed layer of gypsum, where insulation is missing. The area surrounding the location where insulation is missing is also affected as seen in Figure 56. In that area the FRR is greatly reduced, but at the other location the surface temperature remains unaffected. This is due to cavity radiation inside the empty cavity. As it will be discussed further, validation of the cavity radiation model should be done in order to express higher degree of confidence in these results.

Another important factor, which can be seen from the simulation, is the importance of insulation inside the cavity. Results show clearly that a fire resisting barrier has much more chance to withstand the fire for prolonged time if insulated. Indeed, results show lower temperature on the unexposed surface of insulated wall compare to wall with an empty cavity. Furthermore, when the plasterboard layer on the fire side is breached the temperature on the unexposed surface is directly affected. But, if insulation is used, the FRR is reduced less than a wall with an empty cavity. Since the insulation material acts as an extra surface and prevents heat from reaching the unexposed surface. This was found true especially with stone wool insulation, due to its incombustibility, represented in the simulation by lack of ablation. However, as found in section 7.1.5, if the breach reaches the surface it is not possible to prevent the heat transfer through the wall anymore and the resulting FRR falls to almost nothing. Although, the heat transfer from hot gases and from the furnace to the inside of the hole is hard to represent with exactitude in a numerical model, it is without a doubt that the partition is too compromised to be able to perform well under a fire.

On the other hand, when the wall is insulated, because of the low thermal conductivity of insulation, heat is redirected back to gypsum board exposed in the furnace. This results in the exposed gypsum layer to heat up faster, compare to a wall without insulation, as seen in Figure 36. This would result in a failure of the gypsum board faster when the wall is insulated compare to uninsulated. Indeed, as mentioned early in this work, failure of gypsum can be observed at temperature between 600°C and 700°C, therefore, the gypsum of the partition with insulation would be falling off before the partition without, thus, earlier exposing its insulation directly to the fire. Nonetheless, when failure of gypsum wall occurs it is better to have insulation in the cavity to protect the unexposed layer, otherwise the unexposed layer will quickly heat up. Regarding insulation, as it can be seen from Figure 35, stone wool reacts much better at higher temperature compare to Fiber glass wool due to the effect of ablation. Therefore, using such insulation material could be a problem if failure of the gypsum board occurs and insulation is directly exposed to the fire. But, if the gypsum layers do not fail, partition with fiberglass insulation can yield FRR similar to partition with stone wool insulation, see Figure 51. Also, other experiments on LSF showed that when the partition is insulated, lower FRR was found. This was due to bending of the partition resulting from a higher temperature in the steel stud. This could

not be analyzed during this study, but further work with ABAQUS could allow to investigate the effect of expansion and deformation of the steel studs.

Results show that the FRR of partition is greatly affected by leakage, even with tight construction. FRR of under 60min were found for all scenarios investigated, but the worst possible leakage scenario was for localized leakage area. The FRR was improved as the leakage area is reduced.

The cause of the ignition of the cotton pad seemed to be radiation from the surface of the gypsum board. Leakage through the partition increase the temperature on the unexposed surface very close to the ISO-834 and this causes the surface to radiate enough heat to the cotton pad to ignite. However, this means that the failure of the sample is more likely to be due to the insulation criterion since the unexposed reaches the maximum allowed temperature in a matter of minutes while the failure due to integrity is seen after more than 30 minutes.

7.6 Limitations and Uncertainties

When looking at limitations it is important to keep in mind that the results obtained are all the results of numerical simulations. As such simulations are never an exact representation of a real scenario. Also, numerous assumptions have been taken when modeling, not only in the data used, but also in the modeling methods used. One major modeling error can be associated with the cavity radiation in the models. The radiation inside the cavity is complex and will be affected by all the numerous surfaces inside the cavity as well as their temperature. However, the model used in the simulation is rather simple and as such, more validation on this should be done before being able to use the results with more confidence. There are uncertainties related to the heat transfer method used in ABAQUS. For example it is considered that the insulation is in perfect contact with the gypsum board while, in reality, there could be a thin gap of air between which would reduce the conduction. The same could happen between the studs and the gypsum board and the two layers of gypsum board. Also, there certain concern regarding FDS simulations. Since there was no validation done on for furnace test, the severity of the fire and temperature which occurs inside a furnace could exceed the limits of FDS, consequently, the results could be inaccurate.

This study shows the advantages of using mineral wool in fire rated barrier, however, some mineral wool materials are known to cause heat generation, when submitted to external heat flux. This effect was deliberately ignored due to its complexity, but certainly it would cause the temperature on the unexposed side of the wall to rise higher than what was seen in the simulation. Some research is currently being done at DBI on this matter and maybe in the future such phenomenon could be added to simulation. Another aspect, which wasn't considered in this study, is the effect of the vaporized water from gypsum. Indeed, as mentioned in the literature review, crystalline water inside the structure of gypsum vaporized at elevated temperature and

is forced out of the gypsum board. The effect of this water movement inside the partition with regards to the FRR was not considered, a specific study should be done concerning this phenomena.

This work focused on certain features of wall such as: reduced insulation, effect of wall penetration or increased leakage, however it did not consider the impact due to change in thermal properties. Manufacturers offer very wide variety of products with very specific and different properties. As mentioned before, FRR is very dependent on the thermal properties and as such the results obtained would differ for a wall using different types of materials. For example, results from simulation using a Fiberglass wool density equal to 100kg/m^3 showed a reduction on the unexposed surface temperature by 12%. Still, even if the exact results would be different, the impact of the investigated features should affect the FRR in the same way. Also, there are uncertainties related to the values used, these can come from error in the measurement methodology, precision of instruments and more.

In FDS the grid dimension plays an important role in the precision of the results. The coarse grid mesh used limited the number of radiation angles, which could be used, thus affecting the heat transfer inside and outside the furnace. Also, there are uncertainties related to modeling methods used. For example, added vents used to increase oxygen inside the furnace could alter the convective heat transfer coefficient inside the furnace. Also, experimental data would be needed in order to validate the heat transfer through cracks and leakage area, in order to determine how accurate FDS is. Then, the pressure at the top of the furnace exceeds the value required by the code. This causes the exfiltration of smoke to increase as well as the heat transfer. The use of fan in FDS could help maintain the pressure at a lower level. This would require additional work and also increase the computational time. Moreover, as mentioned in the introduction, the cotton pad sample needs to be applied in front of cracks for 30 seconds, then removed. However, it was not possible to simulate this in FDS so the cotton pad was located in front of the crack for all the duration of the test. This causes the cotton pad to reach the ignition temperature faster.

7.7 Validity

This work meant to give an idea on how the FRR barriers change depending on several parameters. Results provided a tendency which show how different parameter can affect the rating of barriers. Still, it is important to keep in mind that those results are valid for the case scenario considered in the scope of this work. A change in the fire-rated wall construction or in the dimension of the investigated parameters would lead to different results. For instance, concrete fire-rated wall would have a much higher thermal capacity and thus would probably take much more time to heat up. Moreover, as mentioned in the introduction, it was assumed that the wall do not collapse or deform excessively at elevated temperature. However, the type

of insulation could influence the temperature found inside the structure, as seen in section 7.1.1, thus influence the FRR based on the stability criterion.

8 Conclusions

Fire rated partition are built according to specifications taken from manufacturers. The objective of this work was to examine what happens to the FRR if the fire-rated barrier is built differently or is altered before it is subject to a fire. This study looked at the reliability of fire resistant structures with regards to the insulation and integrity criterion. This was done using numerical tools such as FDS for the integrity criterion and ABAQUS for the insulation criterion. No experiments were done during this study, however the models were validated using experimental data available. In general it was found that all the tested partitions with increased leakage or reduced insulation had a FRR too low to fulfill their purpose. More precisely the following elements were observed:

- For partition without deficiencies or alteration, stone wool insulation provided a FRR 13% and 40% higher compared to similar partition insulated with Fiberglass wool and uninsulated partition, respectively.
- Small breach (10mm radius) on the exposed layer of gypsum board did not affect the stone wool insulated partition, however the uninsulated partition FRR was found to be reduced by 50%. Also, when breached (10mm radius) Stone wool insulated partition provided a FRR approx. 20% and 70% higher than partition insulated with Fiberglass and uninsulated partition, respectively
- Larger breach (50mm radius) on the exposed layer of gypsum board reduced the FRR by 50% for partition with fiberglass wool and uninsulated partition and by 40% for partition with stone wool. Also, when breached (50mm radius) Stone wool insulated partition provided a FRR approx. 30% and 70% higher than partition insulated with Fiberglass and uninsulated partition, respectively
- Reduction by up to 25 % of the FRR was observed for reduction of the insulation thickness by up to 75%

Results showed that the leakage of hot gases at cracks caused the temperature on the unexposed surface to exceed the acceptable limits in a matter of minutes. Therefore, it is more likely that leaking walls will fail due to the insulation criterion rather than the integrity criterion. Still, the following observation could be made on the FRR of partition according solely to the integrity criterion.

- Leakage occurring through a hole caused a 55% reduction of the FRR, for an average air tight construction

- Leakage occurring on one side of the partition caused a 47% reduction of the FRR, for a very loose air tight construction
- Leakage occurring at all joint of the partition caused a 23% reduction of the FRR, for a very loose air tight construction

The results show clearly that in order to stay reliable, a fire-rated partition must be built and maintained as specified by the manufacturer. The results showed also that using stone wool insulation inside the cavity could help improving the FRR, based on the insulation criterion. This study showed a method to simulate fire resistance test with the help of numerical tools. This could be very useful, especially when considering the high cost of testing samples in furnaces. Still, much work needs to be done in order to accurately model a fire resistance test.

9 Future Work

In order to improve models on fire resistance test, further work should include the following:

- The effect on heat transfer of hot gases leaking through partition should be studied experimentally.
- The effect of heat transfer in empty cavity by radiation during a fire resistance test should be investigated. This would allow to validate the numerical models and help to find a way to reduce the heat transfer to the unexposed gypsum layer in an empty cavity partition.
- Numerical models of thermal expansion and deformation of the partition component such as steel studs, wooden studs and gypsum board, in order to include the stability criterion.
- The impact on the fire resistance rating of lightweight partition using steel or wooden studs.
- The influence of the heat generation in some woolen insulations materials and the impact on the FRR.
- The combustibility of the insulation material inside the cavity and its effect on the FRR.
- The dependency of FRR on the water movement inside the partition caused by water vaporization from the gypsum.

10 Acknowledgements

The author would like to thank Rockwool for support under the form of sponsorship which allowed me to participate in the International Master of Science in Fire Safety Engineering. Also the author wishes to express his gratitude to professor Patrick Van Hees and Bjarne Husted for all their support, guidance and assistance during the master thesis process.

11 References

- [1] P. Kolarkar and M. Mahendran, "Experimental studies of non-load bearing steel wall systems under fire conditions," *Fire Saf. J.*, vol. 53, pp. 85–104, 2012.
- [2] British Standards Institution, "Standards Publication Fire resistance tests Part 1 : General Requirements," 2012.
- [3] CertainTeed, "Gypsum Board Systems Manual," 2012. [Online]. Available: http://www.certainteed.com/resources/CTG_4080_Gypsum_Board_Systems_Manual_Eng.pdf. [Accessed: 21-Apr-2016].
- [4] D. Drysdale, "Heat Transfer," *An Introd. to Fire Dyn.*, pp. 35–82, 2011.
- [5] U. Wickström, R. Jansson, and H. Tuovinen, *Validation fire tests on using the adiabatic surface temperature for predicting heat transfer*, no. 310. 2009.
- [6] U. Wickström, *Methods for Predicting Temperatures in Fire-Exposed Structures*. 2015.
- [7] H. Takeda, "A model to predict fire resistance of non-load bearing wood-stud walls," *Fire Mater.*, vol. 27, no. 1, pp. 19–39, 2003.
- [8] S. Uvsløkk and H. Arnesen, "Thermal insulation performance of reflective material layers in well insulated timber frame structures," *8Th Symp. Build. Phys.*, 2008.
- [9] O. A. Ezekoye, "Conduction of Heat in Solids," *SFPE Handb. Fire Prot. Eng.*, vol. 5th Editio, pp. 25–52, 2015.
- [10] K. Livkiss, B. Andres, N. Johansson, and P. Van Hees, "Uncertainties in material thermal modelling of fire resistance tests," *Eur. Symp. Fire Saf. Sci.*, pp. 1–6, 2015.
- [11] M. A. Sultan, "Incident heat flux measurements in floor and wall furnaces of different sizes," *Fire Mater.*, vol. 30, no. 6, pp. 383–396, 2006.
- [12] C. Beyler, J. Beitel, N. Iwankiw, B. Lattimer, I. Hughes Associates, and N. F. P. Association, *Fire resistance testing for performance-based fire design of buildings*. 2007.
- [13] B. Park, *NFPA Standard for Smoke Control Systems 2012 Edition*. 2012.
- [14] W. Anis, "Commissioning the air barrier system," *ASHRAE J.*, vol. 47, no. 3, pp. 35–44, 2005.
- [15] R. Smith, "Passive fire protection," *Struct. Surv.*, vol. Vol. 11 Is, p. pp.142 – 149, 1993.
- [16] CertainTeed Saint Gobain, "Type X Gypsum Board." [Online]. Available: <http://www.certainteed.com/Products/313675>. [Accessed: 15-Apr-2016].
- [17] J. Lindholm, A. Brink, and M. Hupa, "Cone calorimeter – a tool for measuring heat release rate," *Finnish-Swedish Flame Days 2009*, p. 4B, 2009.
- [18] I. Rahmanian, "Thermal and Mechanical Properties of Gypsum Boards and Their Influences

- on Fire Resistance of Gypsum Board Based Systems,” 2011.
- [19] P. Keerthan and M. Mahendran, “Thermal Performance of Composite Panels Under Fire Conditions Using Numerical Studies: Plasterboards, Rockwool, Glass Fibre and Cellulose Insulations,” *Fire Technol.*, vol. 49, no. 2, pp. 329–356, 2013.
- [20] Andrew H. Buchanan, *Structural Design for Fire Safety*. 2001.
- [21] ENGINEERING TOOLBOX, “Air Properties.” [Online]. Available: http://www.engineeringtoolbox.com/air-properties-d_156.html. [Accessed: 06-Apr-2016].
- [22] THE ENGINEERING TOOLBOX, “Emissivity Coefficients of some common Materials,” 2016. [Online]. Available: http://www.engineeringtoolbox.com/emissivity-coefficients-d_447.html. [Accessed: 06-Apr-2016].
- [23] A. Wolfenden, T. Harmathy, M. Sultan, and J. MacLaurin, “Comparison of Severity of Exposure in ASTM E 119 and ISO 834 Fire Resistance Tests,” *J. Test. Eval.*, vol. 15, no. January, pp. 371–375, 1987.
- [24] THE ENGINEERING TOOLBOX, “Thermal Conductivity of Materials and Gases.” [Online]. Available: http://www.engineeringtoolbox.com/thermal-conductivity-d_429.html. [Accessed: 27-Mar-2016].
- [25] ENGINEERING TOOLBOX, “Densities of Solids.” [Online]. Available: http://www.engineeringtoolbox.com/density-solids-d_1265.html. [Accessed: 27-Mar-2016].
- [26] ENGINEERING TOOLBOX, “Solids - Specific Heats.” [Online]. Available: http://www.engineeringtoolbox.com/specific-heat-solids-d_154.html. [Accessed: 27-Mar-2016].
- [27] K. Mcgrattan and R. Mcdermott, “Fire Dynamics Simulator User ’ s Guide,” 2013.
- [28] D. Drysdale, “Fire Science and Combustion,” *An Introd. to Fire Dyn.*, pp. 1–34, 2011.
- [29] K. J. Overholt, “Simulation of a Fire in a Hillside Residential Structure - San Francisco , CA,” 1856.
- [30] M. Feng, Y. C. Wang, and J. M. Davies, “Thermal performance of cold-formed thin-walled steel panel systems in fire,” *Fire Saf. J.*, vol. 38, no. 4, pp. 365–394, 2003.
- [31] British Standards Institution, “Eurocode 1 — Actions on structures,” no. February, 2013.
- [32] A. Bruls and P. Vandeveldel, *Sécurité contre l ’ incendie dans les bâtiments*, Mai 2000. 1980.
- [33] M. A. Sultan, “A model for predicting heat transfer through noninsulated unloaded steel-stud gypsum board wall assemblies exposed to fire,” *Fire Technol.*, vol. 32, no. 3, pp. 239–

259, 1996.

Appendix A: FDS script file

Following is the script file for the FDS furnace modeling with a very loose air tight construction leaking on one side:

```
&HEAD CHID='nrcc3'/ FURNACE TEST

FYI = 'Room and mesh definition',

&MESH ID='GRID',IJK=24,48,36,XB=0.0,2.4,-2.4,2.4,0.0,3.6/

&TIME T_END= 7200.0/ 2 hours standard fire

&MISC TMPA=20.,

&DUMP DT_DEVC=5/ DATAS EVERY 5 sec

//-----
-----//
//----- FUEL AND BURNERS PARAMETERS -----
-----//
//-----
-----//

//-- RADIATION --//

&RADI RADIATION=.TRUE.,RADIATIVE_FRACTION=0.3, NUMBER_RADIATION_ANGLES=104/

//-- FUEL DESCRIPTION --//

&REAC FUEL = 'PROPANE',

FYI = 'Propane, C_3 H_8',
C= 3.0,
H = 8.0,
O=0.0,
N=0.0,
SOOT_YIELD =0.01,
CO_YIELD =0.02,
HEAT_OF_COMBUSTION=46450.0,
IDEAL=.TRUE./

&SURF ID='FIRE',
HRRPUA=8000,
COLOR='RED'/ HRR in kW/m2

//-- BURNER PORTS --//
```


&VENT XB=0.2,0.2,0.1,0.2,1.6,1.7,SURF_ID='FIRE' ,CTRL_ID='VENT6' /
&VENT XB=0.2,0.2,0.4,0.5,1.6,1.7,SURF_ID='FIRE' , CTRL_ID='VENT6' /
&VENT XB=0.2,0.2,0.7,0.8,1.6,1.7,SURF_ID='FIRE' , CTRL_ID='VENT6' /
&VENT XB=0.2,0.2,1.0,1.1,1.6,1.7,SURF_ID='FIRE' , CTRL_ID='VENT6' /
&VENT XB=0.2,0.2,1.3,1.4,1.6,1.7,SURF_ID='FIRE' , CTRL_ID='VENT6' /

&VENT XB=0.2,0.2, -1.4, -1.3,1.9,2,SURF_ID='FIRE' ,CTRL_ID='VENT3' /
&VENT XB=0.2,0.2, -1.1, -1.0,1.9,2,SURF_ID='FIRE' ,CTRL_ID='VENT3' /
&VENT XB=0.2,0.2, -0.8, -0.7,1.9,2,SURF_ID='FIRE' ,CTRL_ID='VENT3' /
&VENT XB=0.2,0.2, -0.5, -0.4,1.9,2,SURF_ID='FIRE' ,CTRL_ID='VENT3' /
&VENT XB=0.2,0.2, -0.2, -0.1,1.9,2,SURF_ID='FIRE' ,CTRL_ID='VENT3' /
&VENT XB=0.2,0.2,0.1,0.2,1.9,2,SURF_ID='FIRE' , CTRL_ID='VENT4' /
&VENT XB=0.2,0.2,0.4,0.5,1.9,2,SURF_ID='FIRE' ,CTRL_ID='VENT4' /
&VENT XB=0.2,0.2,0.7,0.8,1.9,2,SURF_ID='FIRE' ,CTRL_ID='VENT4' /
&VENT XB=0.2,0.2,1.0,1.1,1.9,2,SURF_ID='FIRE' ,CTRL_ID='VENT4' /
&VENT XB=0.2,0.2,1.3,1.4,1.9,2,SURF_ID='FIRE' ,CTRL_ID='VENT4' /

&VENT XB=0.2,0.2, -1.4, -1.3,2.2,2.3,SURF_ID='FIRE' ,CTRL_ID='VENT3' /
&VENT XB=0.2,0.2, -1.1, -1.0,2.2,2.3,SURF_ID='FIRE' ,CTRL_ID='VENT3' /
&VENT XB=0.2,0.2, -0.8, -0.7,2.2,2.3,SURF_ID='FIRE' ,CTRL_ID='VENT3' /
&VENT XB=0.2,0.2, -0.5, -0.4,2.2,2.3,SURF_ID='FIRE' ,CTRL_ID='VENT3' /
&VENT XB=0.2,0.2, -0.2, -0.1,2.2,2.3,SURF_ID='FIRE' ,CTRL_ID='VENT3' /
&VENT XB=0.2,0.2,0.1,0.2,2.2,2.3,SURF_ID='FIRE' ,CTRL_ID='VENT4' /
&VENT XB=0.2,0.2,0.4,0.5,2.2,2.3,SURF_ID='FIRE' ,CTRL_ID='VENT4' /
&VENT XB=0.2,0.2,0.7,0.8,2.2,2.3,SURF_ID='FIRE' ,CTRL_ID='VENT4' /
&VENT XB=0.2,0.2,1.0,1.1,2.2,2.3,SURF_ID='FIRE' ,CTRL_ID='VENT4' /
&VENT XB=0.2,0.2,1.3,1.4,2.2,2.3,SURF_ID='FIRE' ,CTRL_ID='VENT4' /

&VENT XB=0.2,0.2, -1.4, -1.3,2.5,2.6,SURF_ID='FIRE' ,CTRL_ID='VENT3' /
&VENT XB=0.2,0.2, -1.1, -1.0,2.5,2.6,SURF_ID='FIRE' ,CTRL_ID='VENT3' /
&VENT XB=0.2,0.2, -0.8, -0.7,2.5,2.6,SURF_ID='FIRE' ,CTRL_ID='VENT3' /
&VENT XB=0.2,0.2, -0.5, -0.4,2.5,2.6,SURF_ID='FIRE' ,CTRL_ID='VENT3' /
&VENT XB=0.2,0.2, -0.2, -0.1,2.5,2.6,SURF_ID='FIRE' ,CTRL_ID='VENT3' /
&VENT XB=0.2,0.2,0.1,0.2,2.5,2.6,SURF_ID='FIRE' ,CTRL_ID='VENT4' /
&VENT XB=0.2,0.2,0.4,0.5,2.5,2.6,SURF_ID='FIRE' ,CTRL_ID='VENT4' /
&VENT XB=0.2,0.2,0.7,0.8,2.5,2.6,SURF_ID='FIRE' ,CTRL_ID='VENT4' /
&VENT XB=0.2,0.2,1.0,1.1,2.5,2.6,SURF_ID='FIRE' ,CTRL_ID='VENT4' /
&VENT XB=0.2,0.2,1.3,1.4,2.5,2.6,SURF_ID='FIRE' ,CTRL_ID='VENT4' /

&VENT XB=0.2,0.2, -1.4, -1.3,2.8,2.9,SURF_ID='FIRE' , CTRL_ID='VENT3' /
&VENT XB=0.2,0.2, -1.1, -1.0,2.8,2.9,SURF_ID='FIRE' , CTRL_ID='VENT3' /
&VENT XB=0.2,0.2, -0.8, -0.7,2.8,2.9,SURF_ID='FIRE' , CTRL_ID='VENT3' /
&VENT XB=0.2,0.2, -0.5, -0.4,2.8,2.9,SURF_ID='FIRE' , CTRL_ID='VENT3' /
&VENT XB=0.2,0.2, -0.2, -0.1,2.8,2.9,SURF_ID='FIRE' ,CTRL_ID='VENT3' /
&VENT XB=0.2,0.2,0.1,0.2,2.8,2.9,SURF_ID='FIRE' ,CTRL_ID='VENT4' /
&VENT XB=0.2,0.2,0.4,0.5,2.8,2.9,SURF_ID='FIRE' ,CTRL_ID='VENT4' /
&VENT XB=0.2,0.2,0.7,0.8,2.8,2.9,SURF_ID='FIRE' , CTRL_ID='VENT4' /
&VENT XB=0.2,0.2,1.0,1.1,2.8,2.9,SURF_ID='FIRE' , CTRL_ID='VENT4' /
&VENT XB=0.2,0.2,1.3,1.4,2.8,2.9,SURF_ID='FIRE' , CTRL_ID='VENT4' /

```
//-----  
-----//  
//----- MATERIALS AND SURFACE SETUP -----  
-----//  
//-----  
-----//
```

```
//-- SETTING UP MATERIALS --//
```

```
&MATL ID = 'MATL_FURNACE_WALL'  
CONDUCTIVITY = 0.34  
SPECIFIC_HEAT = 1  
DENSITY = 880 /
```

```
&MATL ID='COTTON PAD',  
EMISSIVITY = 0.8,  
DENSITY = 150,  
SPECIFIC_HEAT = 1.34,  
CONDUCTIVITY = 0.23,/
```

```
&MATL ID='CERAMIC BLANKET',  
EMISSIVITY = 0.8,  
DENSITY = 160,  
SPECIFIC_HEAT = 1.15,  
CONDUCTIVITY = 0.04,/
```

```
&MATL ID = 'ROCKWOOL',  
EMISSIVITY = 0.8,  
DENSITY = 711,
```

```
CONDUCTIVITY_RAMP = 'k_ramp1',
```

```
SPECIFIC_HEAT = 0.9,/
```

```
&RAMP ID='k_ramp1', T= 50., F=0.25 /  
&RAMP ID='k_ramp1', T=200., F=0.26 /  
&RAMP ID='k_ramp1', T=500., F=0.295 /  
&RAMP ID='k_ramp1', T=600., F=.42 /  
&RAMP ID='k_ramp1', T=700., F=.68 /  
&RAMP ID='k_ramp1', T=800., F=.94 /  
&RAMP ID='k_ramp1', T=900., F=1.2 /  
&RAMP ID='k_ramp1', T=1000., F=1.46 /  
&RAMP ID='k_ramp1', T=1200., F=1.98 /
```

```
&MATL ID = 'GYPSUM',  
EMISSIVITY = 0.8,  
DENSITY = 711,  
CONDUCTIVITY_RAMP = 'k_ramp2',
```

```
SPECIFIC_HEAT_RAMP = 'c_ramp2',/
```

```
&RAMP ID='c_ramp2', T= 20., F=1.000 /  
&RAMP ID='c_ramp2', T= 50., F=1.100 /  
&RAMP ID='c_ramp2', T= 100., F=1.500 /  
&RAMP ID='c_ramp2', T= 120., F=1.600 /  
&RAMP ID='c_ramp2', T= 140., F=2.100 /  
&RAMP ID='c_ramp2', T= 160., F=20.000 /  
&RAMP ID='c_ramp2', T= 170., F=7.000 /  
&RAMP ID='c_ramp2', T= 180., F=2.100 /  
&RAMP ID='c_ramp2', T= 200., F=9.000 /  
&RAMP ID='c_ramp2', T= 220., F=1.500 /  
&RAMP ID='c_ramp2', T= 260., F=1.100 /  
&RAMP ID='c_ramp2', T= 400., F=1.000 /  
&RAMP ID='c_ramp2', T= 430., F=.500 /  
&RAMP ID='c_ramp2', T= 450., F=.800 /  
&RAMP ID='c_ramp2', T= 500., F=.900 /  
&RAMP ID='c_ramp2', T= 600., F=1.000 /  
&RAMP ID='c_ramp2', T= 1200., F=1.000 /
```

```
&RAMP ID='k_ramp2', T= 20., F=0.17 /  
&RAMP ID='k_ramp2', T=50., F=0.17 /  
&RAMP ID='k_ramp2', T=100., F=0.18 /  
&RAMP ID='k_ramp2', T=150., F=0.195 /  
&RAMP ID='k_ramp2', T=200., F=0.195 /  
&RAMP ID='k_ramp2', T=250., F=0.197 /  
&RAMP ID='k_ramp2', T=300., F=0.2 /  
&RAMP ID='k_ramp2', T=350., F=0.21 /  
&RAMP ID='k_ramp2', T=400., F=0.22 /  
&RAMP ID='k_ramp2', T=450., F=0.22 /  
&RAMP ID='k_ramp2', T=500., F=0.23 /  
&RAMP ID='k_ramp2', T=550., F=0.24 /  
&RAMP ID='k_ramp2', T=600., F=0.24 /  
&RAMP ID='k_ramp2', T=650., F=0.26 /  
&RAMP ID='k_ramp2', T=700., F=0.28 /  
&RAMP ID='k_ramp2', T=1200., F=0.28 /
```

```
&MATL ID = 'MATL_MIN_WOOL_300'  
CONDUCTIVITY = 0.037  
SPECIFIC_HEAT = 0.8  
DENSITY = 300 /
```

```
&MATL ID = 'MATL_NICKEL'  
CONDUCTIVITY = 90.9  
SPECIFIC_HEAT = 0.44  
DENSITY = 8908 /
```

```
//-- SETTING UP SURFACES --//
```

```
&SURF ID = 'FURNACEWALLS',
DEFAULT=.TRUE.,
MATL_ID='CERAMIC BLANKET',
BACKING = 'INSULATED',
COLOR='BROWN',
Transparency=0.1,
THICKNESS= 0.5,/
```

```
&SURF ID = 'COTTON PAD',
DEFAULT=.TRUE.,
MATL_ID='COTTON PAD',
BACKING = 'INSULATED',
COLOR='WHITE',
THICKNESS= 0.03,/
```

```
&SURF ID = 'DRYWALL INSULATED',
DEFAULT=.TRUE.,
MATL_ID = 'GYPSUM', 'ROCKWOOL', 'GYPSUM',
BACKING = 'EXPOSED',
COLOR='GRAY',
THICKNESS = 0.025,0.045,0.025/
```

```
&SURF ID = 'PLATE_THERMOMETER'
MATL_ID(1,1) = 'MATL_NICKEL'
MATL_ID(2,1) = 'MATL_MIN_WOOL_300'
MATL_ID(3,1) = 'MATL_NICKEL'
BACKING = 'EXPOSED'
EMISSIVITY_BACK = 0.80
THICKNESS = 0.0007,0.097,0.0007 /
```

```
//-----
-----//
//----- ROOM SET UP -----
-----//
//-----
-----//
```

```
//-- FURNACE --//
```

```
FYI = 'Walls for the furnace from 0,2 to 0,8=0,60 from -1.8 to 1.8 =3,6 and
from 0.2 to 3.3 = 3,1',
```

```
&OBST XB=0.2,0.8,1.8,1.9,0.0,3.4,SURF_ID='FURNACEWALLS',/ SIDE WALL&OBST
XB=0.2,0.8,-1.8,-1.9,0.0,3.4,SURF_ID='FURNACEWALLS',/ SIDE WALL
&OBST XB=0.1,0.2,-1.9,1.9,0.0,3.4,SURF_ID='FURNACEWALLS'/ BACK WALL
```

```

&OBST XB=0.2,0.8,-1.8,1.8,0.1,0.2,SURF_ID='FURNACEWALLS' / FLOOR
&OBST XB=0.2,0.8,-1.8,1.8,3.3,3.4,SURF_ID='FURNACEWALLS' / CEILING

//-- SMOKE AND HEAT STOPER --//

&OBST XB=0.7,0.8,1.9,2.4,-0.6,3.6/
&OBST XB=0.7,0.8,-1.9,-2.4,-0.6,3.6/
&OBST XB=0.7,0.8,-1.9,1.9,-0.6,0.1/
&OBST XB=0.7,0.8,-1.9,1.9,3.4,3.6/

//-- TEST SAMPLE --//

FYI = 'Fire barrier',

&OBST XB=0.7,0.8,-1.8,1.8,0.2,3.3,SURF_ID='DRYWALL INSULATED' /

//-- COTTON PAD --//

&OBST XB=0.9,1.0,-1.7,-1.8,3.2,3.3,SURF_ID='COTTON PAD' / 1
&OBST XB=0.9,1.0,-1.7,-1.8,1.6,1.7,SURF_ID='COTTON PAD' / 2
&OBST XB=0.9,1.0,-1.7,-1.8,0.2,0.3,SURF_ID='COTTON PAD' / 3

//-- LEAKAGE --//

&VENT XB=0.7,0.7,-1.7,-1.8,0.2,3.3, SURF_ID='HVAC',ID='IN' /
&VENT XB=0.8,0.8,-1.7,-1.8,0.2,3.3, SURF_ID='HVAC',ID='OUT' /

&HVAC ID='IN',TYPE_ID='NODE',DUCT_ID='DUCT1',VENT_ID='IN' /
&HVAC ID='OUT',TYPE_ID='NODE',DUCT_ID='DUCT1',VENT_ID='OUT' /
&HVAC ID='DUCT1',TYPE_ID='DUCT',NODE_ID='IN','OUT',LENGTH=0.075
,AREA=0.014508,LOSS=1.,1./

//-- SMOKE EXCTRACTION --//

&HOLE XB=0.2,0.6,1.8,-1.8,0.1,0.2, / EXHAUST UNDER FURNACE

&HOLE XB=0.2,0.6,1.8,-1.8,3.2,3.4, CTRL_ID='EXHAUST1' / CONTROLLED EXHAUST TOP
FURNACE

//-- VENTING THE ROOM --//

&VENT MB='XMIN', SURF_ID='OPEN' /
&VENT MB='XMAX', SURF_ID='OPEN' /
&VENT MB='YMIN', SURF_ID='OPEN' /
&VENT MB='YMAX', SURF_ID='OPEN' /
&VENT MB='ZMAX', SURF_ID='OPEN' /
&VENT MB='ZMIN', SURF_ID='OPEN' /

//-- PLATE THERMOMETER OBSTRUCTION --//

```

```

&OBST XB=0.5,0.6,0.8,0.9,0.6,0.7, SURF_ID='PLATE_THERMOMETER' /
&OBST XB=0.5,0.6,-0.8,-0.9,0.6,0.7, SURF_ID='PLATE_THERMOMETER' /
&OBST XB=0.5,0.6,0.8,0.9,2.5,2.6, SURF_ID='PLATE_THERMOMETER' /
&OBST XB=0.5,0.6,-0.8,-0.9,2.5,2.6, SURF_ID='PLATE_THERMOMETER' /
&OBST XB=0.5,0.6,0.0,0.1,1.7,1.8, SURF_ID='PLATE_THERMOMETER' /

//-----
-----//
//----- CONTROLS -----
-----//
//-----
-----//

//-- PRESSURE CONTROL --//

&CTRL ID='EXHAUST1', FUNCTION_TYPE='DEADBAND', INPUT_ID='PRESSUREDEV',
ON_BOUND='UPPER', SETPOINT=28,30, LATCH=.FALSE., INITIAL_STATE=.FALSE./

//-- OXYGEN CONTROL --//

&SPEC ID='OXYGEN' / DEFINE THE OXYGEN
&SURF ID='SUPPLY',SPEC_ID='AIR', MASS_FLUX=1.0,TMP_FRONT=1050. ,
COLOR='BLUE',Transparency=0.1, RAMP_T='RAMP_ISO', / SPECIFY THE QUANTITY OF
OXYGEN INPUT kg/s
&DEVC XB=0.2,0.7,-1.8,1.8,0.2,3.2, QUANTITY='MASS FRACTION',SPEC_ID='OXYGEN',
ID='OXY', STATISTICS='MEAN' /
&CTRL ID='OXYGEN', FUNCTION_TYPE='DEADBAND', INPUT_ID='OXY',
ON_BOUND='LOWER', SETPOINT=0.18,0.20, LATCH=.FALSE.,INITIAL_STATE=.FALSE./
CONTROL THE OXYGEN LEVEL

&VENT XB=0.2,0.2,-1.8,1.8,0.8,1.0,SURF_ID='SUPPLY', CTRL_ID='OXYGEN' / SURFACE
OXYGEN IN
&VENT XB=0.2,0.2,-1.8,1.8,1.1,1.3,SURF_ID='SUPPLY', CTRL_ID='OXYGEN' / SURFACE
OXYGEN IN
&VENT XB=0.2,0.2,-1.8,1.8,1.4,1.6,SURF_ID='SUPPLY', CTRL_ID='OXYGEN' / SURFACE
OXYGEN IN
&VENT XB=0.2,0.2,-1.8,1.8,0.5,0.7,SURF_ID='SUPPLY', CTRL_ID='OXYGEN' / SURFACE
OXYGEN IN
&VENT XB=0.2,0.2,-1.8,1.8,1.7,1.9,SURF_ID='SUPPLY', CTRL_ID='OXYGEN' / SURFACE
OXYGEN IN
&VENT XB=0.2,0.2,-1.8,1.8,2.0,2.2,SURF_ID='SUPPLY', CTRL_ID='OXYGEN' / SURFACE
OXYGEN IN
&VENT XB=0.2,0.2,-1.8,1.8,2.3,2.5,SURF_ID='SUPPLY', CTRL_ID='OXYGEN' / SURFACE
OXYGEN IN
&VENT XB=0.2,0.2,-1.8,1.8,2.6,2.8,SURF_ID='SUPPLY', CTRL_ID='OXYGEN' / SURFACE
OXYGEN IN

//--TEMPERATURE CONTROL--//

```

```
/-- Hot plate in temperature control room at temperature of ISO-curve --/  
  
&SURF ID='HOT_PLATE1', TMP_FRONT=1050. , COLOR='RED', RAMP_T='RAMP_ISO', /  
&OBST XB=2.2,2.4,-0.1,0.1,3.3,3.5, SURF_ID='HOT_PLATE1' /  
&DEVC XYZ=2.3,0.0,3.4, QUANTITY='WALL TEMPERATURE', ID='TEMP_ISO1', IOR=3 /
```

```
/-- ISO Time-temp-curve --/
```

```
&RAMP ID='RAMP_ISO', T= 0000 ,F= 0 /  
&RAMP ID='RAMP_ISO', T= 0001 ,F= 0.018224171 /  
&RAMP ID='RAMP_ISO', T= 0002 ,F= 0.034418995 /  
&RAMP ID='RAMP_ISO', T= 0003 ,F= 0.048991481 /  
&RAMP ID='RAMP_ISO', T= 0004 ,F= 0.062237275 /  
&RAMP ID='RAMP_ISO', T= 0005 ,F= 0.074377916 /  
&RAMP ID='RAMP_ISO', T= 0006 ,F= 0.085583701 /  
&RAMP ID='RAMP_ISO', T= 0007 ,F= 0.095988364 /  
&RAMP ID='RAMP_ISO', T= 0008 ,F= 0.105698851 /  
&RAMP ID='RAMP_ISO', T= 0009 ,F= 0.114802024 /  
&RAMP ID='RAMP_ISO', T= 0010 ,F= 0.123369397 /  
&RAMP ID='RAMP_ISO', T= 0011 ,F= 0.131460553 /  
&RAMP ID='RAMP_ISO', T= 0012 ,F= 0.139125656 /  
&RAMP ID='RAMP_ISO', T= 0013 ,F= 0.14640734 /  
&RAMP ID='RAMP_ISO', T= 0014 ,F= 0.153342143 /  
&RAMP ID='RAMP_ISO', T= 0015 ,F= 0.159961617 /  
&RAMP ID='RAMP_ISO', T= 0016 ,F= 0.166293194 /  
&RAMP ID='RAMP_ISO', T= 0017 ,F= 0.172360878 /  
&RAMP ID='RAMP_ISO', T= 0018 ,F= 0.178185788 /  
&RAMP ID='RAMP_ISO', T= 0019 ,F= 0.183786607 /  
&RAMP ID='RAMP_ISO', T= 0020 ,F= 0.18917994 /  
&RAMP ID='RAMP_ISO', T= 0022 ,F= 0.199401914 /  
&RAMP ID='RAMP_ISO', T= 0024 ,F= 0.208953097 /  
&RAMP ID='RAMP_ISO', T= 0026 ,F= 0.217916132 /  
&RAMP ID='RAMP_ISO', T= 0030 ,F= 0.234339533 /  
&RAMP ID='RAMP_ISO', T= 0032 ,F= 0.241905044 /  
&RAMP ID='RAMP_ISO', T= 0034 ,F= 0.249096794 /  
&RAMP ID='RAMP_ISO', T= 0036 ,F= 0.255949981 /  
&RAMP ID='RAMP_ISO', T= 0038 ,F= 0.262495053 /  
&RAMP ID='RAMP_ISO', T= 0040 ,F= 0.268758528 /  
&RAMP ID='RAMP_ISO', T= 0045 ,F= 0.283331013 /  
&RAMP ID='RAMP_ISO', T= 0050 ,F= 0.296576808 /  
&RAMP ID='RAMP_ISO', T= 0055 ,F= 0.308717449 /  
&RAMP ID='RAMP_ISO', T= 0060 ,F= 0.319923233 /  
&RAMP ID='RAMP_ISO', T= 0065 ,F= 0.330327897 /  
&RAMP ID='RAMP_ISO', T= 0070 ,F= 0.340038383 /  
&RAMP ID='RAMP_ISO', T= 0075 ,F= 0.349141556 /  
&RAMP ID='RAMP_ISO', T= 0080 ,F= 0.357708929 /  
&RAMP ID='RAMP_ISO', T= 0090 ,F= 0.373465189 /  
&RAMP ID='RAMP_ISO', T= 0100 ,F= 0.387681676 /  
&RAMP ID='RAMP_ISO', T= 0110 ,F= 0.400632727 /  
&RAMP ID='RAMP_ISO', T= 0120 ,F= 0.41252532 /
```

&RAMP ID='RAMP_ISO', T= 0130 ,F= 0.423519472 /
&RAMP ID='RAMP_ISO', T= 0140 ,F= 0.433741447 /
&RAMP ID='RAMP_ISO', T= 0150 ,F= 0.44329263 /
&RAMP ID='RAMP_ISO', T= 0175 ,F= 0.4647436 /
&RAMP ID='RAMP_ISO', T= 0200 ,F= 0.483436327 /
&RAMP ID='RAMP_ISO', T= 0225 ,F= 0.5 /
&RAMP ID='RAMP_ISO', T= 0250 ,F= 0.514870395 /
&RAMP ID='RAMP_ISO', T= 0275 ,F= 0.52836183 /
&RAMP ID='RAMP_ISO', T= 0300 ,F= 0.540708489 /
&RAMP ID='RAMP_ISO', T= 0325 ,F= 0.552089541 /
&RAMP ID='RAMP_ISO', T= 0350 ,F= 0.562645128 /
&RAMP ID='RAMP_ISO', T= 0375 ,F= 0.572486937 /
&RAMP ID='RAMP_ISO', T= 0400 ,F= 0.581705416 /
&RAMP ID='RAMP_ISO', T= 0425 ,F= 0.590374842 /
&RAMP ID='RAMP_ISO', T= 0450 ,F= 0.598556957 /
&RAMP ID='RAMP_ISO', T= 0500 ,F= 0.61365891 /
&RAMP ID='RAMP_ISO', T= 0550 ,F= 0.627340643 /
&RAMP ID='RAMP_ISO', T= 0600 ,F= 0.639846466 /
&RAMP ID='RAMP_ISO', T= 0650 ,F= 0.651362611 /
&RAMP ID='RAMP_ISO', T= 0700 ,F= 0.662034297 /
&RAMP ID='RAMP_ISO', T= 0750 ,F= 0.671976953 /
&RAMP ID='RAMP_ISO', T= 0800 ,F= 0.681283848 /
&RAMP ID='RAMP_ISO', T= 0900 ,F= 0.698283112 /
&RAMP ID='RAMP_ISO', T= 1000 ,F= 0.713503572 /
&RAMP ID='RAMP_ISO', T= 1100 ,F= 0.727282483 /
&RAMP ID='RAMP_ISO', T= 1200 ,F= 0.739869438 /
&RAMP ID='RAMP_ISO', T= 1300 ,F= 0.75145434 /
&RAMP ID='RAMP_ISO', T= 1400 ,F= 0.762185039 /
&RAMP ID='RAMP_ISO', T= 1600 ,F= 0.78153064 /
&RAMP ID='RAMP_ISO', T= 1800 ,F= 0.798604742 /
&RAMP ID='RAMP_ISO', T= 2000 ,F= 0.813885156 /
&RAMP ID='RAMP_ISO', T= 2200 ,F= 0.827713176 /
&RAMP ID='RAMP_ISO', T= 2400 ,F= 0.840341093 /
&RAMP ID='RAMP_ISO', T= 2600 ,F= 0.851960683 /
&RAMP ID='RAMP_ISO', T= 2800 ,F= 0.862721133 /
&RAMP ID='RAMP_ISO', T= 3000 ,F= 0.872740792 /
&RAMP ID='RAMP_ISO', T= 3400 ,F= 0.89092224 /
&RAMP ID='RAMP_ISO', T= 3800 ,F= 0.907083325 /
&RAMP ID='RAMP_ISO', T= 4200 ,F= 0.921628493 /
&RAMP ID='RAMP_ISO', T= 4600 ,F= 0.934851717 /
&RAMP ID='RAMP_ISO', T= 5000 ,F= 0.946973396 /
&RAMP ID='RAMP_ISO', T= 5500 ,F= 0.960831049 /
&RAMP ID='RAMP_ISO', T= 6000 ,F= 0.973483672 /
&RAMP ID='RAMP_ISO', T= 6500 ,F= 0.985124174 /
&RAMP ID='RAMP_ISO', T= 7000 ,F= 0.995902555 /
&RAMP ID='RAMP_ISO', T= 7200 ,F= 1 /
&RAMP ID='RAMP_ISO', T= 7300 ,F= 1 /

//-- Control of heater in furnace --//

```

&CTRL ID='VENT1', FUNCTION_TYPE='SUBTRACT',
INPUT_ID='TEMP_IS01','PLATE_T_01', SETPOINT=0,
LATCH=.FALSE., INITIAL_STATE=.TRUE.,TRIP_DIRECTION=-1 /
&CTRL ID='VENT2', FUNCTION_TYPE='SUBTRACT',
INPUT_ID='TEMP_IS01','PLATE_T_02', SETPOINT=0,
LATCH=.FALSE., INITIAL_STATE=.TRUE. ,TRIP_DIRECTION=-1/
&CTRL ID='VENT3', FUNCTION_TYPE='SUBTRACT',
INPUT_ID='TEMP_IS01','PLATE_T_03', SETPOINT=0,
LATCH=.FALSE., INITIAL_STATE=.TRUE.,TRIP_DIRECTION=-1 /
&CTRL ID='VENT4', FUNCTION_TYPE='SUBTRACT',
INPUT_ID='TEMP_IS01','PLATE_T_04', SETPOINT=0,
LATCH=.FALSE., INITIAL_STATE=.TRUE.,TRIP_DIRECTION=-1 /
&CTRL ID='VENT6', FUNCTION_TYPE='SUBTRACT',
INPUT_ID='TEMP_IS01','PLATE_T_05', SETPOINT=0,
LATCH=.FALSE., INITIAL_STATE=.TRUE.,TRIP_DIRECTION=-1 /

```

```

//-----
-----//
//----- MEASUREMENTS -----
-----//
//-----
-----//

```

```

//-- AVERAGE TEMPERATURE INSIDE FURNACE --//

```

```

&DEVC XB=0.2,0.7,-1.8,1.8,0.2,3.2,
QUANTITY='TEMPERATURE',ID='TEMP_FURN_TOP_AVE', STATISTICS='MEAN' /

```

```

//-- INSTRUMENT --//

```

```

&PROP ID='TC18', BEAD_DIAMETER=0.001245/
&PROP ID='HF18', BEAD_DIAMETER=0.025/

```

```

//-- PLATE THERMOMETER --//

```

```

&DEVC XYZ=0.55,0.85,0.65, QUANTITY='WALL TEMPERATURE', ID='PLATE_T_01', IOR=-
1 /
&DEVC XYZ=0.55,-0.85,0.65, QUANTITY='WALL TEMPERATURE', ID='PLATE_T_02',
IOR=-1 /
&DEVC XYZ=0.55,-0.85,2.55, QUANTITY='WALL TEMPERATURE', ID='PLATE_T_03',
IOR=-1 /
&DEVC XYZ=0.55,0.85,2.55, QUANTITY='WALL TEMPERATURE', ID='PLATE_T_04', IOR=-
1 /
&DEVC XYZ=0.55,0.05,1.75, QUANTITY='WALL TEMPERATURE', ID='PLATE_T_05', IOR=-
1 /

```

```

//-- GAUGE HEAT FLUX --//

```

```
&DEVC XYZ=0.55,0.85,0.65, QUANTITY='GAUGE HEAT FLUX', ID='PLATE_GAUGE_HF_01',  
PROP_ID='HF18',IOR=-1 /  
&DEVC XYZ=0.55,-0.85,0.65, QUANTITY='GAUGE HEAT FLUX',  
ID='PLATE_GAUGE_HF_02', PROP_ID='HF18' ,IOR=-1 /  
&DEVC XYZ=0.55,-0.85,2.55, QUANTITY='GAUGE HEAT FLUX',  
ID='PLATE_GAUGE_HF_03', PROP_ID='HF18', IOR=-1 /  
&DEVC XYZ=0.55,0.85,2.55, QUANTITY='GAUGE HEAT FLUX', ID='PLATE_GAUGE_HF_04',  
PROP_ID='HF18',IOR=-1 /  
&DEVC XYZ=0.55,0.05,1.75, QUANTITY='GAUGE HEAT FLUX', ID='PLATE_GAUGE_HF_05',  
PROP_ID='HF18', IOR=-1 /
```

```
//-- DEVICES --//
```

```
&PROP ID='TC18', BEAD_DIAMETER=0.001245/  
&PROP ID='HF18', BEAD_DIAMETER=0.025/
```

```
//-- WALL TEMPERATURE --//
```

```
&DEVC ID='TC_OUT_1',XYZ=0.8,0.6,0.5, QUANTITY='WALL TEMPERATURE' ,IOR=1/  
OUTSIDE WALL SURFACE TEMPERATURE  
&DEVC ID='TC_OUT_2',XYZ=0.8,-0.6,0.5, QUANTITY='WALL TEMPERATURE',IOR=1/  
OUTSIDE WALL SURFACE TEMPERATURE  
&DEVC ID='TC_OUT_3',XYZ=0.8,-0.6,2.4, QUANTITY='WALL TEMPERATURE',IOR=1/  
OUTSIDE WALL SURFACE TEMPERATURE  
&DEVC ID='TC_OUT_4',XYZ=0.8,0.6,2.4, QUANTITY='WALL TEMPERATURE' ,IOR=1/  
OUTSIDE WALL SURFACE TEMPERATURE  
&DEVC ID='TC_OUT_5',XYZ=0.8,0,1.6, QUANTITY='WALL TEMPERATURE' ,IOR=1/  
OUTSIDE WALL SURFACE TEMPERATURE
```

```
&DEVC ID='TC_IN_1',XYZ=0.7,0.6,0.5, QUANTITY='WALL TEMPERATURE' ,IOR=-1/  
OUTSIDE WALL SURFACE TEMPERATURE  
&DEVC ID='TC_IN_2',XYZ=0.7,-0.6,0.5, QUANTITY='WALL TEMPERATURE' ,IOR=-1/  
OUTSIDE WALL SURFACE TEMPERATURE  
&DEVC ID='TC_IN_3',XYZ=0.7,-0.6,2.4, QUANTITY='WALL TEMPERATURE' ,IOR=-1/  
OUTSIDE WALL SURFACE TEMPERATURE  
&DEVC ID='TC_IN_4',XYZ=0.7,0.6,2.4, QUANTITY='WALL TEMPERATURE' ,IOR=-1/  
OUTSIDE WALL SURFACE TEMPERATURE  
&DEVC ID='TC_IN_5',XYZ=0.7,0,1.6, QUANTITY='WALL TEMPERATURE' ,IOR=-1/  
OUTSIDE WALL SURFACE TEMPERATURE
```

```
//-- TEMPERATURE INSIDE WALL --//
```

```
&DEVC XYZ=0.7,0,1.5, QUANTITY='INSIDE WALL TEMPERATURE', DEPTH=0.005,  
IOR=1,ID='Temp 5 mm'/  
&DEVC XYZ=0.7,0,1.5, QUANTITY='INSIDE WALL TEMPERATURE', DEPTH=0.010,  
IOR=1,ID='Temp 10 mm'/  
&DEVC XYZ=0.7,0,1.5, QUANTITY='INSIDE WALL TEMPERATURE', DEPTH=0.040,  
IOR=1,ID='Temp 40 mm'/
```

```

&DEVC XYZ=0.7,0,1.5, QUANTITY='INSIDE WALL TEMPERATURE', DEPTH=0.062,
IOR=1,ID='Temp 62 mm'/

/-- COTTON PAD RADIATION TEMPERATURE READING --//

&DEVC ID='COTTON PAD RADIATIVE HEAT FLUX', QUANTITY='RADIATIVE HEAT FLUX',
XYZ=0.9,-1.75,3.25, IOR=-1/
&DEVC ID='COTTON PAD SURFACE TEMPERATURE', QUANTITY='WALL TEMPERATURE',
XYZ=0.9,-1.75,3.25, IOR=-1, /
&DEVC ID='Temp inside cotton 15 mm', QUANTITY='INSIDE WALL
TEMPERATURE', XYZ=0.9,-1.75,3.25, DEPTH=0.005, IOR=-1,/

&DEVC ID='COTTON PAD RADIATIVE HEAT FLUX 2', QUANTITY='RADIATIVE HEAT
FLUX', XYZ=0.9,-1.75,1.65, IOR=-1/
&DEVC ID='COTTON PAD SURFACE TEMPERATURE 2', QUANTITY='WALL TEMPERATURE',
XYZ=0.9,-1.75,1.65, IOR=-1, /
&DEVC ID='Temp inside cotton 15 mm 2', QUANTITY='INSIDE WALL
TEMPERATURE', XYZ=0.9,-1.75,1.65, DEPTH=0.005, IOR=-1,/

&DEVC ID='COTTON PAD RADIATIVE HEAT FLUX 3', QUANTITY='RADIATIVE HEAT
FLUX', XYZ=0.9,-1.75,0.25, IOR=-1/
&DEVC ID='COTTON PAD SURFACE TEMPERATURE 3', QUANTITY='WALL TEMPERATURE',
XYZ=0.9,-1.75,0.25, IOR=-1, /
&DEVC ID='Temp inside cotton 15 mm 3', QUANTITY='INSIDE WALL
TEMPERATURE', XYZ=0.9,-1.75,0.25, DEPTH=0.005, IOR=-1,/

/-- VELOCITY READING --//

&DEVC ID='Velocity', QUANTITY='DUCT VELOCITY',DUCT_ID='DUCT1'/
&DEVC ID='Velocity', QUANTITY='DUCT VOLUME FLOW',DUCT_ID='DUCT1'/

/-- PRESSURE READING --//

&DEVC XYZ=0.7,0.0,3.2 QUANTITY='PRESSURE', /

&DEVC XB=0.2,0.7,-1.8,1.8,3.0,3.2, QUANTITY='PRESSURE',ID='PRESSUREDEV',
STATISTICS='MEAN' /

/-- SLICE FILE --//

&SLCF PBY=0.0, QUANTITY='TEMPERATURE'/
&SLCF PBY=0.0, QUANTITY='VELOCITY',VECTOR=.TRUE./
&SLCF PBZ=0.0, QUANTITY='PRESSURE' /

/-- BOUNDARY FILE --//

&BNDF QUANTITY='RADIATIVE HEAT FLUX'/

```

&BNDF QUANTITY='RADIOMETER'/
&BNDF QUANTITY='WALL TEMPERATURE'/

&TAIL/

Appendix B: ABAQUS script file

Following is a sample of the INP code from ABAQUS for the partition type A insulated with stone wool. The mesh used for this INP file is coarse in order to keep the appendix short.

*Heading

** Job name: 2x13mmROCKWOOLcode Model name: Model-1

** Generated by: Abaqus/CAE 6.14-2

*Preprint, echo=NO, model=NO, history=NO, contact=NO

**

** PARTS

**

*Part, name="C studs"

*Node

1,	-0.0130000003,	0.0259117652,	0.
2,	0.0185000002,	0.0259117652,	0.
3,	-0.0130000003,	0.0264117643,	0.
4,	0.0189999994,	0.0264117643,	0.
5,	0.0189999994,	-0.0235882346,	0.
6,	-0.0130000003,	-0.0235882346,	0.
7,	-0.0130000003,	-0.0227882359,	0.
8,	0.0185000002,	-0.0227882359,	0.
9,	0.0189999994,	0.00141176477,	0.
10,	0.0185000002,	0.00156176474,	0.
11,	-0.0130000003,	0.0259117652,	0.501666665
12,	0.0185000002,	0.0259117652,	0.501666665

13, -0.0130000003, 0.0264117643, 0.501666665
14, 0.0189999994, 0.0264117643, 0.501666665
15, 0.0189999994, -0.0235882346, 0.501666665
16, -0.0130000003, -0.0235882346, 0.501666665
17, -0.0130000003, -0.0227882359, 0.501666665
18, 0.0185000002, -0.0227882359, 0.501666665
19, 0.0189999994, 0.00141176477, 0.501666665
20, 0.0185000002, 0.00156176474, 0.501666665
21, -0.0130000003, 0.0259117652, 1.00333333
22, 0.0185000002, 0.0259117652, 1.00333333
23, -0.0130000003, 0.0264117643, 1.00333333
24, 0.0189999994, 0.0264117643, 1.00333333
25, 0.0189999994, -0.0235882346, 1.00333333
26, -0.0130000003, -0.0235882346, 1.00333333
27, -0.0130000003, -0.0227882359, 1.00333333
28, 0.0185000002, -0.0227882359, 1.00333333
29, 0.0189999994, 0.00141176477, 1.00333333
30, 0.0185000002, 0.00156176474, 1.00333333
31, -0.0130000003, 0.0259117652, 1.505
32, 0.0185000002, 0.0259117652, 1.505
33, -0.0130000003, 0.0264117643, 1.505
34, 0.0189999994, 0.0264117643, 1.505
35, 0.0189999994, -0.0235882346, 1.505
36, -0.0130000003, -0.0235882346, 1.505

37, -0.0130000003, -0.0227882359, 1.505
38, 0.0185000002, -0.0227882359, 1.505
39, 0.0189999994, 0.00141176477, 1.505
40, 0.0185000002, 0.00156176474, 1.505
41, -0.0130000003, 0.0259117652, 2.00666666
42, 0.0185000002, 0.0259117652, 2.00666666
43, -0.0130000003, 0.0264117643, 2.00666666
44, 0.0189999994, 0.0264117643, 2.00666666
45, 0.0189999994, -0.0235882346, 2.00666666
46, -0.0130000003, -0.0235882346, 2.00666666
47, -0.0130000003, -0.0227882359, 2.00666666
48, 0.0185000002, -0.0227882359, 2.00666666
49, 0.0189999994, 0.00141176477, 2.00666666
50, 0.0185000002, 0.00156176474, 2.00666666
51, -0.0130000003, 0.0259117652, 2.50833344
52, 0.0185000002, 0.0259117652, 2.50833344
53, -0.0130000003, 0.0264117643, 2.50833344
54, 0.0189999994, 0.0264117643, 2.50833344
55, 0.0189999994, -0.0235882346, 2.50833344
56, -0.0130000003, -0.0235882346, 2.50833344
57, -0.0130000003, -0.0227882359, 2.50833344
58, 0.0185000002, -0.0227882359, 2.50833344
59, 0.0189999994, 0.00141176477, 2.50833344
60, 0.0185000002, 0.00156176474, 2.50833344

61, -0.0130000003, 0.0259117652, 3.00999999
62, 0.0185000002, 0.0259117652, 3.00999999
63, -0.0130000003, 0.0264117643, 3.00999999
64, 0.0189999994, 0.0264117643, 3.00999999
65, 0.0189999994, -0.0235882346, 3.00999999
66, -0.0130000003, -0.0235882346, 3.00999999
67, -0.0130000003, -0.0227882359, 3.00999999
68, 0.0185000002, -0.0227882359, 3.00999999
69, 0.0189999994, 0.00141176477, 3.00999999
70, 0.0185000002, 0.00156176474, 3.00999999

*Element, type=DC3D8

1, 4, 3, 1, 2, 14, 13, 11, 12
2, 10, 8, 5, 9, 20, 18, 15, 19
3, 7, 6, 5, 8, 17, 16, 15, 18
4, 4, 2, 10, 9, 14, 12, 20, 19
5, 14, 13, 11, 12, 24, 23, 21, 22
6, 20, 18, 15, 19, 30, 28, 25, 29
7, 17, 16, 15, 18, 27, 26, 25, 28
8, 14, 12, 20, 19, 24, 22, 30, 29
9, 24, 23, 21, 22, 34, 33, 31, 32
10, 30, 28, 25, 29, 40, 38, 35, 39
11, 27, 26, 25, 28, 37, 36, 35, 38
12, 24, 22, 30, 29, 34, 32, 40, 39
13, 34, 33, 31, 32, 44, 43, 41, 42

```
14, 40, 38, 35, 39, 50, 48, 45, 49
15, 37, 36, 35, 38, 47, 46, 45, 48
16, 34, 32, 40, 39, 44, 42, 50, 49
17, 44, 43, 41, 42, 54, 53, 51, 52
18, 50, 48, 45, 49, 60, 58, 55, 59
19, 47, 46, 45, 48, 57, 56, 55, 58
20, 44, 42, 50, 49, 54, 52, 60, 59
21, 54, 53, 51, 52, 64, 63, 61, 62
22, 60, 58, 55, 59, 70, 68, 65, 69
23, 57, 56, 55, 58, 67, 66, 65, 68
24, 54, 52, 60, 59, 64, 62, 70, 69

*Nset, nset=Set-21, generate
  1, 70, 1

*Elset, elset=Set-21, generate
  1, 24, 1

** Section: STEEL

*Solid Section, elset=Set-21, material=STEEL

,

*End Part

**

*Part, name="C- Studs Bottom Top"

*Node
  1, -0.0130000003, 0.0259117652, 0.
  2, 0.0185000002, 0.0259117652, 0.
```

3, -0.0130000003, 0.0264117643, 0.
4, 0.0189999994, 0.0264117643, 0.
5, 0.0189999994, -0.0235882346, 0.
6, -0.0130000003, -0.0235882346, 0.
7, -0.0130000003, -0.0227882359, 0.
8, 0.0185000002, -0.0227882359, 0.
9, 0.0189999994, 0.00141176477, 0.
10, 0.0185000002, 0.00156176474, 0.
11, -0.0130000003, 0.0259117652, 0.515714288
12, 0.0185000002, 0.0259117652, 0.515714288
13, -0.0130000003, 0.0264117643, 0.515714288
14, 0.0189999994, 0.0264117643, 0.515714288
15, 0.0189999994, -0.0235882346, 0.515714288
16, -0.0130000003, -0.0235882346, 0.515714288
17, -0.0130000003, -0.0227882359, 0.515714288
18, 0.0185000002, -0.0227882359, 0.515714288
19, 0.0189999994, 0.00141176477, 0.515714288
20, 0.0185000002, 0.00156176474, 0.515714288
21, -0.0130000003, 0.0259117652, 1.03142858
22, 0.0185000002, 0.0259117652, 1.03142858
23, -0.0130000003, 0.0264117643, 1.03142858
24, 0.0189999994, 0.0264117643, 1.03142858
25, 0.0189999994, -0.0235882346, 1.03142858
26, -0.0130000003, -0.0235882346, 1.03142858

27, -0.0130000003, -0.0227882359, 1.03142858
28, 0.0185000002, -0.0227882359, 1.03142858
29, 0.0189999994, 0.00141176477, 1.03142858
30, 0.0185000002, 0.00156176474, 1.03142858
31, -0.0130000003, 0.0259117652, 1.54714286
32, 0.0185000002, 0.0259117652, 1.54714286
33, -0.0130000003, 0.0264117643, 1.54714286
34, 0.0189999994, 0.0264117643, 1.54714286
35, 0.0189999994, -0.0235882346, 1.54714286
36, -0.0130000003, -0.0235882346, 1.54714286
37, -0.0130000003, -0.0227882359, 1.54714286
38, 0.0185000002, -0.0227882359, 1.54714286
39, 0.0189999994, 0.00141176477, 1.54714286
40, 0.0185000002, 0.00156176474, 1.54714286
41, -0.0130000003, 0.0259117652, 2.06285715
42, 0.0185000002, 0.0259117652, 2.06285715
43, -0.0130000003, 0.0264117643, 2.06285715
44, 0.0189999994, 0.0264117643, 2.06285715
45, 0.0189999994, -0.0235882346, 2.06285715
46, -0.0130000003, -0.0235882346, 2.06285715
47, -0.0130000003, -0.0227882359, 2.06285715
48, 0.0185000002, -0.0227882359, 2.06285715
49, 0.0189999994, 0.00141176477, 2.06285715
50, 0.0185000002, 0.00156176474, 2.06285715

51, -0.0130000003, 0.0259117652, 2.57857132
52, 0.0185000002, 0.0259117652, 2.57857132
53, -0.0130000003, 0.0264117643, 2.57857132
54, 0.0189999994, 0.0264117643, 2.57857132
55, 0.0189999994, -0.0235882346, 2.57857132
56, -0.0130000003, -0.0235882346, 2.57857132
57, -0.0130000003, -0.0227882359, 2.57857132
58, 0.0185000002, -0.0227882359, 2.57857132
59, 0.0189999994, 0.00141176477, 2.57857132
60, 0.0185000002, 0.00156176474, 2.57857132
61, -0.0130000003, 0.0259117652, 3.09428573
62, 0.0185000002, 0.0259117652, 3.09428573
63, -0.0130000003, 0.0264117643, 3.09428573
64, 0.0189999994, 0.0264117643, 3.09428573
65, 0.0189999994, -0.0235882346, 3.09428573
66, -0.0130000003, -0.0235882346, 3.09428573
67, -0.0130000003, -0.0227882359, 3.09428573
68, 0.0185000002, -0.0227882359, 3.09428573
69, 0.0189999994, 0.00141176477, 3.09428573
70, 0.0185000002, 0.00156176474, 3.09428573
71, -0.0130000003, 0.0259117652, 3.6099999
72, 0.0185000002, 0.0259117652, 3.6099999
73, -0.0130000003, 0.0264117643, 3.6099999
74, 0.0189999994, 0.0264117643, 3.6099999

75, 0.0189999994, -0.0235882346, 3.6099999
76, -0.0130000003, -0.0235882346, 3.6099999
77, -0.0130000003, -0.0227882359, 3.6099999
78, 0.0185000002, -0.0227882359, 3.6099999
79, 0.0189999994, 0.00141176477, 3.6099999
80, 0.0185000002, 0.00156176474, 3.6099999

*Element, type=DC3D8

1, 4, 3, 1, 2, 14, 13, 11, 12
2, 7, 6, 5, 8, 17, 16, 15, 18
3, 4, 2, 10, 9, 14, 12, 20, 19
4, 10, 8, 5, 9, 20, 18, 15, 19
5, 14, 13, 11, 12, 24, 23, 21, 22
6, 17, 16, 15, 18, 27, 26, 25, 28
7, 14, 12, 20, 19, 24, 22, 30, 29
8, 20, 18, 15, 19, 30, 28, 25, 29
9, 24, 23, 21, 22, 34, 33, 31, 32
10, 27, 26, 25, 28, 37, 36, 35, 38
11, 24, 22, 30, 29, 34, 32, 40, 39
12, 30, 28, 25, 29, 40, 38, 35, 39
13, 34, 33, 31, 32, 44, 43, 41, 42
14, 37, 36, 35, 38, 47, 46, 45, 48
15, 34, 32, 40, 39, 44, 42, 50, 49
16, 40, 38, 35, 39, 50, 48, 45, 49
17, 44, 43, 41, 42, 54, 53, 51, 52

18, 47, 46, 45, 48, 57, 56, 55, 58

19, 44, 42, 50, 49, 54, 52, 60, 59

20, 50, 48, 45, 49, 60, 58, 55, 59

21, 54, 53, 51, 52, 64, 63, 61, 62

22, 57, 56, 55, 58, 67, 66, 65, 68

23, 54, 52, 60, 59, 64, 62, 70, 69

24, 60, 58, 55, 59, 70, 68, 65, 69

25, 64, 63, 61, 62, 74, 73, 71, 72

26, 67, 66, 65, 68, 77, 76, 75, 78

27, 64, 62, 70, 69, 74, 72, 80, 79

28, 70, 68, 65, 69, 80, 78, 75, 79

*Nset, nset=Set-21, generate

1, 80, 1

*Elset, elset=Set-21, generate

1, 28, 1

** Section: STEEL

*Solid Section, elset=Set-21, material=STEEL

,

*End Part

**

*Part, name=Gypsum

*Node

1, -1.80499995, 1.505, 0.

2, -0.902499974, 1.505, 0.

3, 0., 1.505, 0.
4, 0.902499974, 1.505, 0.
5, 1.80499995, 1.505, 0.
6, -1.80499995, 0.501666665, 0.
7, -0.902499974, 0.501666665, 0.
8, 0., 0.501666665, 0.
9, 0.902499974, 0.501666665, 0.
10, 1.80499995, 0.501666665, 0.
11, -1.80499995, -0.501666665, 0.
12, -0.902499974, -0.501666665, 0.
13, 0., -0.501666665, 0.
14, 0.902499974, -0.501666665, 0.
15, 1.80499995, -0.501666665, 0.
16, -1.80499995, -1.505, 0.
17, -0.902499974, -1.505, 0.
18, 0., -1.505, 0.
19, 0.902499974, -1.505, 0.
20, 1.80499995, -1.505, 0.
21, -1.80499995, 1.505, 0.00949999969
22, -0.902499974, 1.505, 0.00949999969
23, 0., 1.505, 0.00949999969
24, 0.902499974, 1.505, 0.00949999969
25, 1.80499995, 1.505, 0.00949999969
26, -1.80499995, 0.501666665, 0.00949999969

27, -0.902499974, 0.501666665, 0.00949999969
28, 0., 0.501666665, 0.00949999969
29, 0.902499974, 0.501666665, 0.00949999969
30, 1.80499995, 0.501666665, 0.00949999969
31, -1.80499995, -0.501666665, 0.00949999969
32, -0.902499974, -0.501666665, 0.00949999969
33, 0., -0.501666665, 0.00949999969
34, 0.902499974, -0.501666665, 0.00949999969
35, 1.80499995, -0.501666665, 0.00949999969
36, -1.80499995, -1.505, 0.00949999969
37, -0.902499974, -1.505, 0.00949999969
38, 0., -1.505, 0.00949999969
39, 0.902499974, -1.505, 0.00949999969
40, 1.80499995, -1.505, 0.00949999969

*Element, type=DC3D8

1, 6, 7, 2, 1, 26, 27, 22, 21
2, 7, 8, 3, 2, 27, 28, 23, 22
3, 8, 9, 4, 3, 28, 29, 24, 23
4, 9, 10, 5, 4, 29, 30, 25, 24
5, 11, 12, 7, 6, 31, 32, 27, 26
6, 12, 13, 8, 7, 32, 33, 28, 27
7, 13, 14, 9, 8, 33, 34, 29, 28
8, 14, 15, 10, 9, 34, 35, 30, 29
9, 16, 17, 12, 11, 36, 37, 32, 31

10, 17, 18, 13, 12, 37, 38, 33, 32

11, 18, 19, 14, 13, 38, 39, 34, 33

12, 19, 20, 15, 14, 39, 40, 35, 34

*Nset, nset=Set-7, generate

1, 40, 1

*Elset, elset=Set-7, generate

1, 12, 1

*Elset, elset=_Surf-1_S2, internal, generate

1, 12, 1

*Surface, type=ELEMENT, name=Surf-1

_Surf-1_S2, S2

*Elset, elset=_Surf-2_S1, internal, generate

1, 12, 1

*Surface, type=ELEMENT, name=Surf-2

_Surf-2_S1, S1

** Section: GYPSUM

*Solid Section, elset=Set-7, material=DRYWALL

,

*End Part

**

*Part, name=Insulation

*Node

1, -1.79999995, -1.505, 0.0500000007

2, -1.79999995, -0.501666665, 0.0500000007

3, -1.79999995, 0.501666665, 0.0500000007
4, -1.79999995, 1.505, 0.0500000007
5, -1.79999995, -1.505, 0.
6, -1.79999995, -0.501666665, 0.
7, -1.79999995, 0.501666665, 0.
8, -1.79999995, 1.505, 0.
9, -0.897499979, -1.505, 0.0500000007
10, -0.897499979, -0.501666665, 0.0500000007
11, -0.897499979, 0.501666665, 0.0500000007
12, -0.897499979, 1.505, 0.0500000007
13, -0.897499979, -1.505, 0.
14, -0.897499979, -0.501666665, 0.
15, -0.897499979, 0.501666665, 0.
16, -0.897499979, 1.505, 0.
17, 0.0049999989, -1.505, 0.0500000007
18, 0.0049999989, -0.501666665, 0.0500000007
19, 0.0049999989, 0.501666665, 0.0500000007
20, 0.0049999989, 1.505, 0.0500000007
21, 0.0049999989, -1.505, 0.
22, 0.0049999989, -0.501666665, 0.
23, 0.0049999989, 0.501666665, 0.
24, 0.0049999989, 1.505, 0.
25, 0.907500029, -1.505, 0.0500000007
26, 0.907500029, -0.501666665, 0.0500000007

27, 0.907500029, 0.501666665, 0.0500000007
28, 0.907500029, 1.505, 0.0500000007
29, 0.907500029, -1.505, 0.
30, 0.907500029, -0.501666665, 0.
31, 0.907500029, 0.501666665, 0.
32, 0.907500029, 1.505, 0.
33, 1.809999994, -1.505, 0.0500000007
34, 1.809999994, -0.501666665, 0.0500000007
35, 1.809999994, 0.501666665, 0.0500000007
36, 1.809999994, 1.505, 0.0500000007
37, 1.809999994, -1.505, 0.
38, 1.809999994, -0.501666665, 0.
39, 1.809999994, 0.501666665, 0.
40, 1.809999994, 1.505, 0.

*Element, type=DC3D8

1, 9, 10, 14, 13, 1, 2, 6, 5
2, 10, 11, 15, 14, 2, 3, 7, 6
3, 11, 12, 16, 15, 3, 4, 8, 7
4, 17, 18, 22, 21, 9, 10, 14, 13
5, 18, 19, 23, 22, 10, 11, 15, 14
6, 19, 20, 24, 23, 11, 12, 16, 15
7, 25, 26, 30, 29, 17, 18, 22, 21
8, 26, 27, 31, 30, 18, 19, 23, 22
9, 27, 28, 32, 31, 19, 20, 24, 23

10, 33, 34, 38, 37, 25, 26, 30, 29

11, 34, 35, 39, 38, 26, 27, 31, 30

12, 35, 36, 40, 39, 27, 28, 32, 31

*Nset, nset=Set-1, generate

1, 40, 1

*Elset, elset=Set-1, generate

1, 12, 1

*Elset, elset=_Surf-1_S3, internal, generate

1, 12, 1

*Surface, type=ELEMENT, name=Surf-1

_Surf-1_S3, S3

*Elset, elset=_Surf-2_S5, internal, generate

1, 12, 1

*Surface, type=ELEMENT, name=Surf-2

_Surf-2_S5, S5

** Section: STONE WOOL

*Solid Section, elset=Set-1, material="STONE WOOL"

,

*End Part

**

**

** ASSEMBLY

**

*Assembly, name=Assembly

**

*Instance, name="Gypsum out", part=Gypsum

0., 0., -0.0095

*End Instance

**

*Instance, name="Gypsum In", part=Gypsum

0., -4.22503145705837e-18, -0.06900000000000001

*End Instance

**

*Instance, name=C-1, part="C studs"

0., 1.50499999999988, -0.0359117647423686

0., 1.50499999999988, -0.0359117647423686, 1., 1.50499999999988, -
0.0359117647423686, 90.

*End Instance

**

*Instance, name=C-2, part="C studs"

-1.78599999999984, -1.50500000000012, -0.0359117647423685

-1.78599999999984, -1.50500000000012, -0.0359117647423685, -1.78599999999984, -
0.797893188768337, 0.671195046489412, 180.

*End Instance

**

*Instance, name=C-3, part="C studs"

1.78599999999984, 1.50499999999988, -0.0359117647423685

1.78599999999984, 1.50499999999988, -0.0359117647423685, 2.78599999999984,
1.50499999999988, -0.0359117647423685, 90.

*End Instance

**

*Instance, name=C-1-lin-2-1, part="C studs"

0.6, 1.50499999999988, -0.0359117647423684

0.6, 1.50499999999988, -0.0359117647423684, 1.6, 1.50499999999988, -
0.0359117647423684, 90.

*End Instance

**

*Instance, name=C-1-lin-3-1, part="C studs"

1.2, 1.50499999999988, -0.0359117647423684

1.2, 1.50499999999988, -0.0359117647423684, 2.2, 1.50499999999988, -
0.0359117647423684, 90.

*End Instance

**

*Instance, name=C-1-lin-2-1-1, part="C studs"

-0.6, 1.50499999999988, -0.0359117647423684

-0.6, 1.50499999999988, -0.0359117647423684, 0.4, 1.50499999999988, -
0.0359117647423684, 90.

*End Instance

**

*Instance, name=C-1-lin-3-1-1, part="C studs"

-1.2, 1.50499999999988, -0.0359117647423684

-1.2, 1.50499999999988, -0.0359117647423684, -0.2, 1.50499999999988, -
0.0359117647423684, 90.

*End Instance

**

*Instance, name=C-Bottom-1, part="C- Studs Bottom Top"

1.80500000000016, -1.48599999999988, -0.0359117647423686

1.80500000000016, -1.48599999999988, -0.0359117647423686, 2.38235027955221, -
2.06335027955192, -0.613262044294411, 119.999999109416

*End Instance

**

*Instance, name=C-Top-2, part="C- Studs Bottom Top"

1.80500000000016, 1.48599999999988, -0.0330882352576318

1.80500000000016, 1.48599999999988, -0.0330882352576318, 1.22764972044812,
0.908649720447835, 0.54426204429441, 119.999999109416

*End Instance

**

*Instance, name=Insulation-1, part=Insulation

-0.00500000000016421, -4.88498130835066e-15, -0.0595000000000001

*End Instance

**

*Nset, nset=Set-1, instance="Gypsum out", generate

1, 20, 1

*Elset, elset=Set-1, instance="Gypsum out", generate

1, 12, 1

*Nset, nset=Set-2, instance="Gypsum out", generate

1, 40, 1

*Nset, nset=Set-2, instance="Gypsum In", generate

1, 40, 1

*Elset, elset=Set-2, instance="Gypsum out", generate

1, 12, 1

*Elset, elset=Set-2, instance="Gypsum In", generate

1, 12, 1

*Nset, nset=Set-3, instance="Gypsum In", generate

21, 40, 1

*Elset, elset=Set-3, instance="Gypsum In", generate

1, 12, 1

*Elset, elset=_CP-1-C-1_S3, internal, instance=C-1, generate

1, 21, 4

*Surface, type=ELEMENT, name=CP-1-C-1

_CP-1-C-1_S3, S3

*Elset, elset="_CP-1-Gypsum out_S1", internal, instance="Gypsum out", generate

1, 12, 1

*Surface, type=ELEMENT, name="CP-1-Gypsum out"

"_CP-1-Gypsum out_S1", S1

*Elset, elset=_CP-2-C-2_S3, internal, instance=C-2, generate

1, 21, 4

*Surface, type=ELEMENT, name=CP-2-C-2

_CP-2-C-2_S3, S3

*Elset, elset="_CP-2-Gypsum out_S1", internal, instance="Gypsum out", generate

1, 12, 1

*Surface, type=ELEMENT, name="CP-2-Gypsum out"

"_CP-2-Gypsum out_S1", S1

*Elset, elset=_CP-3-C-3_S3, internal, instance=C-3, generate

1, 21, 4

*Surface, type=ELEMENT, name=CP-3-C-3

_CP-3-C-3_S3, S3

*Elset, elset="_CP-3-Gypsum out_S1", internal, instance="Gypsum out", generate

1, 12, 1

*Surface, type=ELEMENT, name="CP-3-Gypsum out"

"_CP-3-Gypsum out_S1", S1

*Elset, elset=_CP-4-C-1-lin-2-1_S3, internal, instance=C-1-lin-2-1, generate

1, 21, 4

*Surface, type=ELEMENT, name=CP-4-C-1-lin-2-1

_CP-4-C-1-lin-2-1_S3, S3

*Elset, elset="_CP-4-Gypsum out_S1", internal, instance="Gypsum out", generate

1, 12, 1

*Surface, type=ELEMENT, name="CP-4-Gypsum out"

"_CP-4-Gypsum out_S1", S1

*Elset, elset=_CP-5-C-1-lin-3-1_S3, internal, instance=C-1-lin-3-1, generate

1, 21, 4

*Surface, type=ELEMENT, name=CP-5-C-1-lin-3-1

_CP-5-C-1-lin-3-1_S3, S3

*Elset, elset="_CP-5-Gypsum out_S1", internal, instance="Gypsum out", generate

1, 12, 1

*Surface, type=ELEMENT, name="CP-5-Gypsum out"

"_CP-5-Gypsum out_S1", S1

*Elset, elset=_CP-6-C-1-lin-2-1-1_S3, internal, instance=C-1-lin-2-1-1, generate

1, 21, 4

*Surface, type=ELEMENT, name=CP-6-C-1-lin-2-1-1

_CP-6-C-1-lin-2-1-1_S3, S3

*Elset, elset="_CP-6-Gypsum out_S1", internal, instance="Gypsum out", generate

1, 12, 1

*Surface, type=ELEMENT, name="CP-6-Gypsum out"

"_CP-6-Gypsum out_S1", S1

*Elset, elset=_CP-7-C-1-lin-3-1-1_S3, internal, instance=C-1-lin-3-1-1, generate

1, 21, 4

*Surface, type=ELEMENT, name=CP-7-C-1-lin-3-1-1

_CP-7-C-1-lin-3-1-1_S3, S3

*Elset, elset="_CP-7-Gypsum out_S1", internal, instance="Gypsum out", generate

1, 12, 1

*Surface, type=ELEMENT, name="CP-7-Gypsum out"

"_CP-7-Gypsum out_S1", S1

*Elset, elset=_CP-8-C-Bottom-1_S3, internal, instance=C-Bottom-1, generate

1, 25, 4

*Surface, type=ELEMENT, name=CP-8-C-Bottom-1

_CP-8-C-Bottom-1_S3, S3

*Elset, elset="_CP-8-Gypsum out_S1", internal, instance="Gypsum out", generate

1, 12, 1

*Surface, type=ELEMENT, name="CP-8-Gypsum out"

"_CP-8-Gypsum out_S1", S1

*Elset, elset=_CP-9-C-Top-2_S4, internal, instance=C-Top-2, generate

2, 26, 4

*Surface, type=ELEMENT, name=CP-9-C-Top-2

_CP-9-C-Top-2_S4, S4

*Elset, elset="_CP-9-Gypsum out_S1", internal, instance="Gypsum out", generate

1, 12, 1

*Surface, type=ELEMENT, name="CP-9-Gypsum out"

"_CP-9-Gypsum out_S1", S1

*Elset, elset="_CP-10-Gypsum out_S1", internal, instance="Gypsum out", generate

1, 12, 1

*Surface, type=ELEMENT, name="CP-10-Gypsum out"

"_CP-10-Gypsum out_S1", S1

*Elset, elset=_CP-10-Insulation-1_S3, internal, instance=Insulation-1, generate

1, 12, 1

*Surface, type=ELEMENT, name=CP-10-Insulation-1

_CP-10-Insulation-1_S3, S3

*Elset, elset=_CP-11-C-1_S4, internal, instance=C-1, generate

3, 23, 4

*Surface, type=ELEMENT, name=CP-11-C-1

_CP-11-C-1_S4, S4

*Elset, elset="_CP-11-Gypsum In_S2", internal, instance="Gypsum In", generate

1, 12, 1

*Surface, type=ELEMENT, name="CP-11-Gypsum In"

"_CP-11-Gypsum In_S2", S2

*Elset, elset=_CP-12-C-2_S4, internal, instance=C-2, generate

3, 23, 4

*Surface, type=ELEMENT, name=CP-12-C-2

_CP-12-C-2_S4, S4

*Elset, elset="_CP-12-Gypsum In_S2", internal, instance="Gypsum In", generate

1, 12, 1

*Surface, type=ELEMENT, name="CP-12-Gypsum In"

"_CP-12-Gypsum In_S2", S2

*Elset, elset=_CP-13-C-3_S4, internal, instance=C-3, generate

3, 23, 4

*Surface, type=ELEMENT, name=CP-13-C-3

_CP-13-C-3_S4, S4

*Elset, elset="_CP-13-Gypsum In_S2", internal, instance="Gypsum In", generate

1, 12, 1

*Surface, type=ELEMENT, name="CP-13-Gypsum In"

"_CP-13-Gypsum In_S2", S2

*Elset, elset=_CP-14-C-1-lin-2-1_S4, internal, instance=C-1-lin-2-1, generate

3, 23, 4

*Surface, type=ELEMENT, name=CP-14-C-1-lin-2-1

_CP-14-C-1-lin-2-1_S4, S4

*Elset, elset="_CP-14-Gypsum In_S2", internal, instance="Gypsum In", generate

1, 12, 1

*Surface, type=ELEMENT, name="CP-14-Gypsum In"

"_CP-14-Gypsum In_S2", S2

*Elset, elset=_CP-15-C-1-lin-3-1_S4, internal, instance=C-1-lin-3-1, generate

3, 23, 4

*Surface, type=ELEMENT, name=CP-15-C-1-lin-3-1

_CP-15-C-1-lin-3-1_S4, S4

*Elset, elset="_CP-15-Gypsum In_S2", internal, instance="Gypsum In", generate

1, 12, 1

*Surface, type=ELEMENT, name="CP-15-Gypsum In"

"_CP-15-Gypsum In_S2", S2

*Elset, elset=_CP-16-C-1-lin-2-1-1_S4, internal, instance=C-1-lin-2-1-1, generate

3, 23, 4

*Surface, type=ELEMENT, name=CP-16-C-1-lin-2-1-1

_CP-16-C-1-lin-2-1-1_S4, S4

*Elset, elset="_CP-16-Gypsum In_S2", internal, instance="Gypsum In", generate

1, 12, 1

*Surface, type=ELEMENT, name="CP-16-Gypsum In"

"_CP-16-Gypsum In_S2", S2

*Elset, elset=_CP-17-C-1-lin-3-1-1_S4, internal, instance=C-1-lin-3-1-1, generate

3, 23, 4

*Surface, type=ELEMENT, name=CP-17-C-1-lin-3-1-1

_CP-17-C-1-lin-3-1-1_S4, S4

*Elset, elset="_CP-17-Gypsum In_S2", internal, instance="Gypsum In", generate

1, 12, 1

*Surface, type=ELEMENT, name="CP-17-Gypsum In"

"_CP-17-Gypsum In_S2", S2

*Elset, elset=_CP-18-C-Bottom-1_S4, internal, instance=C-Bottom-1, generate

2, 26, 4

*Surface, type=ELEMENT, name=CP-18-C-Bottom-1

_CP-18-C-Bottom-1_S4, S4

*Elset, elset="_CP-18-Gypsum In_S2", internal, instance="Gypsum In", generate

1, 12, 1

*Surface, type=ELEMENT, name="CP-18-Gypsum In"

"_CP-18-Gypsum In_S2", S2

*Elset, elset=_CP-19-C-Top-2_S3, internal, instance=C-Top-2, generate

1, 25, 4

*Surface, type=ELEMENT, name=CP-19-C-Top-2

_CP-19-C-Top-2_S3, S3

*Elset, elset="_CP-19-Gypsum In_S2", internal, instance="Gypsum In", generate

1, 12, 1

*Surface, type=ELEMENT, name="CP-19-Gypsum In"

"_CP-19-Gypsum In_S2", S2

*Elset, elset="_CP-20-Gypsum In_S2", internal, instance="Gypsum In", generate

1, 12, 1

*Surface, type=ELEMENT, name="CP-20-Gypsum In"

"_CP-20-Gypsum In_S2", S2

*Elset, elset=_CP-20-Insulation-1_S5, internal, instance=Insulation-1, generate

1, 12, 1

*Surface, type=ELEMENT, name=CP-20-Insulation-1

_CP-20-Insulation-1_S5, S5

*Elset, elset=_Surf-1_S2, internal, instance="Gypsum out", generate

1, 12, 1

*Surface, type=ELEMENT, name=Surf-1

_Surf-1_S2, S2

*Elset, elset=_Surf-2_S1, internal, instance="Gypsum In", generate

1, 12, 1

*Surface, type=ELEMENT, name=Surf-2

_Surf-2_S1, S1

*Elset, elset=_Surf-3_S1, internal, instance="Gypsum In", generate

1, 12, 1

*Surface, type=ELEMENT, name=Surf-3

_Surf-3_S1, S1

** Constraint: CP-1-Gypsum out-C-1

*Tie, name="CP-1-Gypsum out-C-1", adjust=yes, type=SURFACE TO SURFACE

CP-1-C-1, "CP-1-Gypsum out"

** Constraint: CP-2-Gypsum out-C-2

*Tie, name="CP-2-Gypsum out-C-2", adjust=yes, type=SURFACE TO SURFACE

CP-2-C-2, "CP-2-Gypsum out"

** Constraint: CP-3-Gypsum out-C-3

*Tie, name="CP-3-Gypsum out-C-3", adjust=yes, type=SURFACE TO SURFACE

CP-3-C-3, "CP-3-Gypsum out"

** Constraint: CP-4-Gypsum out-C-1-lin-2-1

*Tie, name="CP-4-Gypsum out-C-1-lin-2-1", adjust=yes, type=SURFACE TO SURFACE

CP-4-C-1-lin-2-1, "CP-4-Gypsum out"

** Constraint: CP-5-Gypsum out-C-1-lin-3-1

*Tie, name="CP-5-Gypsum out-C-1-lin-3-1", adjust=yes, type=SURFACE TO SURFACE
CP-5-C-1-lin-3-1, "CP-5-Gypsum out"

** Constraint: CP-6-Gypsum out-C-1-lin-2-1-1

*Tie, name="CP-6-Gypsum out-C-1-lin-2-1-1", adjust=yes, type=SURFACE TO SURFACE
CP-6-C-1-lin-2-1-1, "CP-6-Gypsum out"

** Constraint: CP-7-Gypsum out-C-1-lin-3-1-1

*Tie, name="CP-7-Gypsum out-C-1-lin-3-1-1", adjust=yes, type=SURFACE TO SURFACE
CP-7-C-1-lin-3-1-1, "CP-7-Gypsum out"

** Constraint: CP-8-Gypsum out-C-Bottom-1

*Tie, name="CP-8-Gypsum out-C-Bottom-1", adjust=yes, type=SURFACE TO SURFACE
CP-8-C-Bottom-1, "CP-8-Gypsum out"

** Constraint: CP-9-Gypsum out-C-Top-2

*Tie, name="CP-9-Gypsum out-C-Top-2", adjust=yes, type=SURFACE TO SURFACE
CP-9-C-Top-2, "CP-9-Gypsum out"

** Constraint: CP-10-Insulation-1-Gypsum out

*Tie, name="CP-10-Insulation-1-Gypsum out", adjust=yes, type=SURFACE TO SURFACE
"CP-10-Gypsum out", CP-10-Insulation-1

** Constraint: CP-11-Gypsum In-C-1

*Tie, name="CP-11-Gypsum In-C-1", adjust=yes, type=SURFACE TO SURFACE
CP-11-C-1, "CP-11-Gypsum In"

** Constraint: CP-12-Gypsum In-C-2

*Tie, name="CP-12-Gypsum In-C-2", adjust=yes, type=SURFACE TO SURFACE
CP-12-C-2, "CP-12-Gypsum In"

** Constraint: CP-13-Gypsum In-C-3

*Tie, name="CP-13-Gypsum In-C-3", adjust=yes, type=SURFACE TO SURFACE

CP-13-C-3, "CP-13-Gypsum In"

** Constraint: CP-14-Gypsum In-C-1-lin-2-1

*Tie, name="CP-14-Gypsum In-C-1-lin-2-1", adjust=yes, type=SURFACE TO SURFACE

CP-14-C-1-lin-2-1, "CP-14-Gypsum In"

** Constraint: CP-15-Gypsum In-C-1-lin-3-1

*Tie, name="CP-15-Gypsum In-C-1-lin-3-1", adjust=yes, type=SURFACE TO SURFACE

CP-15-C-1-lin-3-1, "CP-15-Gypsum In"

** Constraint: CP-16-Gypsum In-C-1-lin-2-1-1

*Tie, name="CP-16-Gypsum In-C-1-lin-2-1-1", adjust=yes, type=SURFACE TO SURFACE

CP-16-C-1-lin-2-1-1, "CP-16-Gypsum In"

** Constraint: CP-17-Gypsum In-C-1-lin-3-1-1

*Tie, name="CP-17-Gypsum In-C-1-lin-3-1-1", adjust=yes, type=SURFACE TO SURFACE

CP-17-C-1-lin-3-1-1, "CP-17-Gypsum In"

** Constraint: CP-18-Gypsum In-C-Bottom-1

*Tie, name="CP-18-Gypsum In-C-Bottom-1", adjust=yes, type=SURFACE TO SURFACE

CP-18-C-Bottom-1, "CP-18-Gypsum In"

** Constraint: CP-19-Gypsum In-C-Top-2

*Tie, name="CP-19-Gypsum In-C-Top-2", adjust=yes, type=SURFACE TO SURFACE

CP-19-C-Top-2, "CP-19-Gypsum In"

** Constraint: CP-20-Insulation-1-Gypsum In

*Tie, name="CP-20-Insulation-1-Gypsum In", adjust=yes, type=SURFACE TO SURFACE

"CP-20-Gypsum In", CP-20-Insulation-1

*End Assembly

*Amplitude, name="Heat flux", time=TOTAL TIME

0.,	0.,	600.,	0.357142857,	1200.,	0.428571429,	1800.,	0.5
2400.,	0.642857143,	3000.,	0.714285714,	3600.,	0.714285714,	4200.,	0.785714286
4800.,	0.857142857,	5400.,	0.885714286,	6000.,	0.928571429,	6600.,	0.96
7200.,	1.						

*Amplitude, name="ISO 834", time=TOTAL TIME

0.,	0.02,	180.,	0.48,	360.,	0.57,	540.,	0.63
720.,	0.67,	900.,	0.7,	1080.,	0.73,	1260.,	0.75
1440.,	0.77,	1620.,	0.79,	1800.,	0.8,	1980.,	0.82
2160.,	0.83,	2340.,	0.84,	2520.,	0.85,	2700.,	0.86
2880.,	0.87,	3060.,	0.88,	3240.,	0.89,	3420.,	0.89
3600.,	0.9,	3780.,	0.91,	3960.,	0.91,	4140.,	0.92
4320.,	0.93,	4500.,	0.93,	4680.,	0.94,	4860.,	0.94
5040.,	0.95,	5220.,	0.95,	5400.,	0.96,	5580.,	0.96
5760.,	0.97,	5940.,	0.97,	6120.,	0.98,	6300.,	0.98
6480.,	0.98,	6660.,	0.99,	6840.,	0.99,	7020.,	1.
7200.,	1.						

**

** MATERIALS

**

*Material, name=Air

*Conductivity

0.0243, 0.

0.0257, 20.

0.0271, 40.

0.0285, 60.

0.0299, 80.

0.0314,100.

0.0328,120.

0.0343,140.

0.0358,160.

0.0372,180.

0.0386,200.

0.0421,250.

0.0454,300.

0.0485,350.

0.0515,400.

*Density

1.293, 0.

1.205, 20.

1.127, 40.

1.067, 60.

1., 80.

0.946,100.

0.898,120.

0.854,140.

0.815,160.

0.779,180.

0.746,200.

0.675,250.

0.616,300.

0.566,350.

0.524,400.

*Specific Heat

1005., 0.

1005., 20.

1005., 40.

1009., 60.

1009., 80.

1009.,100.

1013.,120.

1013.,140.

1017.,160.

1022.,180.

1026.,200.

1034.,250.

1047.,300.

1055.,350.

1068.,400.

*Material, name=DRYWALL

*Conductivity

0.17, 20.

0.17, 50.

0.18, 100.

0.18, 150.

0.05, 200.

0.05, 250.

0.2, 300.

0.21, 350.

0.215, 400.

0.22, 450.

0.23, 500.

0.24, 550.

0.25, 600.

0.26, 650.

0.27, 700.

0.3, 1000.

*Density

711., 0.

675.45, 50.

639.9, 100.

607.905, 150.

575.922, 200.

554.608, 300.

554.839, 400.

553.,500.

552.759,600.

558.434,700.

558.434,800.

*Specific Heat

1000., 20.

1100., 50.

1500.,100.

1600.,120.

2100.,140.

20000.,160.

7000.,170.

2100.,180.

9000.,200.

1500.,220.

1100.,260.

1000.,400.

500.,430.

800.,450.

900.,500.

1000.,600.

*Material, name="FIBRE WOOL"

*Conductivity

0.51, 50.

0.524, 100.

0.524, 120.

0.528, 140.

0.532, 160.

0.534, 170.

0.536, 180.

0.54, 200.

0.544, 220.

0.58, 400.

0.586, 430.

0.59, 450.

0.6, 500.

0.6, 600.

2., 700.

10., 800.

18., 900.

26., 1000.

34., 1100.

42., 1200.

*Density

35.,

*Specific Heat

900.,

*Material, name=STEEL

*Conductivity

53., 20.

52., 50.

51., 100.

49., 150.

47., 200.

46., 250.

44., 300.

42., 350.

41., 400.

39., 450.

37., 500.

36., 550.

34., 600.

32., 650.

31., 700.

30., 735.

27., 800.

27., 850.

27., 900.

27., 950.

27., 1000.

27., 1050.

27., 1100.

27.,1150.

27.,1200.

*Density

7850.,

*Specific Heat

440., 20.

460., 50.

488., 100.

510., 150.

530., 200.

547., 250.

565., 300.

584., 350.

606., 400.

633., 450.

667., 500.

708., 550.

760., 600.

814., 650.

1008., 700.

5000., 735.

803., 800.

695., 850.

650., 900.

650., 950.

650.,1000.

650.,1050.

650.,1100.

650.,1150.

650.,1200.

*Material, name="STONE WOOL"

*Conductivity

0.2545, 50.

0.259, 100.

0.2608, 120.

0.2626, 140.

0.2644, 160.

0.2653, 170.

0.2662, 180.

0.268, 200.

0.2698, 220.

0.286, 400.

0.2887, 430.

0.2905, 450.

0.295, 500.

0.4215, 600.

0.6815, 700.

0.9415, 800.

1.2015, 900.

1.4615,1000.

1.7215,1100.

1.9815,1200.

*Density

100.,

*Specific Heat

900.,

**

** INTERACTION PROPERTIES

**

*Surface Interaction, name=Conduction

1.,

*Gap Conductance

0.0257, 0., 20.

0., 1., 20.

0.0271, 0., 40.

0., 1., 40.

0.0285, 0., 60.

0., 1., 60.

0.0299, 0., 80.

0., 1., 80.

0.0314, 0.,100.

0., 1.,100.

0.0328, 0.,120.

0., 1.,120.

0.0343, 0.,140.

0., 1.,140.

0.0358, 0.,160.

0., 1.,160.

0.0372, 0.,180.

0., 1.,180.

0.0386, 0.,200.

0., 1.,200.

0.0421, 0.,250.

0., 1.,250.

0.0454, 0.,300.

0., 1.,300.

0.0485, 0.,350.

0., 1.,350.

0.0515, 0.,400.

0., 1.,400.

**

** PHYSICAL CONSTANTS

**

*Physical Constants, absolute zero=-273., stefan boltzmann=8.67e-08

** -----

**

```
** STEP: Heat transfer
**
*Step, name="Heat transfer", nlgeom=NO, inc=1000000
*Heat Transfer, end=PERIOD, deltmx=10000.
100., 7200., 0.01, 100.,
**
** INTERACTIONS
**
** Interaction: Cold Convection
*Sfilm
Surf-1, F, 20., 4.
** Interaction: Hot Convection
*Sfilm, amplitude="ISO 834"
Surf-2, F, 1049., 25.
** Interaction: Radiation
*Sradiate, amplitude="ISO 834"
Surf-3, R, 1049., 0.8
**
** OUTPUT REQUESTS
**
*Restart, write, frequency=0
**
** FIELD OUTPUT: F-Output-1
**
```

*Output, field, variable=PRESELECT

*Output, history, frequency=0

*End Step